uOttawa

L'Université canadienne
Canada's university

FACULTÉ DES ÉTUDES SUPÉRIEURES ET POSTOCTORALES

uOttawa

L'Université canadienne
Canada's university

FACULTY OF GRADUATE AND POSDOCTORAL STUDIES

Julie E. Wijaya
AUTEUR DE LA THÈSE / AUTHOR OF THESIS

M.A.Sc. (Chemical Engineering)
GRADE / DEGREE

Department of Chemical Engineering
FACULTÉ, ÉCOLE, DÉPARTEMENT / FACULTY, SCHOOL, DEPARTMENT

Formation and Characterization of Solvent Resistant Nanofiltration Membranes

TITRE DE LA THÈSE / TITLE OF THESIS

Ashwani Kumar
DIRECTEUR (DIRECTRICE) DE LA THÈSE / THESIS SUPERVISOR

CO-DIRECTEUR (CO-DIRECTRICE) DE LA THÈSE / THESIS CO-SUPERVISOR

EXAMINATEURS (EXAMINATRICES) DE LA THÈSE / THESIS EXAMINERS

Jules Thibault

Kevin Kennedy

Gary W. Slater
LE DOYEN DE LA FACULTÉ DES ÉTUDES SUPÉRIEURES ET POSTDOCTORALES /
DEAN OF THE FACULTY OF GRADUATE AND POSTDOCORAL STUDIES

FORMATION AND CHARACTERIZATION OF SOLVENT RESISTANT NANOFILTRATION MEMBRANES

by

Julie E. Wijaya

(#2150237)

A thesis submitted to the Faculty of Graduate and Postdoctoral Studies

in partial fulfillment of the requirement for the degree of

Master in Applied Science (M.A.Sc.)

in Chemical Engineering

Department of Chemical Engineering

University of Ottawa

Your file Votre référence
ISBN: 0-494-11455-X
Our file Notre référence
ISBN: 0-494-11455-X

ABSTRACT

Studies on membrane technology have reported that membrane stability in organic solvents depends on the physiochemical characteristics of the solvent and the membrane. Solvents interactions with membranes have been reported to cause swelling, plasticization or dissolution of membrane's material and subsequently loosening of the membrane's structure, leading to changes in separation performance or loss in mechanical strength under pressure. In addition, a small number of membrane types that are currently available on the market are expensive and show either insufficient separation performance with fluxes that are too low and molecular weight cut-off (MWCO) values that are too high.

In this work, a novel approach for preparing nanofiltration membranes using poly(amide imide) (Torlon®)/Chitosan composites by coating the Chitosan solution on top of the Torlon® base membrane and subsequently curing and neutralization with sodium bicarbonate ($NaHCO_3$) has been developed. The effect of surface cross linking of these membranes with various concentrations of the cross linker, diethylene glycol dimethacrylate (DEGDMA), over different cross linking periods has been studied including the characterization of the surface chemical composition and filtration properties such as pure water permeation and molecular weight cut-off of these new membranes. To develop an understanding of the membrane morphology, the formation of a Chitosan layer on the surface of Torlon® base membrane was also characterized by various analytical techniques such as X-ray photoelectron spectroscopy and scanning electron microscopy. These methods indicate the formation of a Chitosan layer on the surface and X-ray spectroscopy also revealed the cross linking of Chitosan with DEGDMA on the membrane surface. Pure water permeation (PWP) and MWCO measurements indicated that pore size reduction

occurs as a result of the formation of Chitosan layer on the pore walls of Torlon® base membrane.

The pH resistance for the Torlon®/Chitosan composite membranes was determined by permeating aqueous acidic (pH 3.0) and basic (pH 11) solutions and swelling studies were performed for permeating solutions over a pH range of 2.0 to 12. PWP, visual examination, and solute (polyethylene glycol) transmission data indicated that membrane was more stable at a pH of 11. It was also observed that this membrane was suitable for use in the pH range of 4.0 - 10. Solvent resistance of the membrane was also determined by swelling, immersion, and permeation studies with laboratory organic solvents, namely methanol, ethanol, iso-propanol, methyl ethyl ketone, ethyl acetate, and hexane. The results showed that the cross linked composite membranes maintain the permeate fluxes for the various solvents for 2.5 h of continuous operation after compaction with no significant change in flux. These results have been explained in terms of polar and hydrophobic interactions between solvent and membrane using the dielectric constant and surface tension of the solvent used.

In general, Torlon®/Chitosan composite nanofiltration membranes were found to be stable in aqueous medium and when contacted with the solvents. A uniform Chitosan dense layer was successfully coated on the base membrane, which reduced the effect of chemical degradation of the membrane. Low permeability of solvents was attributed to the swelling of the Torlon® layer. It is proposed that by increasing the porosity in the Torlon® based membrane or utilizing other polymers which contain amide chains as the support membrane, permeability performance could be enhanced.

RÉSUMÉ

Les études sur la technologie de membrane ont indiqué que la stabilité de membrane dans les solvants organiques dépend des caractéristiques physicochimiques du solvant et de la membrane. Il a été rapporté que les interactions solvant - membranes résultent en un gonflement, à une plastification ou la dissolution de la membrane et affectent la structure de la membrane menant à des changements des propriétés de séparation ou des pertes dans la force mécanique sous pression. En plus, un nombre restreint de types de membrane qui sont actuellement disponibles sur le marché sont chers et montrent une performance insuffisante de séparation avec des flux qui sont trop bas ou des valeurs du seuil de coupure (MWCO) qui sont trop hautes.

Ce travail présente une approche nouvelle pour préparer des membranes de nanofiltration composite en poly (imide amide) (Torlon®)/Chitosan. Une procédure a été développée où la membrane de base faite de Torlon® est enduite d'une solution de Chitosan et ensuite réticulée et neutralisée avec du bicarbonate de soude ($NaHCO_3$). Le phénomène de réticulation de la surface de ces membranes avec diverses concentrations de l'agent réticulant, le dimethacrylate de glycol de diéthylène (DEGDMA), et différentes durées a été étudié et ceci incluant la caractérisation des propriétés de composition chimique de la surface et de filtration, telles que la perméation de l'eau pure et la coupure de poids moléculaire de ces nouvelles membranes. Pour mieux comprendre la morphologie des membranes, la formation d'une couche de Chitosan sur la surface de la membrane de base de Torlon® a été également caractérisée par diverses techniques analytiques telles que la spectroscopie de photoélectron de rayon X et la microscopie électronique par balayage. Ces méthodes indiquent la formation d'une couche de Chitosan sur la surface et la spectroscopie

par rayon X a également montré la réticulation du Chitosan avec DEGDMA sur la surface de la membrane. La perméation pure de l'eau (PWP) et les mesures de MWCO ont indiqué que la réduction de la taille des pores se produit en raison de la formation d'une couche de Chitosan sur les murs des pores de la membrane de base faite de Torlon®.

La résistance des membranes composite de Torlon®/Chitosan au pH a été déterminée par la perméation de solutions acide aqueuses (pH 3.0) et basiques (pH 11). Les études de gonflage ont été réalisées avec des solutions d'imprégnation sur une gamme de pH de 2.0 à 12. Le flux d'eau pure, par inspection visuelle et les données de transmission de solutés dissous (polyéthylène glycol) ont indiqué que la membrane était plus stable à un pH de 11. On a également observé que cette membrane convenait pour un usage dans la gamme de pH de 4.0 à 10. La résistance de la membrane aux solvants a été également déterminée par gonflement, immersion, et études de perméation avec des solvants organiques de laboratoire, comme méthanol, éthanol, iso-propanol, acétone éthylique méthylique, acétate éthylique, et hexane. Les résultats ont prouvé que les membranes composite réticulées maintiennent les flux avec divers solvants pour 2.5 h d'opération continue après compaction sans changement significatif du flux. Ces résultats ont été expliqués en termes d'interactions polaires et hydrophobes entre le solvant et la membrane en utilisant la constante diélectrique et tension superficielle du solvant utilisé.

Généralement des membranes composite de nanofiltration de Torlon®/Chitosan se sont avérées stables dans les milieu aqueux et également après être entrées en contact avec des solvants. Une couche dense uniforme de Chitosan a été enduite avec succès sur la membrane de base ce qui a réduit l'effet de la dégradation chimique de la membrane. La basse perméabilité des solvants a été attribuée au gonflement de la couche de Torlon®. Nous

proposons que la performance en perméabilité pourrait être améliorée .en augmentant la porosité de la membrane de base de Torlon®, ou en utilisant d'autres polymères qui contiennent des chaînes d'amide.

ACKNOWLEDGEMENTS

I appreciatively acknowledge and sincerely thank my supervisor Dr. Ashwani Kumar for giving the opportunity to continue my learning journey. His guidance and advice play a major role to the outcome of this project.

I would like to thank L. Layton for her support and direction, O. Kutowy and J. Kurdi for their helpful discussions, G. Beland and D. Kirpalani for their expertise in LabVIEW programs, A. Bennett for the excellent pictures, F. Toll for his mechanical skill, and other personals in ICPET group for all their help in this particular project. I am also thankful to D. Kingston who kindly produced SEM and XPS analysis and I. Hill for the Raman studies. Furthermore, I gratefully acknowledge the support from K. Cook from the Canada Institute for Scientific and Technical Information (CISTI) for her additional help in conducting the scientific literature searches.

Lastly, but most importantly, a well appreciation and thank you goes to my parents, friends, and those who have supported this project from the beginning to the end, as this project would be impossible to completed without their support, encouragement, and love.

NOMENCLATURE

a	Mark-Houwink constant
A	active membrane surface area (m^2)
J	solvent flux ($lm^{-2}h^{-1}$)
K	Mark-Houwink constant
M	molarity (mole of solute/liter of solution)
MW	molecular weight (g/g.mole)
P	pressure (psi, kPa)
S	swelling (%)
t	time (h)
V	volume of permeate or solvents (m^3)
W	weight (gram, kilogram)

GREEK LETTERS

δ	Hildebrand solubility parameter ($(cal/cm^3)^{1/2}$)
ε	Dielectric constant
ϕ_m	Volume fraction on membrane surface
η	Viscosity ($kg\ m^{-1}\ s^{-1}$)
μm	micrometer

ABBREVIATIONS

DEGDMA	Diethylene glycol Dimethacrylate
EtOAc	Ethyl acetate

EtOH	Ethanol
F^-	Highly electronegative ion
IPA	Iso-propanol
MeOH	Methanol
MEK	Methyl ethyl ketone
MWCO	Molecular Weight Cut-off
$NaHCO_3$	Sodium bicarbonate
NaOH	Sodium hydroxide
NF	Nanofiltration
NMP	N-methylpyrrolidone
PAI	polyamide imide
PEA	Poly(ethylene adipate)
PEG	Polyethylene glycol
PR	Product rate
PVP	polyvinyl pyrrolidone
PWP	Pure Water Permeability ($lm^{-2}h^{-1}$)
RO	Reverse Osmosis
SEM	Scanning electron microscopes
TOC	Total Organic Carbon
Torlon®	Another common name of poly(amide imide)
UF	Ultrafiltration
UV	Ultraviolet
XPS	X-ray photoelectron spectroscopy

TABLE OF CONTENT

LIST OF TABLES

LIST OF FIGURES

PAGE

PAGE

LIST OF APPENDICES

PAGE

PAGE

PAGE

CHAPTER 1

INTRODUCTION

In recent years, the use of membrane-based separation and purification processes has been increasingly applied in the chemical process industry. Membrane technology is gaining increased acceptance due to its ability to overcome limitations in conventional chemical engineering process applications such as distillation, adsorption and chromatographic separations. The benefits of membrane technology include selective permeation, reduced energy consumption and non-thermal processing of sensitive compounds. These technologies are commonly applied in electrochemical, paper and pulp, petrochemical, pharmaceutical and fertilizer industry for treatment of industrial waste effluents and hazardous solvents. Membranes are also used for selective permeation for upgrading of aromatics and aliphatic substances using a wide range of processes such as pervaporation, hyperfiltration, and membrane distillation (Schäfer, 2001; Scott, 1995; Rautenbach and Albrecht, 1989). Although, a large number of commercial membranes have been developed in recent years for processing aqueous streams, there are only a limited number of membranes compatible with non-aqueous solvents. Therefore, there has been a growing need for developing solvent resistant polymers and membranes for a wide range of non-aqueous applications. Nanofiltration (NF) membranes are used in many applications with water treatment as the major application area accounting for 65% approximately followed by the food and dairy industry applications (~25%) and less than 10% for the chemical industry (Bessarabov and Twardowski, 2002)

The use of polymeric nanofiltration membranes for organic or non-aqueous solvent recovery has been suggested in recent research (Wang and Chung, 2005; Zhang *et al.*, 2005; Freger *et al.*, 2005; Geens, *et al.*, 2004; Tsui and Cheryan, 2004; Peeva *et al.*, 2004; Sheth *et al.*, 2003; Bhanushali *et al.*, 2002; Gibbins *et al.*, 2002; Yang *et al.*, 2001). Although, NF

membranes have been extensively researched by the scientific community, practical applications are scant mainly due to their limited solvent stability (Wang and Chung, 2005; Van der Bruggen *et al.*, 2002), lower rejection of solutes in comparison to that obtained with their aqueous counterparts (Nwuha, 2000), low solvent fluxes at high solute concentrations (Whu *et al.*, 2000). A small number of commercial membranes in the operating range of NF membranes are available in the market at very high cost (Razdan *et al.*, 2003). Moreover, the mechanism of the separations with polymeric membranes in organic solvents is not fully understood. Van der Bruggen *et al.* (2002) reported that membrane flux and rejection rates of NF membranes in organic solvents are significantly different from that in aqueous solution. Hence, prediction of the behaviour of a membrane in an organic solvent remains difficult since the mechanism of the separations with polymeric membranes in organic solvents is still poorly understood at this stage.

In order to address the above challenges, studies are currently being conducted for developing new types of NF membranes and also for outlining improved characterization methods by studying the transport behaviour of solvents in them. A majority of the current research is focused on the separation of particular solvents or solute systems rather than the development of experimental methods designed to understand the influence of NF membrane transport fundamentals. Yaroshchuk (2004) concentrated on the modeling of the membrane potential in attempt to explain some qualitative observations that are not well-represented by conventional models. The empirical results reported in this study were inconsistent with estimated values of solute coefficient and solute permeability and were generally lower than the theoretical estimates. This can be explained by the fact that salt rejection increases essentially slower than it could be expected from the Donnan (electrical)

exclusion model through a constant fixed charge density as the feed concentration decreases. Ali *et al.* (2005) used the Donnan predictive model (DPM) to develop general criteria for selection of optimum NF membranes and also to analyze the effect of various NF membrane characteristics on NF membrane economics. It was found that up to 30% of the capital and operating costs in recovering sodium sulphate solution can be saved by using looser membrane compared to the tight membrane structure. Meanwhile, Vankelecom *et al.* (2004) theorized a physico-chemical interpretation of transport mechanisms of the solvent resistant NF membranes. The study revealed that convective flow played a role in membrane transport and top-layer compaction, in spite of being dense, was found to be present. It was also showed that solvent transport for a given membrane, whether it was situated more towards pure convective flow or towards solution-diffusion, would depend on conditions of top-layer swelling, solvent viscosity, support layer porosity, applied pressure, compaction, and top-layer thickness. Other recent research focuses on obtaining improved NF membranes by the development of new pore-filled NF membranes (Zhou *et al.*, 2005), ceramic NF membranes (Guizard et al., 2002), and by the use of negatively and positively charged composite NF membranes (Wu *et al.*, 2005; Du and Zhao, 2004; Mohammad *et al.*, 2004; Jones, 2003).

A brief review of earlier reported studies outlined above shows that NF membranes must maintain the ability to separate desired components while operating in non-aqueous organic solvents. Polymers selected for solvent resistant applications should be rigid and crystalline, thermally stable, resistant to compaction, inert to solvents with no swelling, and stable for longer term usage. Razdan *et al.* (2003) reported that polymers with certain groups like imide as the backbone with rigid segments that impart solvent resistance

properties and fabricated by co-polymerization appear to be suitable. They also pointed out that this membrane type can be produced from modified silicone rubber, methacrylates, polyimide polyurethane, polyimide, poly(amide imide), polyimide aliphatic polyester copolymers, poly(acrylonitrile)-based, liquid crystalline-based, poly(phosphazene), graft or block polymers, inorganic and cross linked polymers.

Based on the literature criterion discussed above, the polymer materials chosen in this work is poly(amide imide) and Chitosan. Aromatic poly(amide imide) is a high performance condensation polymer which brings together both advanced mechanical properties typically associated with polyamides and high thermal stability which also have solvent resistance properties. In addition to its well established use for magnetic wire coatings in under-the-hood automotive applications (Ranade *et al.*, 2002), this polymer has been used for making ultrafiltration membranes (Blume *et al.*, 1992; Ebert *et al.*, 2004), blended membranes (Yoshikawa *et al.*, 2004; Bershtein *et al.*, 2002; Kanapitsas *et al.*, 2002; Šindelář *et al.*, 2001), and composite membranes (Rami Reddy, 2000; Hu and Marand, 1999; Chern and Wu, 1997; Fritsch and Peinemann, 1995). These studies have primarily focused on pervaporation and gas separation membranes since the membranes could achieve high gas permeability and had permselectivity characteristic of polyimides (Hu *et al.*, 1997). Chitosan is a natural hydrophilic biopolymer which has been used as a membrane material for reverse osmosis, pervaporation, gas separation membranes, and composite nanofiltration membranes (Musale and Kumar, 2000) which also has excellent solvent resistance.

To date, there is no reported literature on Torlon®/Chitosan composite NF membranes although studies on Torlon® cross linked with poly(ethylene adipate) for separation of organic vapour and permanent gases are reported by Šindelář *et al.* (2001).

The main objectives of this thesis are formation and characterization of new asymmetric membrane to increase the permeation flux, selectivity, and solvent stability. A thin nonporous selective polymer layer coated onto a porous support membrane is desired. The composite NF membranes comprising poly(amide imide) (Torlon®) as the base support layer and Chitosan as the active membrane layer coated on Torlon® layer. The characterization study involves the development of an understanding of the effects of surface cross linking on the composite membranes resistance with industrially important solvents such as alcohols, ketones, esters, and aliaphatic hydrocarbons. Lack of published literature on the subject of Torlon® as a liquid separation and composite membranes provides a motivating challenge. For instance, determination of a suitable cross linking agent for in-situ reaction that is compatible with both Torlon® and Chitosan, altering the pore size distribution of polymeric materials to obtain membranes cut-off in the NF range, and development of fabrication technique for making such membranes.

In this work, the phase inversion method was used to form a support base membrane layer while Chitosan was coated by in-situ surface reaction on the skin layer with suitable cross linking solution. Polyethylene adipate (PEA) and diethylene glycol dimethacrylate (DEGDMA) were used for cross linking agent so that the coating layer would adhere on to the base surface layer. Two different neutralization solutions, aqueous sodium hydroxide and sodium bicarbonate, were also used in the experiment conducted for this thesis. The main purpose for this neutralization step was to convert Chitosan acetate composite layer to Chitosan during the fabrication process. Potential parameters in membrane formation process were altered to achieve optimum membrane performances. For example, duration of membrane curing process, switching the cross linking and neutralization stages, and

viscosity changes of Chitosan solution by dilution. This thesis primarily focused on the formation process of coating layer onto selected base membrane. The effect of cross linking parameters, specifically poly(ethylene adipate) and di(ethylene glycol) dimethacrylate concentration and cross linking time on solute flux, molecular weight cut-off, and pure water permeation were examined. In addition, effects of surface cross linking of the Torlon®/Chitosan composite membranes on their resistance to pH and commonly used solvents were investigated. Furthermore, swelling and the permeation characteristics including solvent flux of these membranes with selected solvents were also studied.

CHAPTER 2

MEMBRANE PREPARATION

Membrane separation processes involve relative transport of molecules across a film or other physical barrier. This separation technology is increasingly being utilized in the chemicals industry for a wide range of applications. The key drivers for this technology include consumer demand for higher quality and value-added products, increased regulatory requirements, deteriorating natural resources, and also the need for environmental as well as economic sustainability. Furthermore, the need for efficient water treatment processes also encourages constant research and development of reverse osmosis (RO) and NF membrane technologies. In Figure 2.1, an overview of the sizes of solutes as well as particles of interest is presented.[1]

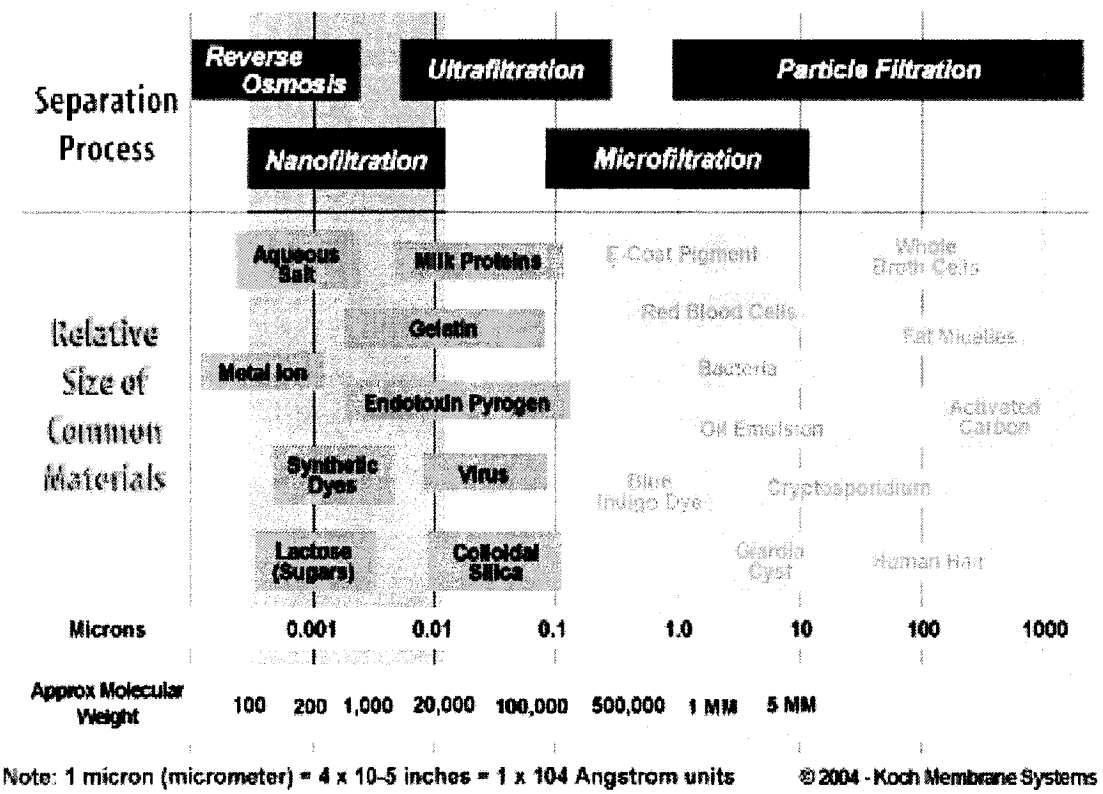

Figure 2.1 – Overview of solutes sizes and particle dimensions in membrane separation process (www.kochmembrane.com)

[1] 1 Dalton ≅ 1.66×10^{-24} gram

Although membrane separation technology has grown tremendously in processing aqueous feed, further research and development are still required for developing membranes for non-aqueous solvents. The goal of researchers has been to evaluate a range of polymer materials to make solvent resistance composite NF membranes for contributions to new membrane separation processes. The selection and design of membrane systems is highly dependent on the selection of appropriate membrane materials and fabrication procedures. The purpose of this chapter is to provide a literature background of materials and methods used in the fabrication and testing of composite membrane separation made from Torlon® and Chitosan.

2.1 Membrane materials

The most important membrane characteristics include high selectivity, high permeability and good mechanical, thermal, and chemical stabilities. These requirements limit the choice of materials considering that membranes have to be hydrophilic to reduce the adsorption of organics. Previous work conducted by Lainé *et al.* (1989) reported that the most important membrane characteristic is indeed hydrophilicity. The first membrane materials used in separation technology was cellulose acetate; however over the years several new materials have been studied and evaluated. Technically relevant membranes, their structure, and their areas of application are summarized by Strathmann in Li and Calo's separation book (1992), with supporting data from Rautenbach and Albrecht (1989). A comprehensive list is presented in Table 2.1.

Table 2.1 – Membrane classifications according to structure, production, essential transport mechanism, and area of application

Membranes	Basic materials	Manufacturing procedures	Structures	Applications
Ceramic membranes	Clay, silicate, aluminium-oxide, graphite, metal powder	Pressing and sintering of fine powders	Pores of 0.1-10μm diameter	Filtering of suspensions, gas separations, separations of isotopes
Stretched membranes	Polytetrafluotoethylene, polyethylene, polypropylene	Stretching of partially crystalline foil perpendicular to the orientation of crystallyts	Pores of 0.1-1μm diameter	Filtration of aggressive media, cleaning of air, sterile filtration, medical technology
Etched polymer films	Polycarbonate	Radiation of a foil and subsequent acid etching	Pores of 0.5-10μm diameter	Analytical and medical chemistry, sterile filtration
Homogeneous membranes	Silicone rubber, hydrophobic liquids	Extruding of homogeneous foils, formation of liquid films	Homogeneous phase, support possible	Gas separations, carrier-mediated transport
Symmetric microporous membranes	Cellulose derivatives, polyamide, polypropylene	Phase inversion reaction	Pores of 50-5000nm diameter	Sterile filtration, dialysis, membrane distillation
Integral asymmetric membranes	Cellulose derivatives, polyamide, polysulfone, etc.	Phase inversion reaction	Homogeneous polymer or pores of 1-10nm diameter	Ultrafiltration, hyperfiltration, gas separations, pervaporation
Composite asymmetric membranes	Cellulose derivatives, polyamide, polysulfone, polydimethylsiloxane	Application of a film to a microporous membrane	Homogeneous polymer or pores of 1-5nm diameter	Ultrafiltration, hyperfiltration, gas separations, pervaporation
Ion exchange membranes	Polyethylene, polysulfone polyvinylchloride, etc.	Foils from ion exchange resins or sulfonation of homogeneous polymers	Matrix with positive or negative charges	Electrodialysis, electrolysis

Rautenbach and Albrecht also provide manufacturing compounds regarding several important membranes (shown in Table 2.2) which was further confirmed by Johns (2000) and Scott (1995).

Table 2.2 – Membrane materials

Modifed natural products : cellulose based	Cellulose acetate (cellulose-2-acetate, cellulose-2,5-diacetate, cellulose-3-acetate), cellulose acetobutyrate, cellulose regenerate, cellulose nitrate
Synthetic products	Polyamide (aromatic polyamide, copolyamide, polyamide hydrazide), polybenzimidazole, polysulphone, vynil polymers, polyfuran, polycarbonate, polyethylene, polypropylene, poly vynil alcohol, polyacrilonitrile, polyether sulphone, polyolefins, polyhydantoin, (cyclic polyurea)
Miscellaneous	Polyelectrolyte complex, porous glass, graphite oxide, ZrO_2-polyacrylic acid, ZrO_2-carbon, oils, Al_2O_3

This study focuses on polyamide imide, commonly known as Torlon®, and Chitosan as membrane materials. Torlon® a high molecular weight polymer is acknowledged to have excellent resistance to chemicals including organic solvents and demonstrate very high thermal stability. Chitosan is a polysaccharide that offers a highly hydrophilic surface for membranes which gives high permeation rates of water soluble drugs and small solutes. Since the objective of this project is to prepare solvent resistance composite membrane, asymmetric membranes are formed using these two substances. Torlon® was cast on a polyester support to form a base membrane layer, whereas Chitosan was coated on Torlon® membrane surface to provide a thin active membrane layer with smaller membrane pore size.

2.1.1 Poly(amide imide), Torlon®

Poly(amide imide) resin, Torlon®, were first introduced by Amoco Chemicals in the early of 1970s and it has been commercially available in the market (Mark *et al.*, 1985). Detailed information regarding aromatic poly(amide imide) preparation is explained by Unishi (1965). And Tan (1999) has also clearly pointed out in Polymer Data Handbook that Torlon® can be prepared by various methods described below:

1. Two-step polycondensation of trimellitic anhydride and aromatic amines,
2. Low temperature polymerization of trimellitic anhydride-based diacid chlorides and aromatic amines,
3. Polycondensation or trimellitic anhydride or dicarboxylic acids derived from trimellitic anhydride with aromatic diisocyanates, and
4. Direct polycondensation of dicarboxylic acids derived from trimellitic anhydride and aromatic amines via Yamazaki-Higashi reaction.

Aside from their excellent resistance to creep, wear, chemical, and wide range of uses in industry, the exact structure of Torlon® is still not commonly known. Robertson *et al.* (2004) recently reported structural determination of a specific Torlon®, namely 4000T poly(amide imide), the polymer used in this work, by nuclear magnetic resonance spectroscopy. This earlier work showed that commercial 4000T poly(amide imide) could be synthesized by trimellitic anhydride chloride, oxydianiline and phenylenedianiline monomers. This work also explained that the sequence of appearance of the polymer's amide and imide functional groups followed certain distribution due to dual reactive sites, acid chloride and anhydride, of the monomer trimellitic anhydride chloride. General

structure for Torlon® 4000T poly(amide imide) can be seen in Figure 2.2 below (Robertson *et al.*, 2004).

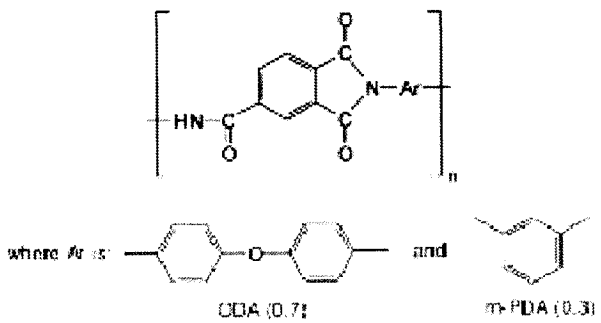

Figure 2.2 – General structure of Torlon® 4000T poly(amide imide)

2.1.2 Chitosan

The structure of Chitosan, illustrated in Figure 2.3, is a polysaccharide based biopolymer and is the deacetylated derivative of chitin. Chitin is a natural water insoluble biopolymer present in insect exoskeletons, outer shells of crabs, shrimps, lobster, krill, and fungal cell walls.

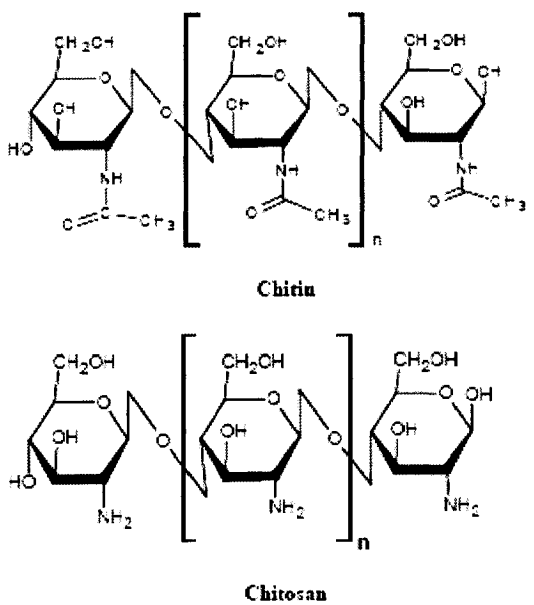

Figure 2.3 – Structure of chitin and Chitosan (Rohindra *et al.*, 2004)

2.2 Asymmetric membranes

A homogeneous or uniform membrane structure is known as symmetric membranes. The simplest example of this symmetric membrane is microporous membrane which is primarily used in filtration but can also be used in pertraction and liquid membranes. Such fabrication usually includes materials like ceramics, metals, carbon, and polymers (Scott, 1995). On the other hand, the membrane structure used in this study is known as an asymmetric membrane that is formed with a non uniform structure comprising of an active top layer supported by a porous support or sub layer. Furthermore, Scott pointed out that asymmetric membranes can be produced either by phase inversion from single polymers or from composite structures. Figure 2.4 illustrates both asymmetric and symmetric membranes.

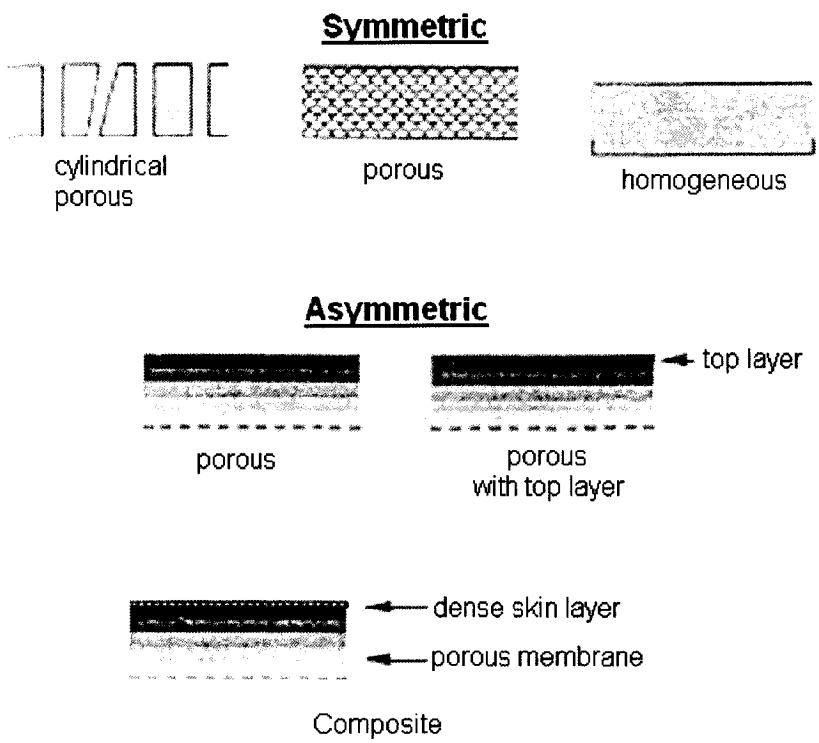

Figure 2.4 – Structure of symmetric and asymmetric membranes (Scott, 1995)

Membranes with high selectivity and high permeability can be obtained by forming a very thin top layer. According to Watson (1998), some practical limits such as minimum thickness of the membrane need to be considered to ensure membrane effectiveness. Watson generalized that the primary practical limitation is the need to maintain sufficient mechanical strength and avoid tears, holes, and other damage during use and handling. In order to decrease the thickness of membranes without extensive loss in mechanical strength, membrane can be fabricated on a denser substrate. The substrate can be strong and relatively thick but highly porous since no separation performance is required from it. The selectivity of the membrane is provided from the thin layer film of active membrane only. This type of membrane can be formed by combining a thin layer of active membrane on a pre-formed porous structure consisting of the same polymer as the porous structure or an alternate material.

2.2.1 Phase inversion membranes

All membranes used in this study were prepared by the phase inversion technique. Phase inversion is the process of forming a single continuous phase by inverting the polymer matrix into a swollen three-dimensional macromolecular complex or gel. Conventionally, porous membranes are produced from two component dope mixture containing polymer and a suitable solvent which is also identified as casting solution (Scott, 1995; Tweddle and Striez, 1994; Rautenbach and Albrecht, 1989; Tremblay, 1989; Sourirajan and Matsuura, 1985). The concept of this phase inversion method is extensively described in the above-mentioned references. Casting solution is spread onto a suitable support using a casting bar, a metal bar with a fixed thickness slot for controlling the membrane thickness. The support

can be a glass plate or the membrane backing material such as non-woven polyester. The cast film is then transferred to a non solvent (normally water) or gelation bath. On immersion in the bath, the polymer present at the gelation bath – the solvent interface immediately precipitates while the solvent is leached out of the polymer solution. The solvent exchanged with the gelling agent by force of diffusion process. Thus the exchanged continues until all of the solvent in the polymer solution leaves the cast layer and a solid structure of porous polymer matrix is formed. Scott (1995) also reported that the microstructure of the membrane from this phase inversion method is determined in the gelation stage. The gelation process is also influenced by the properties of the film, which is formed after precipitation has occurred at the surface of the membrane that was exposed to the air. He observed that finger-like voids in the membrane matrixes were formed by the occurrence of rapid polymer precipitation, i.e. where solvents with little affinity for the polymer are used or where the gelation bath has a high salinity.

2.2.2 Composite membranes

Composite membranes are generally known as an improvement over phase inversion membranes. The membranes are formed onto a porous, compaction-resistant, or a support layer which is usually ultrafiltration (UF) membrane that gives most of the desired properties of a support layer. Generally, the advantage of the composite membrane is that each layer can be chosen independently to give an optimum performance of permeation, selectivity, and stability for a particular purpose. The critical stage in composite membranes formation is the formation of the ultra thin active skin layer. As the skin formed is very thin, it is very fragile and requires further processing for handling and use in applications. One of

several methods available to make the layer stronger is by in-situ surface reaction on the skin layer with suitable cross linking solution. Thus the thin active skin layer is bonded chemically to the support film and the physical stability is improved.

Several parameters such as the casting solution composition, cross linking time and concentration, and evaporation time affect the resulting composite membrane. The effect of these factors on the formation of Torlon®/Chitosan composite membranes was studied in this work. Flux and rejection properties of the composite membrane when exposed to aqueous alcohol along with other selected solutes have also been described in this work.

CHAPTER 3

MATERIALS AND METHODS

3.1 Materials

Amorphous poly(amide imide) (Torlon®, grade 4000T-40) in powder form was procured from BP Amoco Chemicals Polymer Inc., USA (now known as Solvay Advanced Polymer). Chitosan crab shells, poly(ethylene adipate), and di(ethylene glycol) dimethacrylate were procured from Aldrich Chemical Co. Inc., USA. Anhydrous N-Methyl-2-Pyrrolidone (NMP) and polyethylene glycols (PEG) of different molecular weights were procured from Anachemia, Canada and Fluka, USA respectively.

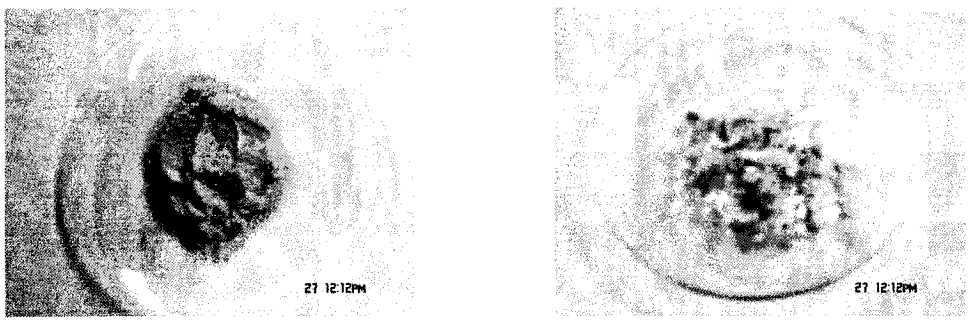

Figure 3.1 – Illustration of Torlon® powder (a) and Chitosan flake (b) used in experiments

Methanol (MeOH), ethyl acetate (EtOAc), and hexane were obtained from EMD Chemicals Inc., USA, while iso-propanol (IPA) and methyl ethyl ketone (MEK) were obtained from Fisher Scientific Limited, Canada. Anhydrous ethanol (EtOH) was supplied by Commercial Alcohols Inc., Canada. All solvents were used as received. Reverse osmosis ice water with a conductivity of 5×10^{-4} S m^{-1} was used for the gelation media and other purposes throughout the conducted experiments.

3.2 Pretreatment of Chitosan

Chitosan was purified using the same method described by Musale *et al.* (1999). This method involved dissolving Chitosan in 2% w/w aqueous acetic acid and precipitating in 4% w/w aqueous sodium hydroxide. The authors determined the molecular weight of Chitosan as 1.16 x 10^5 Da using Mark-Houwink-Sakurda equation ($[\eta] = K M^a$) where intrinsic viscosity $[\eta]$ measured in a buffer solvent system (0.3 M acetic acid and 0.2 M sodium acetate) at 25 °C and Mark-Houwink constants (K = 7.4 x 10^{-4} dl g^{-1} and a = 0.76). The constant K and a, were literature values obtained from the double logarithmic plot of intrinsic viscosity versus molecular weight if polymer and are functions of solvent and polymer types. Above method and molecular weight value were adopted for this experiment.

3.3 Preparation of base membranes casting solution

Torlon® poly(amide imide) polymer was dried overnight in the glove box at 21 °C with relative humidity of 9.3%. Two polymer solutions with different concentration, 25% and 20% (w/w), were prepared by dissolving Torlon® powder in NMP solvent (labeled as Torlon® 25-0 and Torlon® 20-0 where zero signifies the absence of co-polymer or additive). In order to ensure that the solutions were prepared in a clean and dry environment, casting was conducted in a glove box using the following steps:

- Two glass bottles of 400 ml. were weighed on an analytical balance with a least count of ± 0.001 gram.
- For each solution, the desired quantity of NMP was placed into the bottle before the addition of Torlon® using a spatula. Bottles were shaken gently

during this step to avoid the formation of encapsulated sphere, which would prolong dissolution process in the viscous solution.

- The bottles were then labeled and the lids were securely held in place using electrical tapes to avoid leakage and moisture.
- The solutions were then rolled with variable speed for at least three days for complete dissolution of Torlon® in the NMP solvent.
- Both Torlon® 25-0 and Torlon® 20-0 solutions were set aside for 24 hours to eliminate any air bubbles that may have formed on the surface or were trapped in the solutions during the rolling process.

3.4 Phase inversion of base membranes (Torlon®)

Non-woven porous polyester supplied by Ahlstrom Filtration Corp., USA, under the trade name of Hollytex 3329, was used as backing material or support layer in base membrane formation. It was cut to fit the clean glass plates, which were used for the casting purposes and have been left at room temperature prior to use.

The base membranes, using both Torlon® 25-0 and Torlon® 20-0 solutions, were prepared by performing phase inversion on the backing material within the 12 to 15 seconds of casting the film. The relative humidity and temperature of the casting environment were 15.9% and 17.9 °C, respectively. The conditions of precipitation or gelation water bath used in this experiment method were measured at 6.7 °C with thermal conductivity of 23.3 μS.

The phase inversion process for the Torlon® base membranes production is described as follows:

1. The glass plate and casting bar with a gap of 450 μm were cleaned with distilled RO water and dried completely with lint free paper towels.
2. The plate was placed on the table and leveled to be horizontal.
3. Backing material was attached on the plate and taped accordingly that the material will remain stationary and smooth on top of the plate.
4. The polymer solution was then poured evenly onto the prepared plate in front of the casting bar at room temperature in order to form a thin film layer.
5. The casting bar with the appropriate thickness slot traverses over the polymer solution along the length of the glass plate at a constant speed and pressure to spread the solution evenly resulting in the formation of a film of uniform thickness. This procedure is illustrated in Figure 3.2 below.

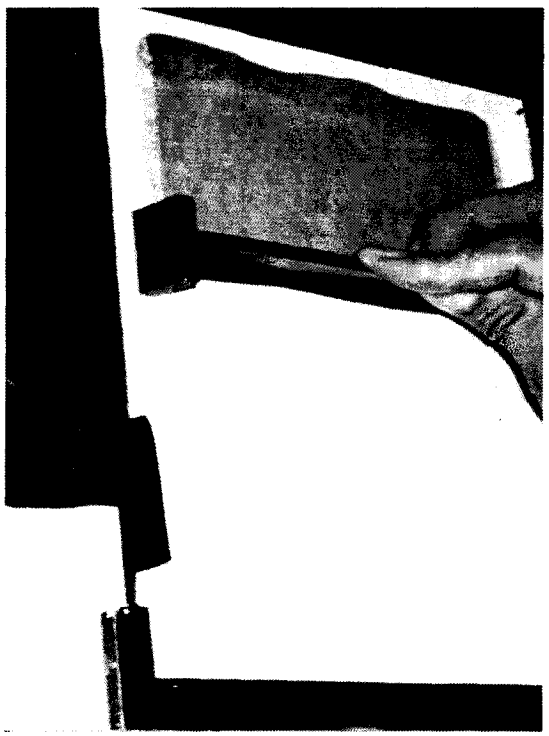

Figure 3.2 – Illustration of hand casting on the glass plate procedure

6. The polymer films were then immersed in a smooth and even manner in a precipitation bath that had been prepared earlier. As mentioned previously, solvent exchange will lead to precipitation and gel formation at this stage.
7. The nascent films or membranes were left in the gelatin water for approximately 30 minutes before they were immersed into fresh RO water at room temperature and stored overnight in a clean container.
8. Finally, membrane films were cut into 6.6 cm in diameter coupons for further test and characterization.

Unfortunately, Torlon® 25-0 membranes did not provide a desired molecular weight cut-off or permeation rates. During pore size measurement experiments using automated UF test system, Torlon® 25-0 membrane coupons did not provide any product rate or flux at a pressure of 344.74 kPa or at 689.48 kPa. Hence, it was concluded that desired membrane pore size in UF range could not be formed using 25% w/w Torlon® in NMP and subsequent experiments were conducted only with Torlon® 20-0 membranes. It was estimated that 20% w/w Torlon® in NMP would give a suitable porous membrane in UF range and after additional coating with Chitosan, the membrane porous would reduce to NF range.

3.5 Surface cross linked Torlon®/Chitosan composite membranes

Two set of experiments were performed in order to validate alternate novel concepts for preparing the membranes. The first set of experiments explored the preparation of composite membranes. While the second set was used to study the effects of cross linking time and concentrations on the performance of composite membranes. Torlon®/Chitosan composite membranes were made by coating Chitosan solution on the surface of the Torlon®

base membranes. Degassed and purified Chitosan was diluted in salt buffer (0.3 M acetic acid and 0.2 M sodium acetate) while a concentration 2.5% (w/w) was maintained. This viscous solution was filtered through permeate carrier using pressure valve that was connected to nitrogen cylinder to eradicate remaining dirt and undissolved Chitosan chunk. One factor considered in first category is choosing all possible solvent that could be used to improve viscosity of the coating solution. Subsequently, Chitosan solution was diluted further to 36% w/w in MeOH, EtOH, IPA, MEK, and acetone. Both EtOH and IPA showed potentially interesting results by forming a clear and relatively less viscous coating solution compared to Chitosan solution itself. Other solvents formed translucent pasty gels like solution which were not suitable for coating.

Chitosan solution, diluted by EtOH and IPA, was transferred onto Torlon® base membrane surface by a hypodermic syringe which was filled with the coating solution. The content of the syringe was extruded as a bead, counting twenty beads for each membrane coupons, approximately one centimeter from the membrane surface. The bead of coating solution was then spread evenly across the surface using a fine paint brush (illustration shown in Figure 3.3). This method left a thin layer of coating solution on the base membrane surface that was previously flattened on a glass plate with electrical tape. In an alternate procedure 2.5% w/w Chitosan solution was coated on base membrane surface by a finely polished glass rod. Regardless of the method of coating, the membranes were placed in a forced air convection oven and held at a set temperature of 50 °C, for a given period of time. Air was fed to the oven in order to limit the accumulation of solvent in the oven and permit a constant supply of fresh air to the surface of the coated membrane coupons during the evaporation or curing step.

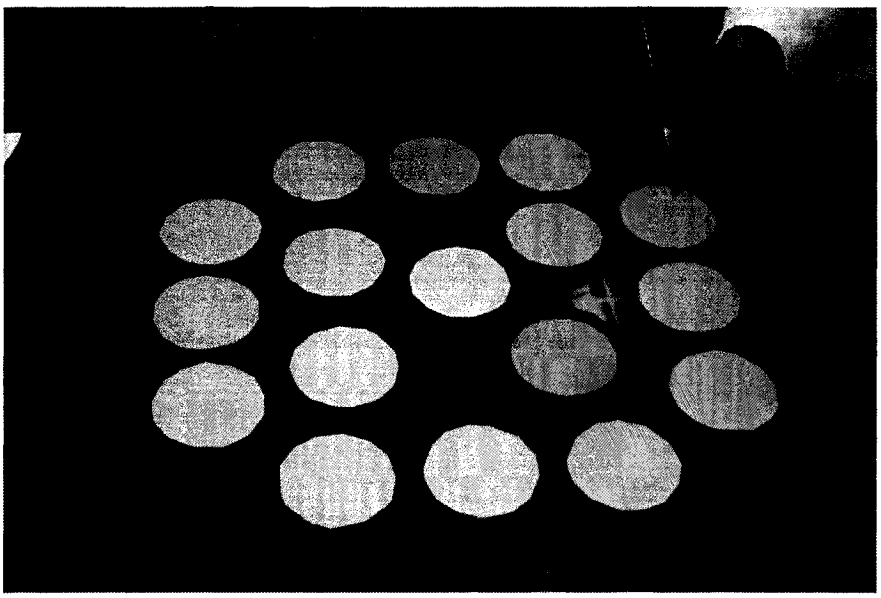

Figure 3.3 – Illustration of composite membrane thin film coating procedure

The first set of experiments also included two different solutions i.e. aqueous sodium hydroxide and aqueous sodium bicarbonate, which were used in neutralization step. The purpose was to figure out which of the solutions would provide better performance in neutralizing acid compound used in Chitosan buffer without damaging membrane matrix. Consequently this experiment also employed poly(ethylene adipate) (PEA) and di(ethylene glycol) dimethacrylate (DEGDMA) as two different cross linking agents. A comprehensive step by step procedure is shown in process flow diagrams illustrated in Figure(s) 3.4, 3.5 and 3.6 respectively.

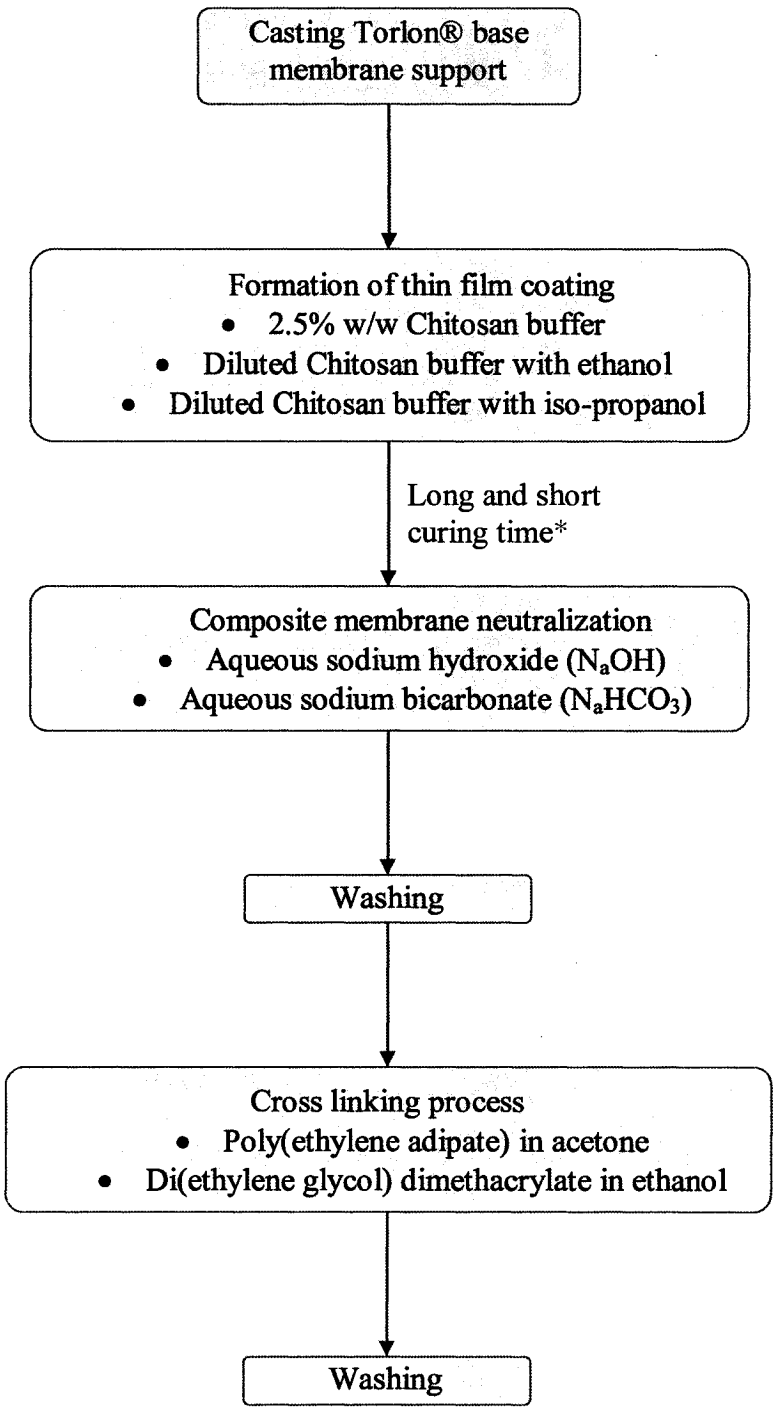

Figure 3.4 – Surface cross linked Torlon®/Chitosan composite membranes procedure

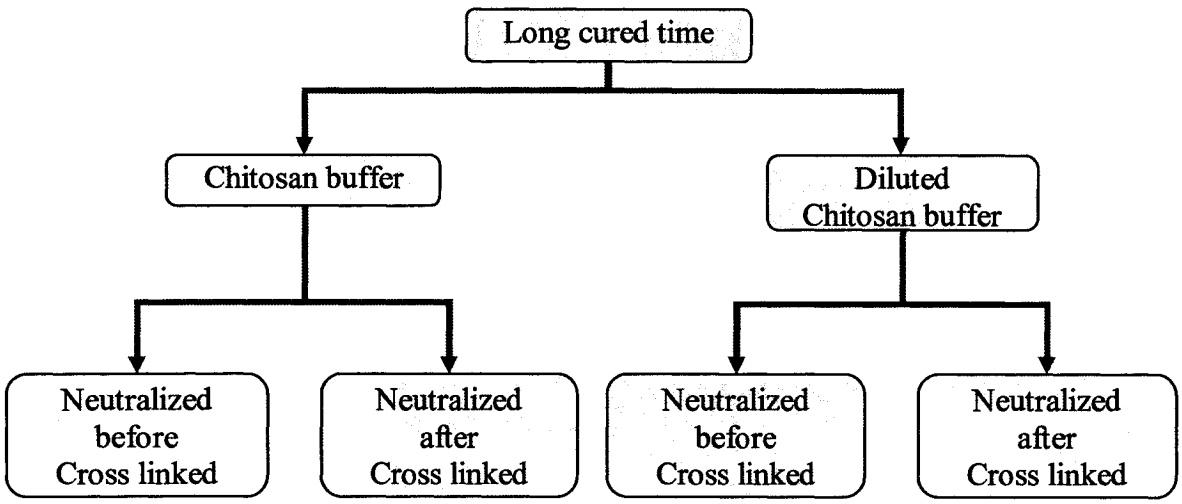

Figure 3.5 – Torlon®/Chitosan composite NF membranes procedure based on long curing period (6 days in convection oven)

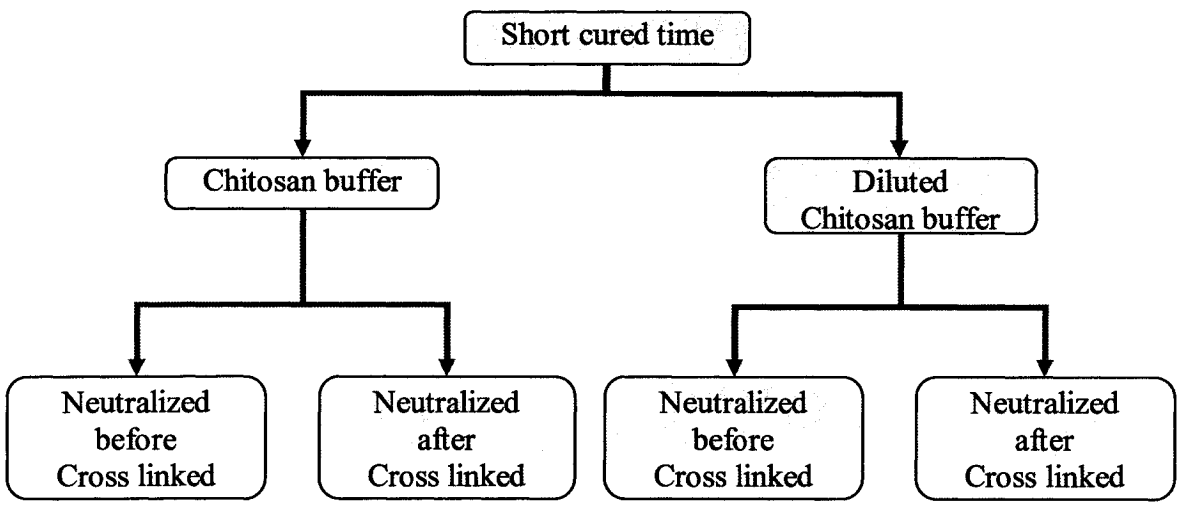

Figure 3.6 – Torlon®/Chitosan composite NF membranes procedure based on short curing period (24 hours in convection oven)

The cross linking concentrations and times studied for PEA and DEGDMA in the second set of experiments are listed in Table 3.1. The membrane procedure described above was used in all subsequent experiments. After cross linking, composite membranes were washed several times and immersed under water for 24 hours before they were tested for PEG separation and permeation.

Table 3.1 – Compositions of cross linking agents and cross linking period used to produce composite membranes

Cross linking time (hours)	Cross linking concentration, % (w/v)				
0.5	0.2	1	3	5	10
1	0.2	1	3	5	10
4	0.2	1	3	5	10
9	0.2	1	3	5	10
17	0.2	1	3	5	10
24	0.2	1	3	5	10

3.6 Membrane testing and characterization

Molecular weight cut-off (MWCO) and pure water permeation (PWP) measurements were used to characterize composite membranes that were prepared earlier. Torlon® 20-0 base membranes, which were presumably UF membranes, were tested using an automatic UF membrane test apparatus. All other composite membranes were tested using a conventional or manual membrane system.

3.6.1 Automatic ultrafiltration (UF) system

The details of this particular automated system have been described by other authors (Dal-Cin *et al.*, 2005; Daligaux, 1999; Tremblay, 1989) and a photograph of system can be seen below. The test system consisted of two banks of parallel test cells and each bank was assembled with six test cells that were connected in series. The temperature of the feed solution was set to be at 25 °C and the system was operated at proposed inlet pressure of 344.74 kPa.

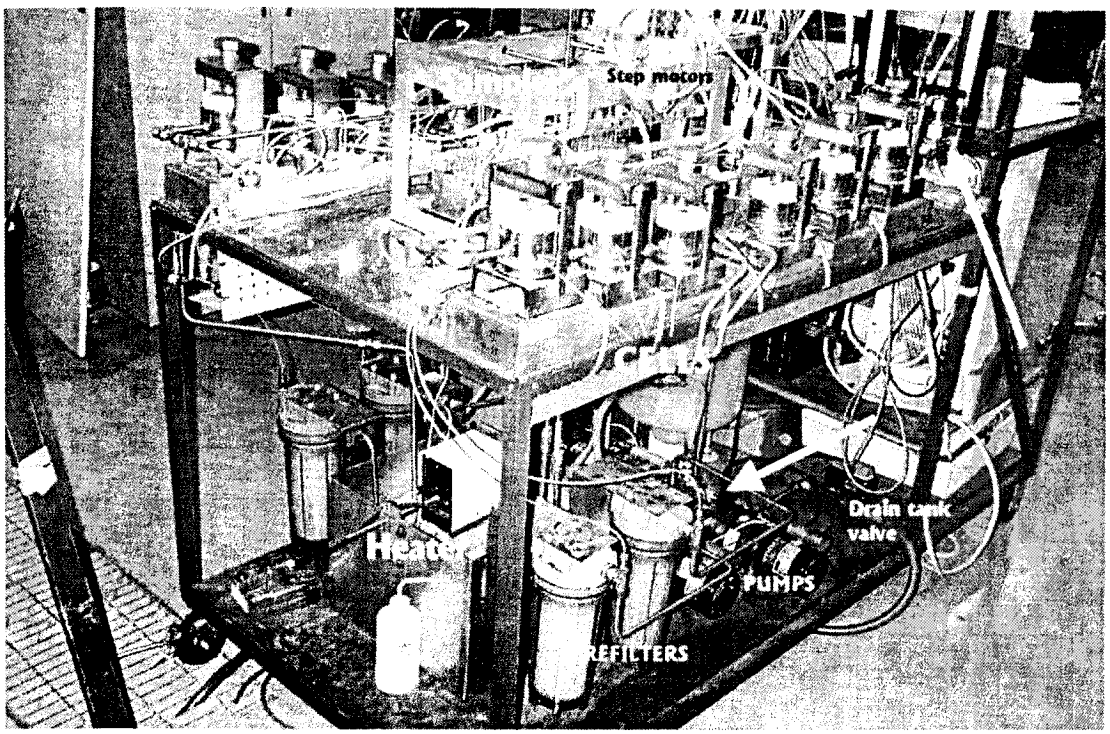

Figure 3.7 – Sample image of the automatic UF system

The experiment started by pressurizing the membranes in the test cells for five hours before readings were taken using LabVIEW program. The program would start by doing a valve checked, draining feed tank, rinsing tank, and purging four times before taking PWP

samples followed by PEG solute samples. This experiment used permeation of 200 ppm dilute solutions of PEG with various molecular weights (200, 3k, 12k, 17.5 k, and 20k Daltons) to evaluate the membrane's MWCO or pore size. The program was also designed to keep track of all data produced by the automated systems (such as PWP and product rate of PEG solutes) and transferred them into a file which can be processed by Excel. A Shimadzu 5000 Total Organic Carbon (TOC) analyzer was used to determine the concentration of permeate and feed samples collected for separation purposes or MWCO calculations.

3.6.2 Conventional membrane system

Photographs of the test cell used and schematic diagrams of the conventional membrane system are shown in Figures 3.8 and 3.9. Four banks of three test cells connected in parallel and linked to a pump, flow control valves, rotameters, filter, temperature bath, and feed solution reservoir. The feed reservoir was designed to hold up to ten liter solution and permeate samples were discharged to the atmosphere and simply collected in sample bottles. Since the composite membranes fabricated in this experiment fell into NF ranges, this testing system was set at pressure 689.48 kPa and temperature at 23 °C.

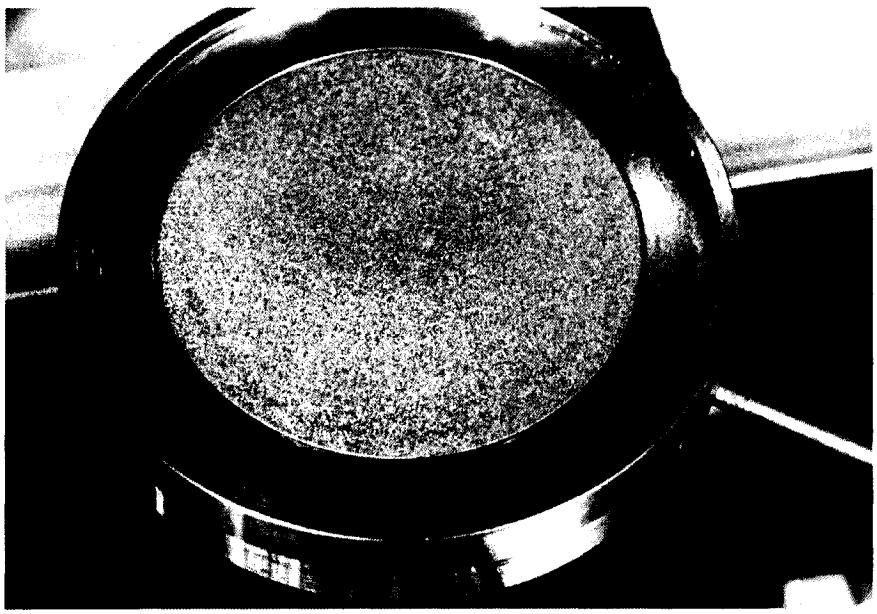

(a)

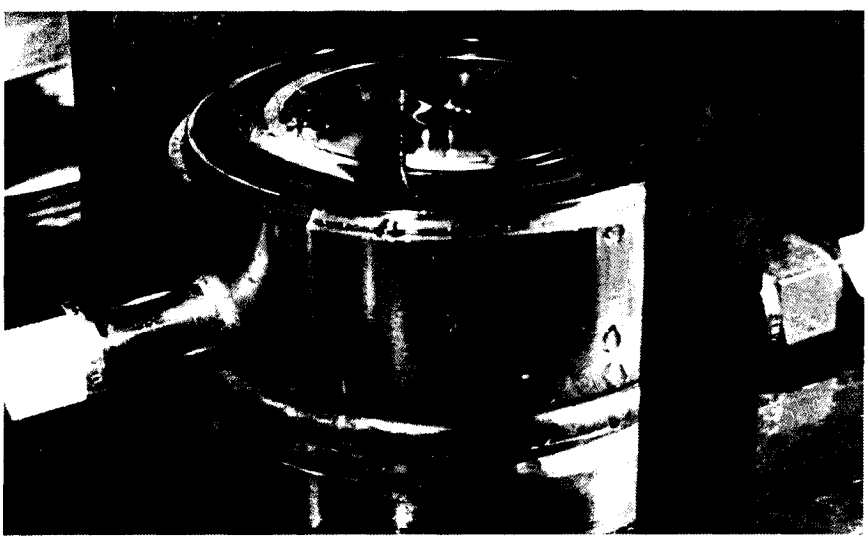

(b)

Figure 3.8 – Photograph of membrane test cell (a) top cell and (b) bottom cell (Tweddle *et al.*, 1990)

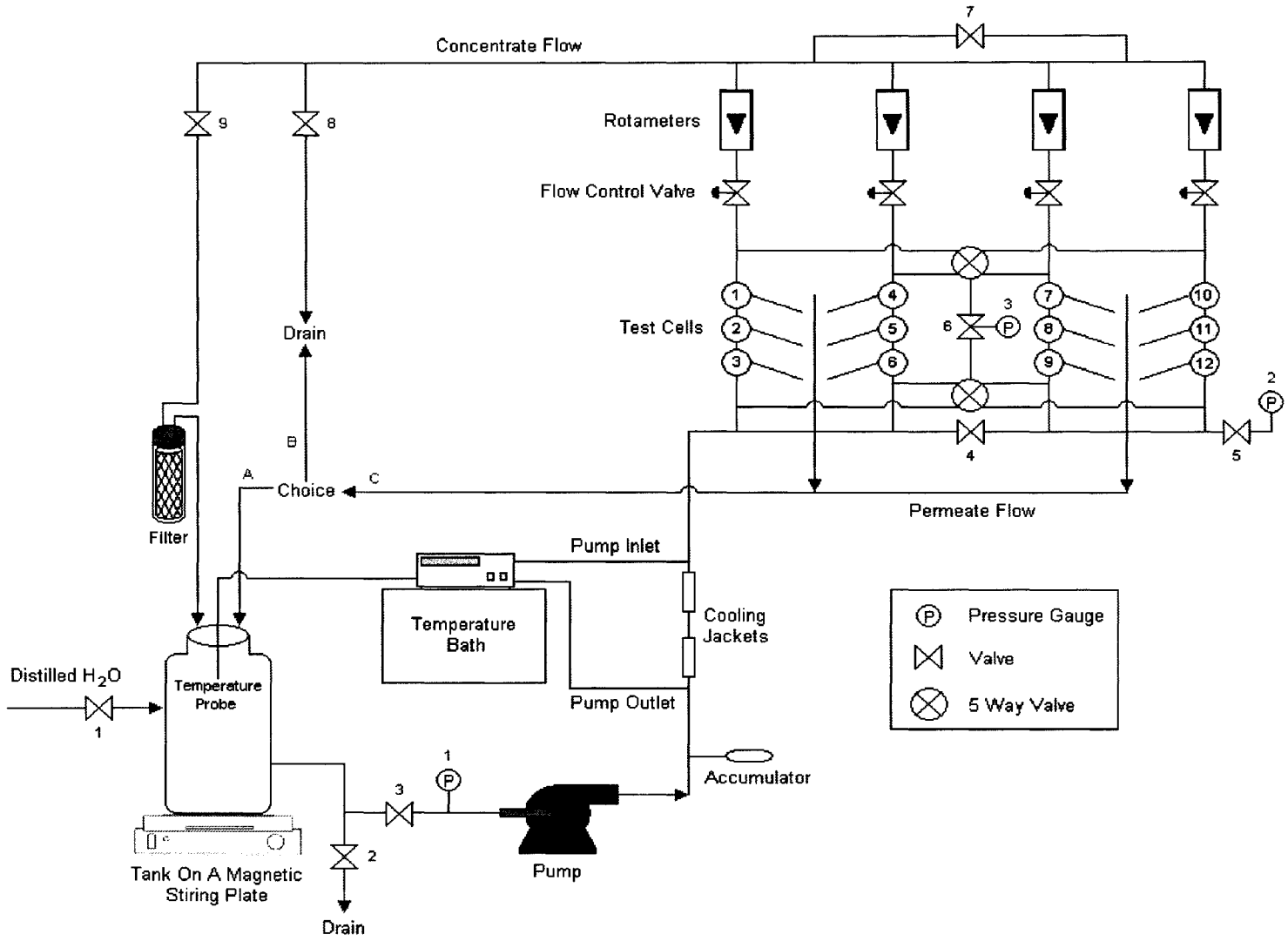

Figure 3.9 – Schematic diagram of the conventional membrane system used in this study

Distilled RO water was circulated under pressure throughout the test system for a sufficient period of time to flush out approximately 20 ml. of permeate. This ensures purging of all impurities through all the tubing and connections of the flow system (Tweddle *et al.*, 1990). During the experiments, approximately 10 ml. of permeate was collected and the mass flow rate of permeate, which is also described as PWP, was determined by the difference in weights prior to and after the experiment. Analogous to experiments conducted in the automated UF system, a 200 ppm dilute solution of PEG (feed solution) was circulated under the same operating pressure through out the system. An additional 10 ml. of permeate was also collected to determine the mass flow rate of permeate, which has been frequently described as product rate in this work and was determined by weight difference. The concentrations of both permeate and feed solutions were determined by TOC machine as described in Section 3.6.1 earlier. The above-mentioned procedure was repeated for four (4) PEG solutions with molecular weight of 200, 400, 600, and 1k Daltons. The PWP, product rate, and TOC values for all solutes were entered manually in an Excel worksheet to determine the membrane's MWCO and separation curves.

3.7 Membrane morphology and surface characterization

The physical and chemical properties of composite NF membrane utilizing Chitosan as active layer on Torlon® support was characterized by scanning electron microscopy (SEM) and X-ray photoelectron spectroscopy (XPS). In light of the large volume of literature available on characterization, a brief summary has been provided here that focuses on the specific application to membranes.

3.7.1 Scanning electron microscopy (SEM)

SEM is a microscope that employs electrons rather than light to form an image. It has a large depth of field, which allows a large amount of the sample to be in focus at one time. It also produces images of high resolution meaning that closely spaced features can be examined at a high magnification. Thus, the combination of higher magnification, larger depth of focus, and greater resolution makes the SEM a powerful technique for surface studies. In this work, SEM was carried out on gold sputtered membrane samples using Jeol JSM 5300 scanning electron microscope for as long as one minutes with 10 kV accelerating voltage. Membrane samples were prepared by soaking in anhydrous EtOH for 30 minutes followed by hexane for 30 minutes respectively before drying in convection oven at 40 °C overnight.

3.7.2 X-ray photoelectron spectroscopy (XPS)

XPS is an analytical technique based on the photoelectric affect. The X-ray photoemission is utilized to obtain information on elements and in their chemical bonds, allowing the identification of different chemical compounds on the surfaces. It can be used to study all solid samples such as glasses and polymers along with its non destructive nature, which does not change the chemical and physical properties of the sample during measurements. An additional characteristic feature of this spectroscopy is the probable function on complex materials including buried and curved interfaces, wet samples such as biological and environmental, and vacuum and radiation sensitive materials. XPS measurements were conducted using Kratos axis ultra X-ray photoelectron spectrometer equipped with a hemispherical analyzer, a DLD (delay line detector), monochromatic Al K_α

X-radiation, and charge neutralizer. Each sample for XPS experiments was mounted on a piece of conductive carbon tape. The spectrometer was operated in fixed analyzer transmission mode using electrostatic magnification. High resolution spectra were collected using an accelerating voltage of 14 kV, a current of 10 mA, 40 eV pass energy.

3.8 pH Stability

Change of PWP and PEG product rate of Torlon®/Chitosan composite NF membranes before and after the immersion in aqueous acidic and aqueous basic solutions for one hour were measured for pH stability studies. The acidic and basic pH chosen for this work were pH 3.0 and pH 11, respectively. Aqueous pH test solutions were prepared by adding 2 N HCl or 2 N NaOH in distilled RO water. Swelling (*%S*) measurements for composite membrane at pH 2.0 to 12.0 under static condition were also determined by using formulae shown below (Geens *et al.*, 2004; Li *et al.*, 2002; Musale and Kumar, 2000; Rohindra *et al.*, 2004; Nam and Lee, 1997).

$$\%S = \frac{W_w - W_d}{W_d} \cdot 100 \qquad (1)$$

Where W_w and W_d are the weights of wet and dry membrane samples, respectively. The wet weight was obtained by immersing membranes in aqueous pH solution for 24 hours at room temperature. Any excess solution was removed by blotting the membranes with tissue paper gently prior to weighing step. The dry weight were prepared by solvent exchange first in anhydrous EtOH then in hexane for length of 30 minutes each before drying in convection oven at 40 °C overnight. This procedure was also used for SEM samples mentioned before.

3.9 Static swelling for solvents

Static swelling of membranes in contact with solvents were determined by measuring the weight difference of dried membranes after 24 hours immersion in selected test solvents (alcohols i.e. MeOH, EtOH, IPA; ketones i.e. MEK; esters i.e. EtOAc; and aliphatic hydrocarbons i.e. hexane) at room temperature (23 °C) under stagnant conditions. The same drying technique stated before was used in preparing dried membranes weight. Hence, swelling (*%S*) for each solvent was calculated using Equation #1 and procedure described in Section 3.8.

3.10 Immersion studies

Immersion studies were determined by measuring the change in PWP before and after membranes were soaked in test solvents for 24 hours at room temperature of 22 °C. In the case of alcohols, the sequence of solvent immersion was 50% aqueous alcohol for 30 minutes, corresponding pure alcohol for 24 hours, 50% aqueous alcohol for 30 minutes and finally with RO water for at least 24 hours. In the case of MEK, EtOAc, and hexane; the sequence was 50% aqueous IPA for 30 minutes, MEK, EtOAc, or hexane for 24 hours, IPA for 30 minutes, 50% aqueous IPA for another 30 minutes and finally with water (Musale and Kumar, 2000). The conventional membrane system was used for these PWP measurements.

3.11 Solvent permeation

In addition to static swelling and immersion studies, solvent resistance of Torlon®/Chitosan composite NF membranes were also determined by measuring the actual

permeation rates of test solvents as a function of time. In order to avoid effects of "polymer memory" (Machado *et al.*, 1999), a different membrane sample was used in the flux measurement of each of the solvents. However, the permeation rates of MEK and EtOAc could not be completed due to incompatibility of available test cell.

Stirred UF cells model 8200 (Amicon Canada Ltd., Millipore Corporation) with 28.7 cm^2 effective membrane area was used. The cell was modified to hold approximately 180 ml. of feed solution with 63.5 mm accessible membrane diameter. The membrane was installed at the bottom of the cell which was filled with test solvent. During this work pure solvents were only tested hence the cell stirrer was removed from the cell. Compressed nitrogen gas was used to pressurize the cell and the solvent permeate flowed into a beaker which was placed onto an analytical balance. Both the high precision laboratory balance and pressure transducer were connected to a computer through a National Instruments card and LabVIEW program. Weight of permeate in the beaker and applied pressure were continuously recorded at a pre-selected sampling time interval. A schematic diagram of the apparatus is shown in Figure 3.10.

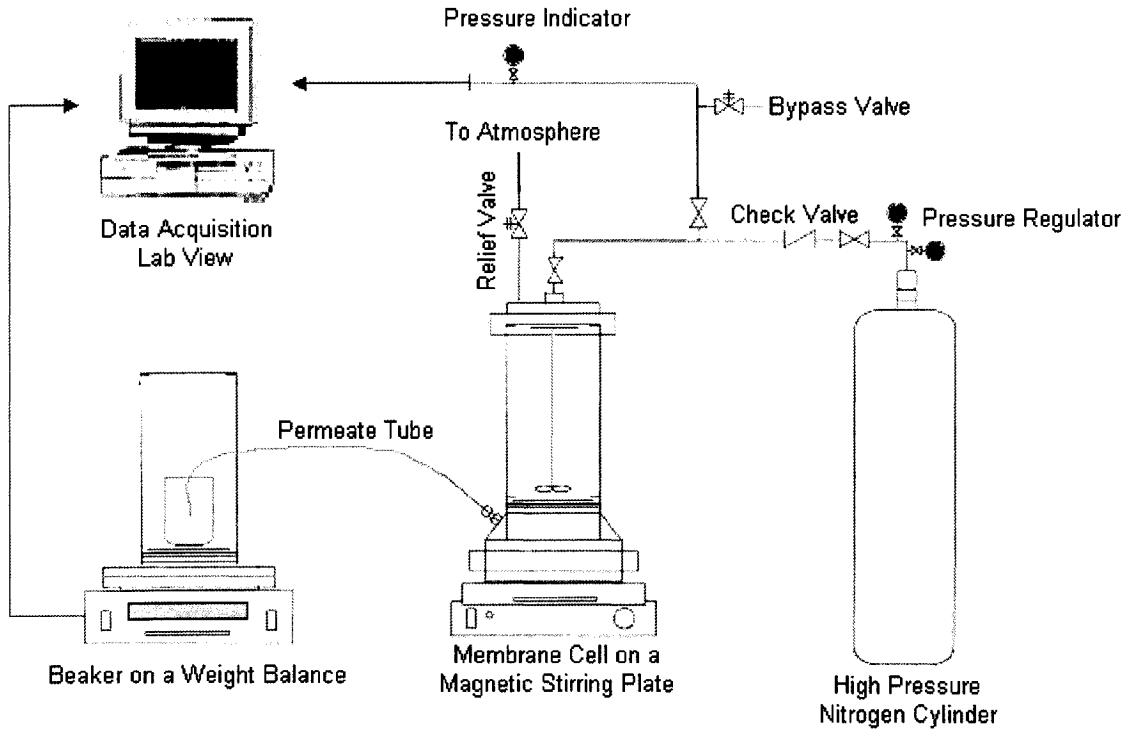

Figure 3.10 – Schematic diagram of membrane test setup for solvent permeation

To avoid damaging the pore structure of membranes due to higher difference in surface tension of water and test solvents, composite membranes were immersed in solvents with decreasing surface tension prior to testing (Musale and Kumar, 2000). For example in case of alcohol, membranes were first immersed in 50% aqueous alcohol and then twice in corresponding pure alcohol for 30 minutes in each solvent before placing the membrane in test cell. Procedures were repeated for other test solvents and all experiments were carried out at 22 °C at ambient conditions. Recorded data of permeate weight, time, and pressure applied were used to calculate solvent flux (J) which can be obtained by (Yang *et al.*, 2001)

$$J = \frac{V}{A \cdot t} \tag{2}$$

Where V is the volume of permeate, A is the active membrane are, and t as time.

CHAPTER 4

RESULTS AND DISCUSSION

4.1 Selection of base membranes

Experiments were performed by casting Torlon® 20-0 base membranes. The average molecular weight cut-off in this work is taken as the point where the separation curve reaches 90% separation for the range of solutes. The product rate is the permeation rate through the membrane when a solution is used as a replacement for pure water. Twelve membrane coupons or samples were taken randomly from the entire membrane sheets. The average pore size of the base membranes was calculated using the PEG rejection data (Figures 4.1 and 4.2). Due to mechanical limitations in the automated membrane testing system, product rate through these twelve membranes coupons could not be determined. Subsequently, the experiments were performed again with a new set of membrane coupons that were cut from the same membrane sheets to eliminate the effect of "polymer memory" or membrane damage. Figures 4.2 and 4.3 show the percent separation and flux result of the Torlon® base membrane coupons for a range of PEG solutes used. These results will be used for future reference.

From Figures 4.1 and 4.2, it is clear that Torlon® 20-0 base membrane coupons have comparable performance. The average molecular weight cut-off (MWCO) calculated from both figures is around 13 000 Daltons with a standard deviation of 4%, which could be considered to be in the UF category. T201-5 and T202-3 in Figure 4.1 were suspected of having pinholes[2] or accumulation of dirt on the membrane surfaces. This explained the behaviour of the separation curve that is 48% higher (T201-5) and 31% lower (T202-3) than the calculated average MWCO. Defect on membrane surface could also be accounted from a scratch on surface while cutting the membrane sheet into small coupons to fit the test cell.

[2] Pinholes are also known as small holes through the selective layer of the membrane which sometime can not be detected visually.

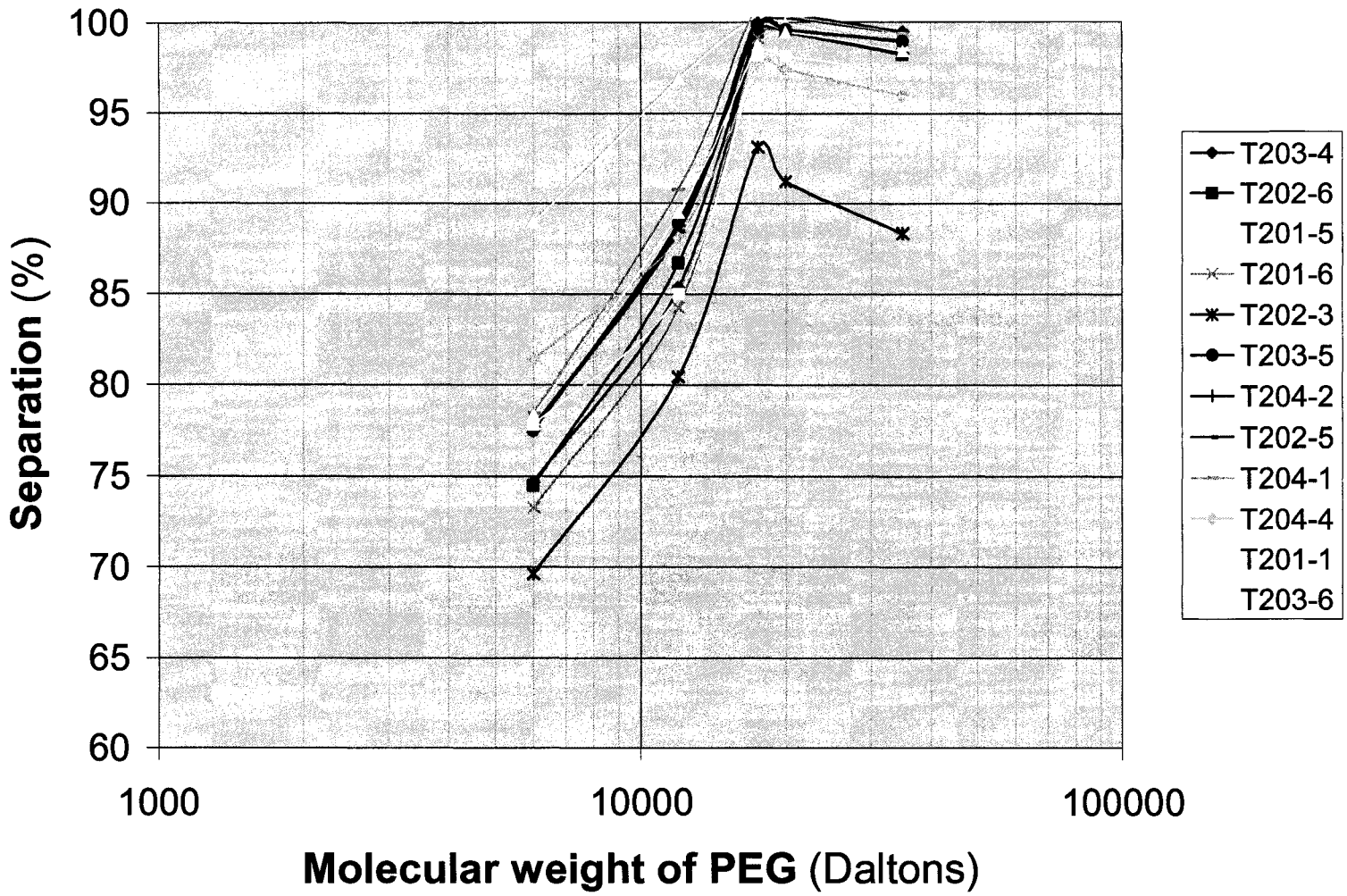

Figure 4.1 – PEG separation as function of molecular weight for Torlon® 20-0 (first trial) at 23 °C and 344.74 kPa

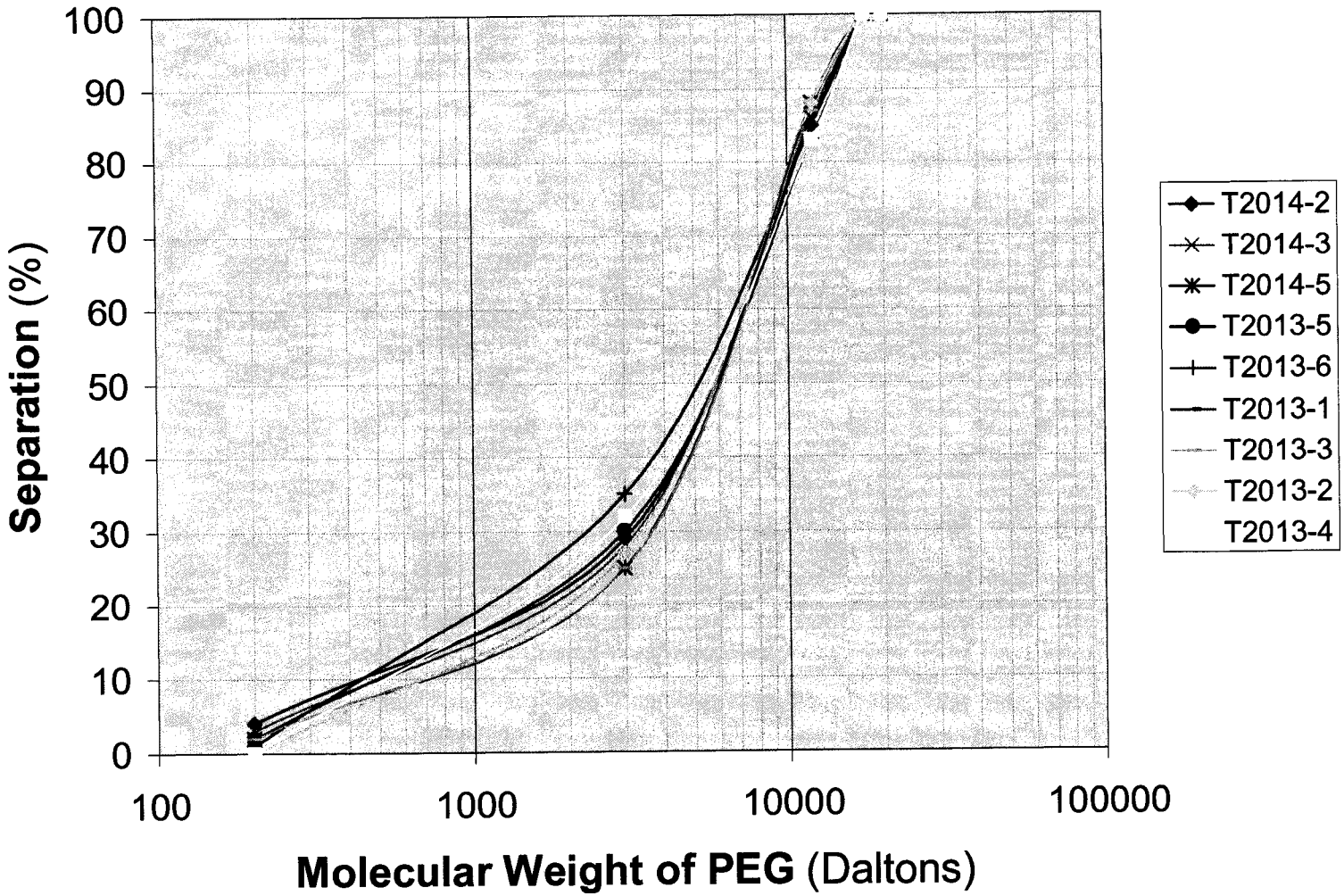

Figure 4.2 – PEG separation as function of molecular weight for Torlon® 20-0 (second trial) at 23 °C and 344.74 kPa

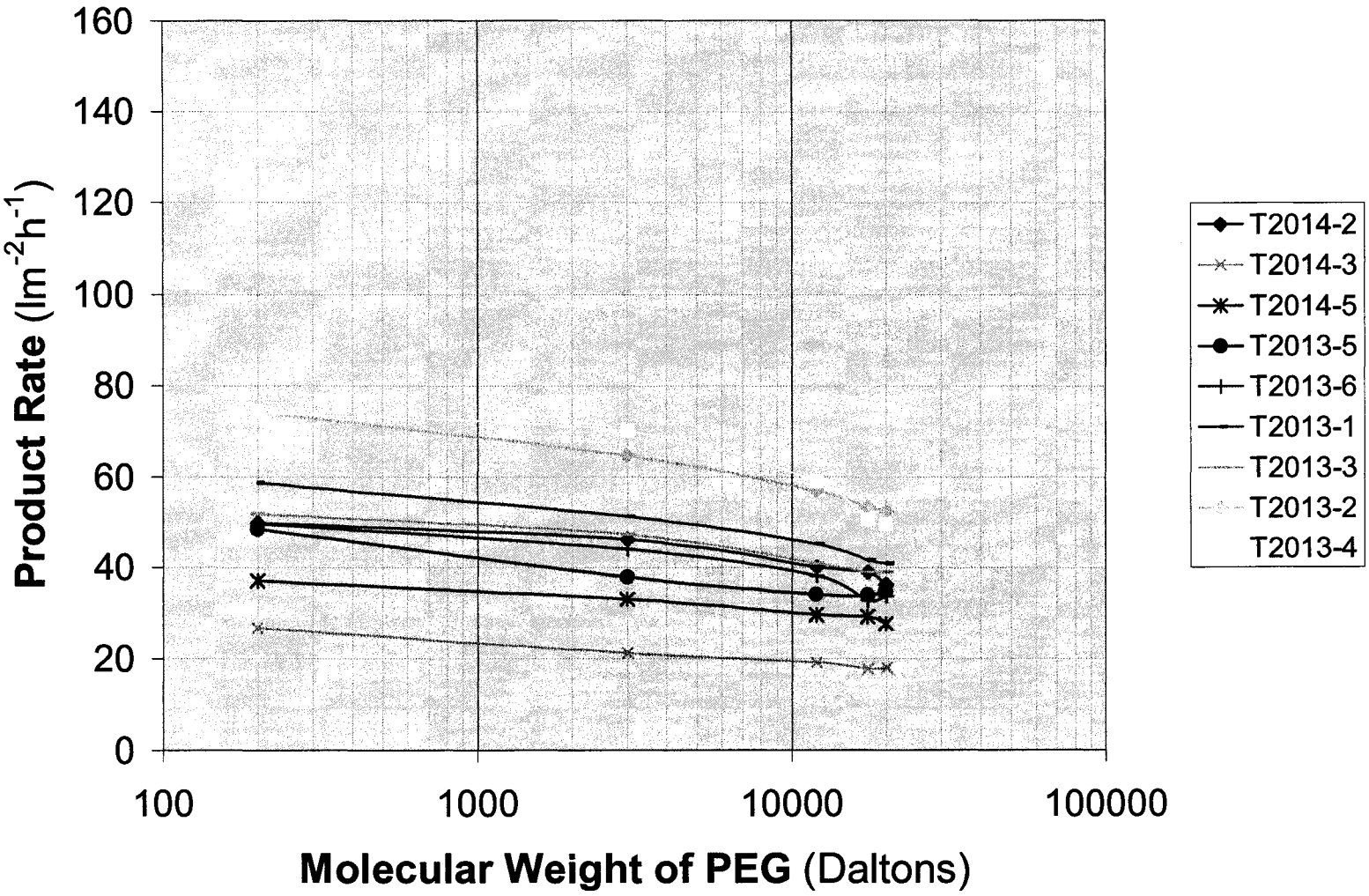

Figure 4.3 – Product rate as a function of molecular weight of solute for Torlon® 20-0 (second trial) at 23 °C and 344.74 kPa

Strange behaviour of the separation curves also found in Figure 4.1. As the PEG solute increase, the separation curve is expected to increase until it reaches the maximum 100% separation and stabilized. Oddly; all coupons showed that as the PEG increased from 20000 (20k) Daltons to 45k Daltons, the separation curves decreased instead of reaching their constant rate. From this point, there are no theoretical explanations to this behaviour but the possible rationalization that can be drawn is because of the impurities in PEG solutes used as it was procured from the manufacturer.

The consistency of the measured performance of coupons cut from single membranes sheet is known as intra-membrane reproducibility whereas inter-membrane reproducibility is identified as the ability to make the same membrane in separate casting environments. Inter-membrane consistency, at this stage, is desired since the focus of this work is to establish repeatable results for making thin film composites. Aside from the coupons suspected to have pinholes or defects in them, separation curves for the PEG solutions for both first and second trial were obtained and were found to have similar separation values and a low deviation from the average separation value. However product rate of each membrane coupon in Figure 4.3 did not show a similar behaviour. It has been experimentally verified that coupon production rates can range from 24 to 74 $lm^{-2}h^{-1}$. Thus, it can be argued that there is lack of homogeneity in the membrane sheets. To explain this behaviour, it is postulated that the product rate variability can be a result of the use of different casting conditions such as, casting speed leading to different pre-evaporation, pressure applied on the casting bar, which commonly performed by hand casting process.

One potential approach that can be used to achieve better inter-membrane reproducibility is utilizing more coupons in the test. Dal-Cin *et al.* (1991) pointed that the

inter-membrane reproducibility could be increased by reducing the actual variance. Conversely there was no indication of how it could be done since the variance took into account all specific processes used in membrane formation such as accuracy of TOC determination, testing procedures and the reproducibility of the membrane casting itself. Dal-Cin *et al.* (1991) also mentioned that using automated casting machine allowed more consistent castings which would enhance the reproducibility of membrane separation and product rate performances from hand cast membranes.

Aside from rate differences, the coupons show that the highest product rates were observed at lowest molecular weight of solute while the lowest product rates were observed for highest molecular weight of solute. This behaviour can be expected since larger sizes of the solute molecules show lower permeation through the membranes compared to the smaller ones. Larger solute molecules tend to form thicker gel or polarize on the surface of the membrane thereby increasing the resistance to permeate flow. The blockage of pores by solute molecules could very well be the reason for the decrease in product rate. This phenomenon could be avoided by using a membrane with pore sizes smaller than the solutes to be separated. As a result, the solute molecules would not enter the pore structure and would be deflected off the membrane surface. However, this method will also lead to concentration polarization or gel formation as described earlier leading to the fouling of the membrane and more often the results gathered from these test solutes would not be repeatable.

Focusing on the work objective of forming solvent resistance composite NF membranes, Torlon® 20-0 UF membrane was found to be suitable as a support membrane with good reproducibility of separation curves. The average thickness of this membrane is

0.251 mm with standard deviation of 0.015 mm. This average number was obtained by measuring the thickness of approximately hundred membrane coupons. Measurement was taken in the center of the coupon perimeter given that most surface contact occurred around this region. The processes were performed carefully to avoid scratches or damages on membrane surface.

4.2 Torlon®/Chitosan composite NF membranes

Membrane formation process was continued through Chitosan coating on Torlon® 20-0 UF membrane using the procedures explained in experimental section. Preliminary experiments were done using 2.5% w/w Chitosan buffer as the coating solution (without any dilution agent at this point) followed by short curing time (24 hours). The purpose of this was to determine the optimal cross linking and neutralization agents that could be used to obtain the desired membrane performance. The results are summarized in Table 4.1 below.

Table 4.1 – Summary of Torlon®/Chitosan composite NF membranes based on visual examination of the possible detachment of Chitosan on Torlon® support layer at the first category of experiments using short curing time as reference

Case	Neutralization before cross linked	Cross linking agents		Degree of success
		PEA	DEGDMA	
1	4% w/v aq. NaOH	0.08% w/w in acetone	-	poor
2	4% w/v aq. NaOH	0.2% w/w in acetone	-	poor
3	4% w/v aq. NaOH	-	10% w/v in MeOH	poor
4	4% w/v aq. NaOH	-	10% w/v in EtOH	fair
5	1% w/v aq. $NaHCO_3$	-	10% w/v in EtOH	good

Case 1 illustrates the situation when the formation of composite membranes was completed via polyethylene adipate (PEA) solution. The process began with instantaneous liquid-liquid mixing in aqueous sodium hydroxide (NaOH) for 5 minutes to convert Chitosan acetate to Chitosan, followed by several washings with water. Accordingly membrane was immersed in cross linking solution for 0.5 h which later was extended to 1 h. The top Chitosan layer (transparent in colour) can be seen delaminated from Torlon® base which was yellow in colour. Evidently 0.08% w/w PEA in acetone did not provide any cross linking reaction for this composite membrane even though the cross linking time was extended to 1 h.

It was found that the PEA concentration was not sufficient to provide the desired cross linking effects, therefore, additional experiments were done by increasing cross linking agent concentration to 0.2% w/w as described in Case 2. This experiment also gave detached Chitosan layer and trace amount of Torlon® was left attached on non-woven material as the membrane was immersed in water after cross linking process. The hypothesis is that NaOH was too strong of a base that caused Torlon® to change the matrix (swollen and moved). Considering that Chitosan is hydrophilic, water caused swelling in Chitosan layer and formed bubbles. Since PEA did not cross link properly, the bubbles present in between the base and the active layer caused the added potential for detachment. In order to ascertain the most significant parameter that affects performance, a new cross linking agent diethylene glycol dimethacrylate (DEGDMA) was used in this work.

DEGDMA solutions were prepared in MeOH and EtOH as shown in Cases 3 and 4. Case 3 did not show adequate cross linking and Case 4 showed much better cross linking. No detachment of Chitosan layer from base membrane was observed; however, there were a

few noticeable white spots on the membrane. Further examination revealed that the spots appeared to be small pockets of entrapped air or liquid bubbles between two layers. These pockets are postulated to form when the membrane is soaked in the aqueous NaOH solution. It could be argued that degree of hydrophobicity and hydrophilicity of both Torlon® and Chitosan layer are not compatible with the use of NaOH as a neutralization agent.

Consequently, a two-pronged approach was taken at this point.

1. The first approach entailed the testing of alternate coating solutions. The option of 10% w/w PEA blended in Chitosan buffer was studied since acetic acid contained in Chitosan buffer can also be used as a solvent for PEA. This method also did not give positive results as PEA polymer is not compatible with strong oxidizing agents and might have decomposed on exposure to moist air or water. Immediate contact of PEA solution with Chitosan buffer triggered a reaction where PEA became solidified, forming white plastic like layer.
2. In the second approach, a less basic aqueous sodium bicarbonate ($NaHCO_3$) solution, with a pH of 8 was used in the preparation of Case 5. Case 5 offered a significant level of cross linking breakthrough when compared with the earlier cases and detachment of the membrane layer was not visible similar to Case 1-3. Also, white spots were not observed on visual inspection as in Case 4. Chitosan active layer was completely attached to Torlon® base membrane without any damage on membrane surface and backing material.

This suggests that using aqueous $NaHCO_3$ and DEGDMA as neutralization and cross linking agent respectively is indeed a good starting point for the formation of

Torlon®/Chitosan composite NF membrane. Since hand casting was the only method used for Torlon® base membranes, the composite membrane procedures illustrated in Figures 3.4, 3.5, and 3.6 were used with the first two coating solutions, which are 2.5% w/w Chitosan buffer and diluted Chitosan buffer with EtOH.

In practice, supplementary Torlon® membrane sheets can be cast, but higher discrepancy in the performance of membrane coupons tends to arise when membranes were cast in different casting environments. Membrane sheets produced from this uncontrolled environment tend to have diverse MWCO, product rate, and thickness. The casting environments that can affect the membrane formed include humidity and temperature of casting room, temperature and thermal conductivity of the gelation bath, and the speed and pressure used in casting itself. The effects of these factors must be studied and subsequently controlled to ensure good reproducibility. Thus, composite membrane from diluted Chitosan buffer via IPA is done with the most feasible technique concluded from the preliminary work.

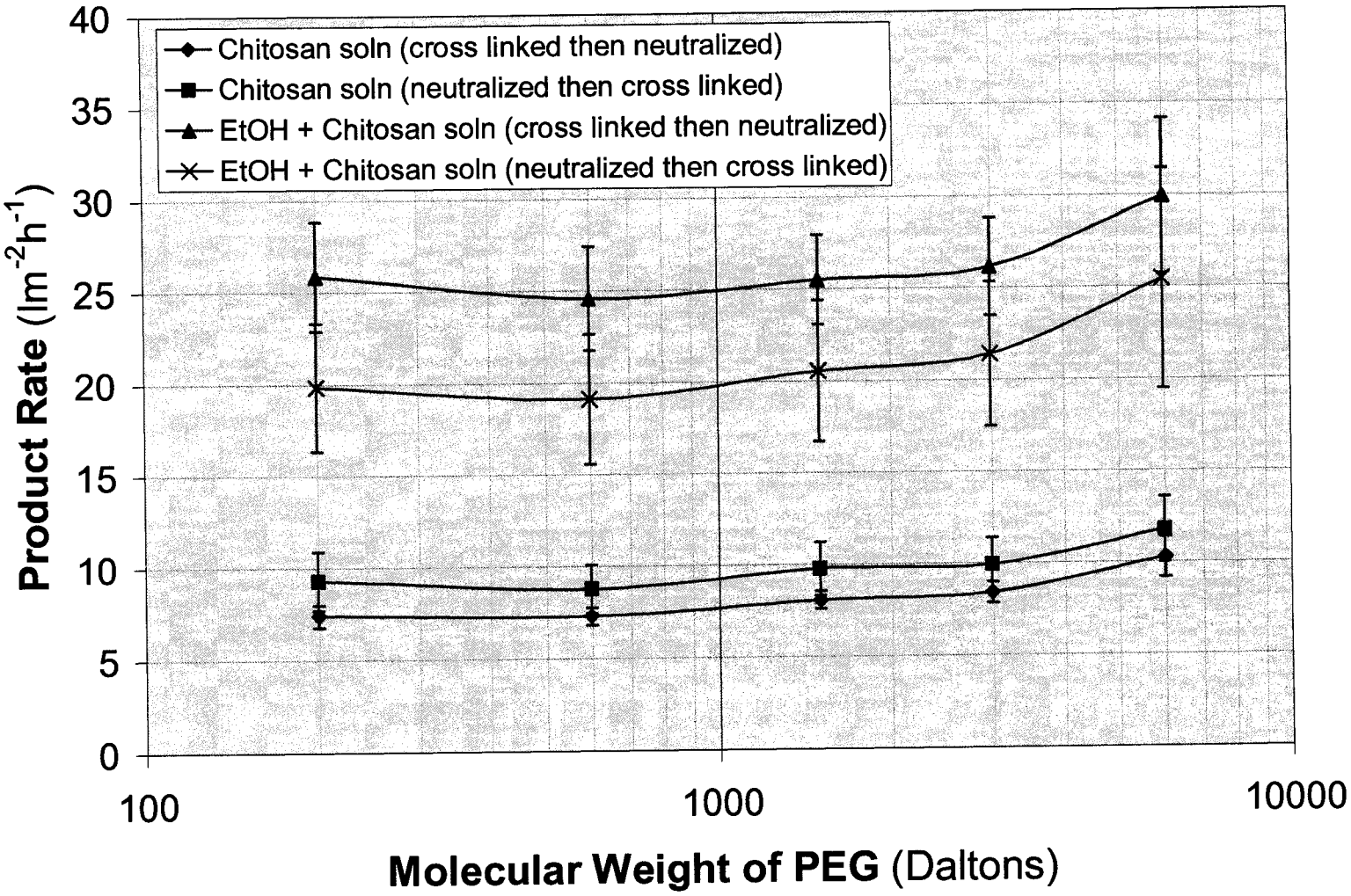

Figure 4.4 – Permeation flux of PEG solutes for composite NF membranes based on 6 days curing period at 23 °C and 689.48 kPa

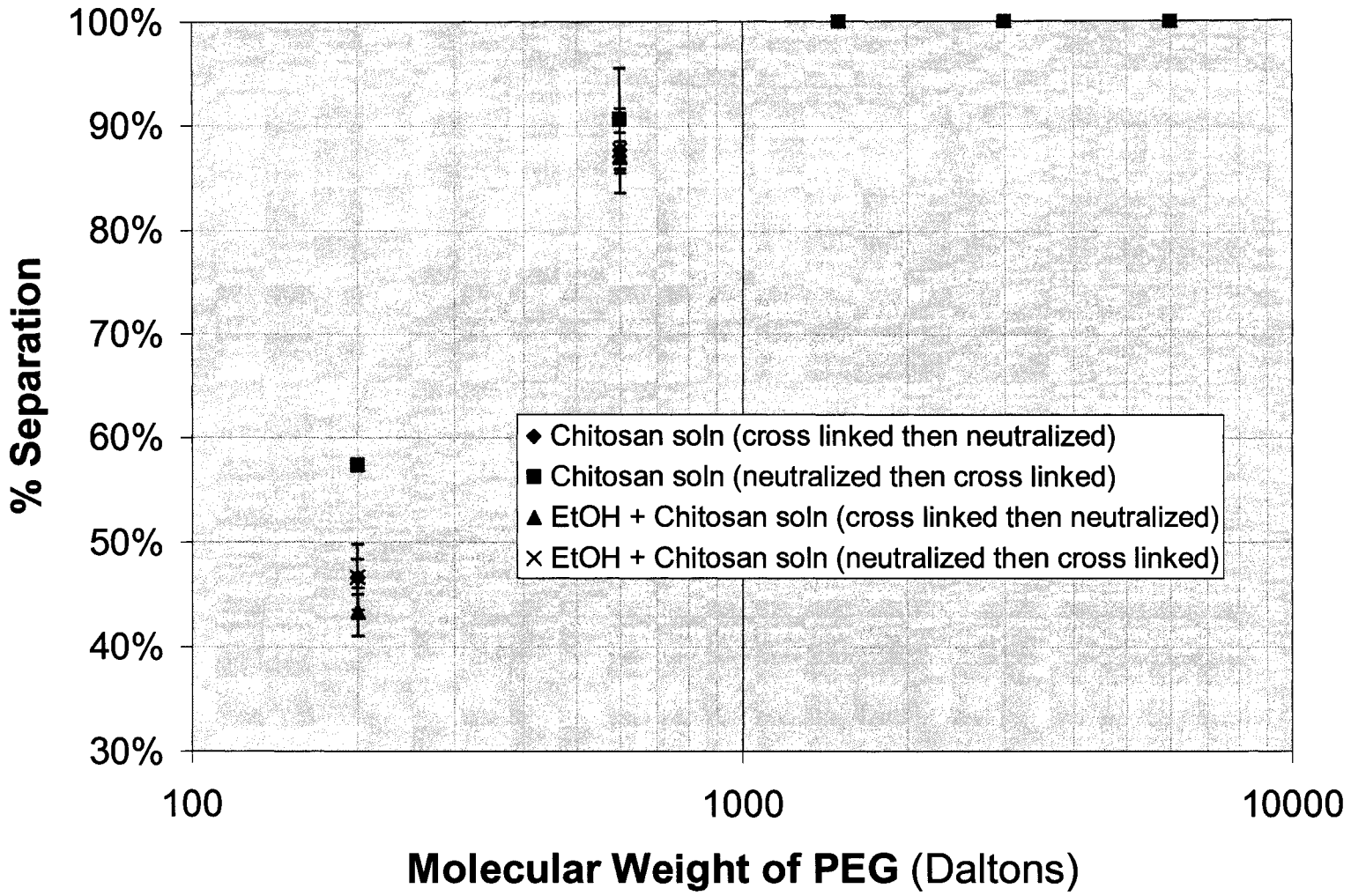

Figure 4.5 – % Separation of PEG solutes for composite NF membranes based on 6 days curing period at 23 °C and 689.48 kPa

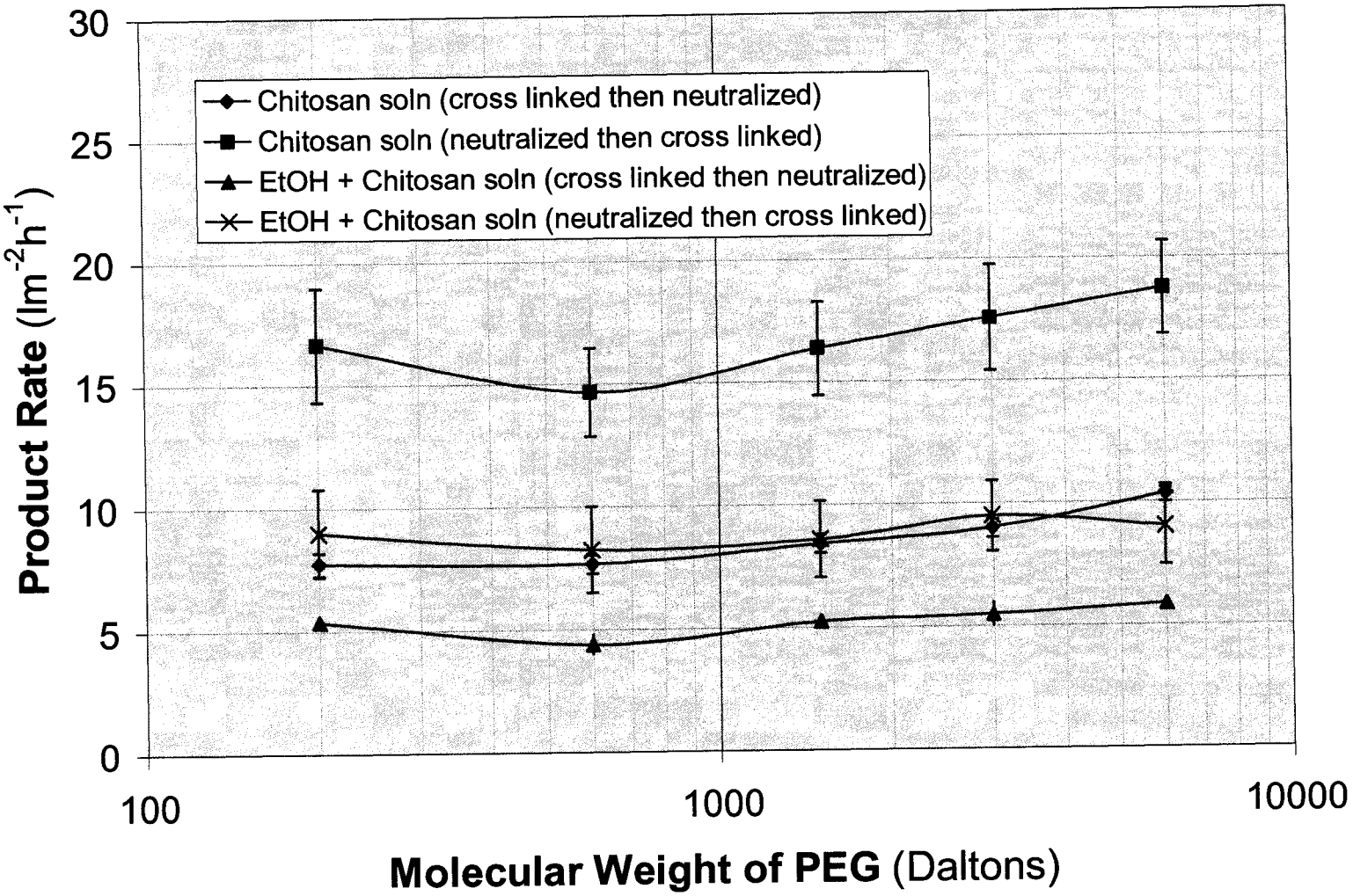

Figure 4.6 – Permeation flux of PEG solutes for composite NF membranes based on 24 hours curing period at 23 °C and 689.48 kPa

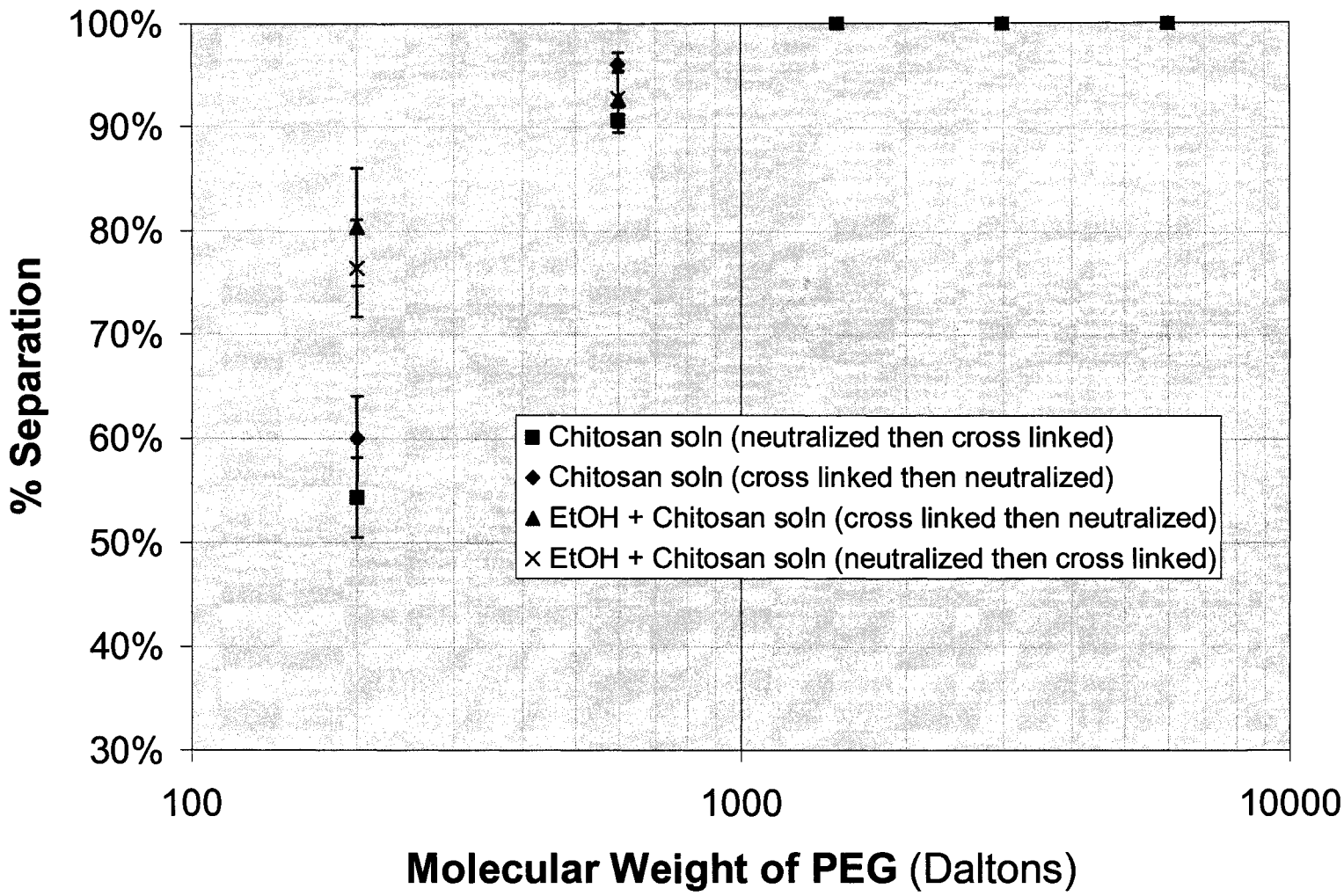

Figure 4.7 – % Separation of PEG solutes for composite NF membranes based on 24 hours curing period at 23 °C and 689.48 kPa

The performance of Torlon®/Chitosan composite membranes data shown in Figures 4.4 – 4.7 were collected with the automatic UF system. Figures showed that the average value of three membrane coupons for each specific procedure (details for each membrane coupon are tabled and listed in Appendix A). The percent separation of solutes and the product rates of composite membranes treated with neutralization process prior to cross linking step gave higher product rates and smaller MWCO which were desirable (200 to 1000 Daltons) compared to composite membranes treated with cross linking step prior to neutralization process. Composite membranes using diluted Chitosan buffer with IPA coating solution were prepared via neutralization step (24 h) prior to washing (24 h) and cross linking (24 h).

Although the separation curves show the expected trend, product rate of membranes showed a peculiar drift from Figure 4.3. As the molecular weight of PEG increased, the overall product rate increased instead of decreasing. But focusing on the bend at lower PEG solutes (200 to 600 Daltons), data actually show that the product rates decreased before it actually increased. This section is expected since larger solutes will permeate less through membrane pores. When the membranes pore size is bigger than the solute size and considering that the solute itself is more viscous than water, product rate will decrease to the minimum. The hypothesis drawn from the increasing product rate behaviour is that as the molecular weight of solute increases, less solute passed through the membrane pores. Subsequently, by measuring the PEG concentration in permeate stream; more water is permeated through the membrane which leads to increase of flux and separation. If the experiment is continued with higher molecular weight PEG solutes, the curves are expected to reach constant rate unless there is a cake formation (concentration polarization) or fouling

on membrane surface then the product rate will decrease. In general, the increased change of product rate (up to 5 $lm^{-2}h^{-1}$) of this Torlon®/Chitosan composite membrane is not significant for this study considering that pore size distribution of each membrane coupons also play a big role in observed discrepancies. .

Other possible explanation that can be referred to is the study done by Bhattacharjee *et al.* (1999). The authors pointed that an enhancement in inter-particle repulsion leads to higher diffusion and osmotic pressure. Higher diffusion resulted in a lower volume fraction on the membrane surface (ϕ_m) and less accumulation of solute on the membrane thus higher permeate flux will be observed (illustrated in Figure 4.8). The studies done on a repulsive colloidal systems also showed that the permeate flux increased with increasing particle size and decreasing ionic strengths.

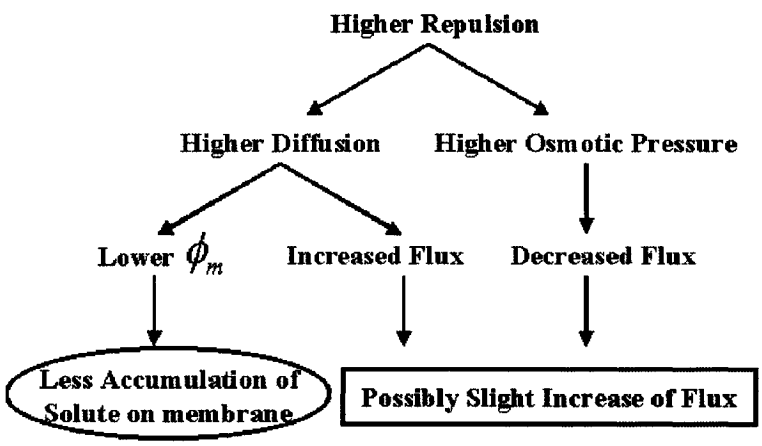

Figure 4.8 – Effect of interparticle interaction on permeate flux (Bhattacharjee *et al.*, 1999)

In order to distinguish specific composite membrane types, individual membranes will be identified with different acronyms (L or S was added at the end of each acronym to indicate if membrane was processed with 6 days (L) or 24 hours (S) curing in convection oven).

- CS(XN) is membrane coated with Chitosan, going through cross linking step prior neutralization process and followed by the curing period.
- CS(NX) is membrane coated with Chitosan, going through neutralization process prior cross linking and followed by the curing period.
- ECS(XN) is membrane coated by diluted Chitosan with EtOH, going through cross linking step prior neutralization and followed by the curing period.
- ECS(NX) is membrane coated by diluted Chitosan with EtOH, going through neutralization process prior cross linking and followed by the curing period.
- IPACS(NX) is membrane coated by diluted Chitosan with IPA, going through neutralization process prior cross linking and followed by the curing period.

Table 4.2 – Summary of Torlon®/Chitosan composite NF membranes based on different formation technique

Methods	MWCO (Daltons)	PWP ($lm^{-2}h^{-1}$) ± standard deviation	Total organic carbon content in PWP (ppm)
CS(XN)L	657	7.2 ± 1.1	<15
CS(NX)L	587	8.2 ± 2.3	<15
ECS(XN)L	671	24.0 ± 3.9	<15
ECS(NX)L	657	17.0 ± 5.1	<15
CS(XN)S	588	7.7 ± 0.7	12 – 25
CS(NX)S	480	16.0 ± 4.3	24 – 25
ECS(XN)S	480	5.2 ± 0.2	29 – 30
ECS(NX)S	495	9.0 ± 3.0	24 – 37
IPACS(NX)L	640	19.0 ± 4.3	<10

Table 4.2 summarized the performance of all the composite coupons tested using conventional membrane system. Again, the results provided are averages from three composite coupons based on each fabrication technique. MWCO was determined by reading the average separation curve at 90% separation of PEG solutes with a standard deviation of 2% to 8%. Comparing MWCO values, membranes fabricated with short curing time method provide a dense cross-linked membrane structure which is desired in NF but pure water permeability (PWP) are lower and the impurities in the PWP flux are much higher. Impurities outside the membranes can be washed out by soaking the membranes in water and the storage water is replaced every day or two. The impurities shown in Table 4.2 are a result of the compounds formed during the membrane making process. The conventional system for testing NF membranes was run continuously for 8 h per day for 5 to 8 days with clean RO water in feed solution to ensure that no more than trace amounts of impurities were left in the membranes before the PEG measurements were conducted.

A 24-hour curing time was found to be insufficient for completion of the reaction between Chitosan coating and Torlon® base. Therefore, free compound or excess material that contained carbon was washed off from the membrane. This impurity was washed out by water hence high TOC was observed. As the curing time increased, more unused solvents such as alcohol and water evaporate from the membranes. Also the Chitosan chains become closely linked together. A more stable membrane was thus developed since additional space became available as a result of solvent displacement which allowed additional cross linking to occur. As a result of all the preliminary experiments performed on composite membranes, IPACS(NX)L composite NF membrane was selected for further optimization and solvent resistance studies due to its overall suitability.

4.3 Effect of cross linking time and concentration

A range of cross linking time (0.5 h to 24 h) and DEGDMA concentrations (0.2% to 10%) were used to determine their effects on the performance of the IPACS(NX)L composite membranes. The results of PWP and MWCO values for IPACS(NX)L composite membranes along with the cross linking composition (Table 3.1) are listed in Table 4.3 and illustrated in Figure 4.9 (detailed experimental data is provided in Appendix A).

Table 4.3 – Torlon®/Chitosan membranes based on cross linking time and concentration

Composite membrane		MWCO	PWP
Cross linking time	% of DEGDMA	(Dalton)	($lm^{-2}h^{-1}$)
0.5 h	0.2%	500	12 ± 2.2
	1%	780	15 ± 3.3
	3%	860	17 ± 0.8
	5%	600	16 ± 2.8
	10%	740	32 ± 6.5
1 h	0.2%	860	17 ± 1.9
	1%	600	15 ± 0.8
	3%	860	18 ± 2.4
9 h	1%	560	21 ± 7.7
	3%	600	14 ± 1.3
	5%	660	17 ± 1.5
	10%	600	17 ± 1.3
17 h	0.2%	570	16 ± 4.2
	1%	540	17 ± 2.3
	3%	580	13 ± 2.3
	5%	510	15 ± 1.2
	10%	700	23 ± 1.5
24 h	0.2%	900	19 ± 1.8
	1%	540	15 ± 1.3
	3%	800	11 ± 1.0
	5%	620	16 ± 2.6
	10%	660	19 ± 2.4

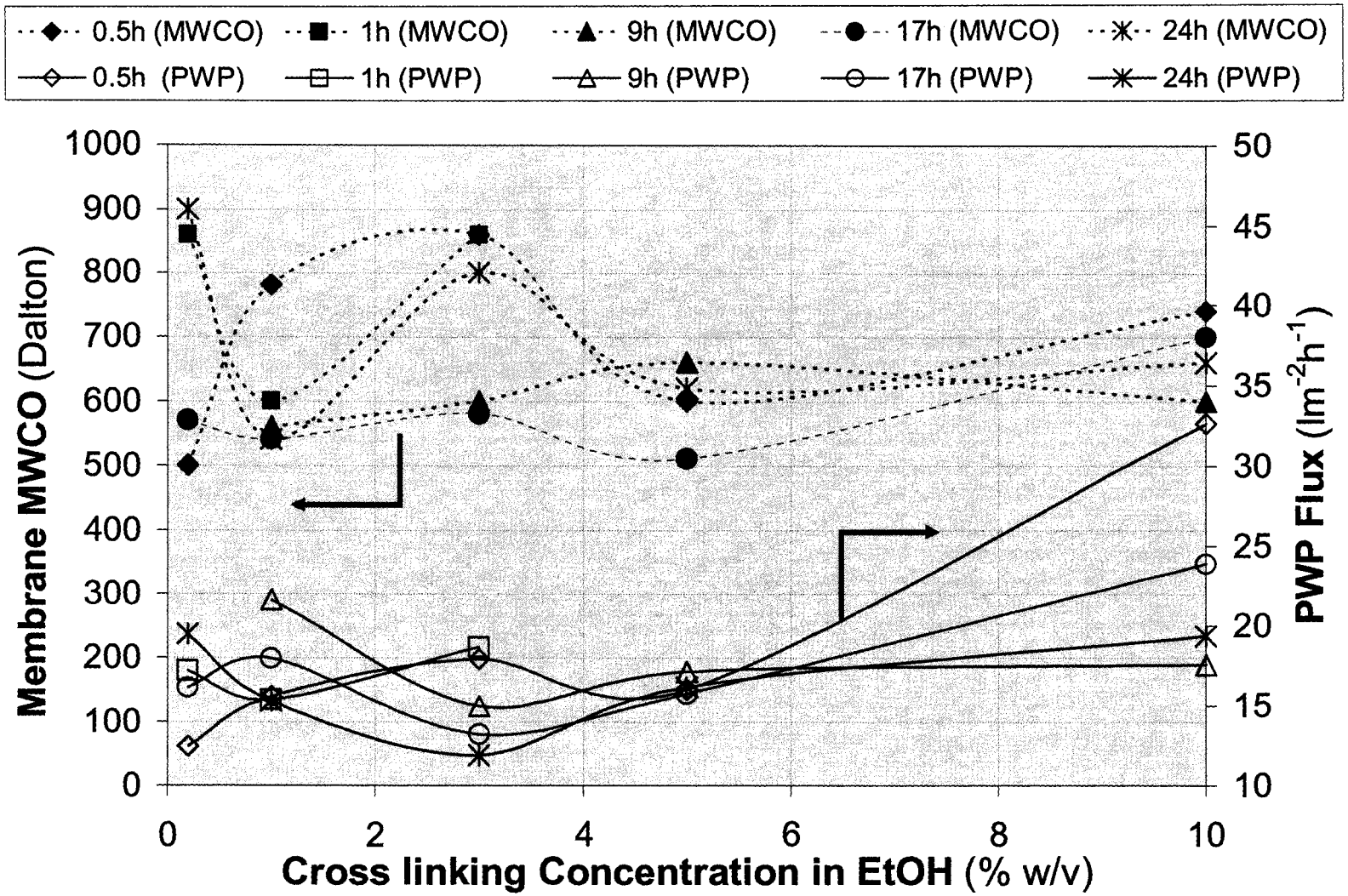

Figure 4.9 – MWCOs and PWP results of IPACS(NX)L composite membranes based on cross linking time and concentration

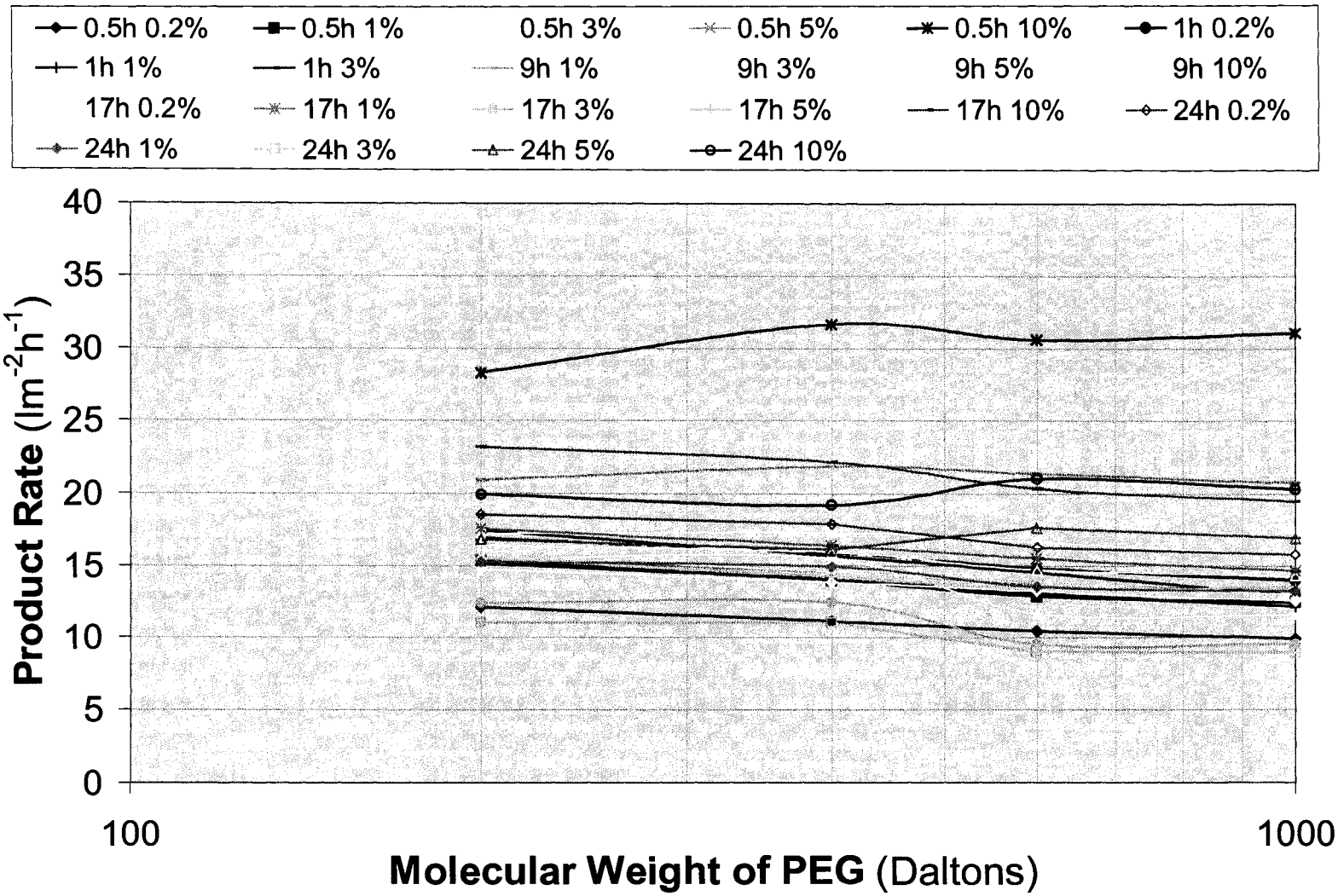

Figure 4.10 – Product rate of PEG solutes for IPACS(NX)L composite membranes based on cross linking time and concentration

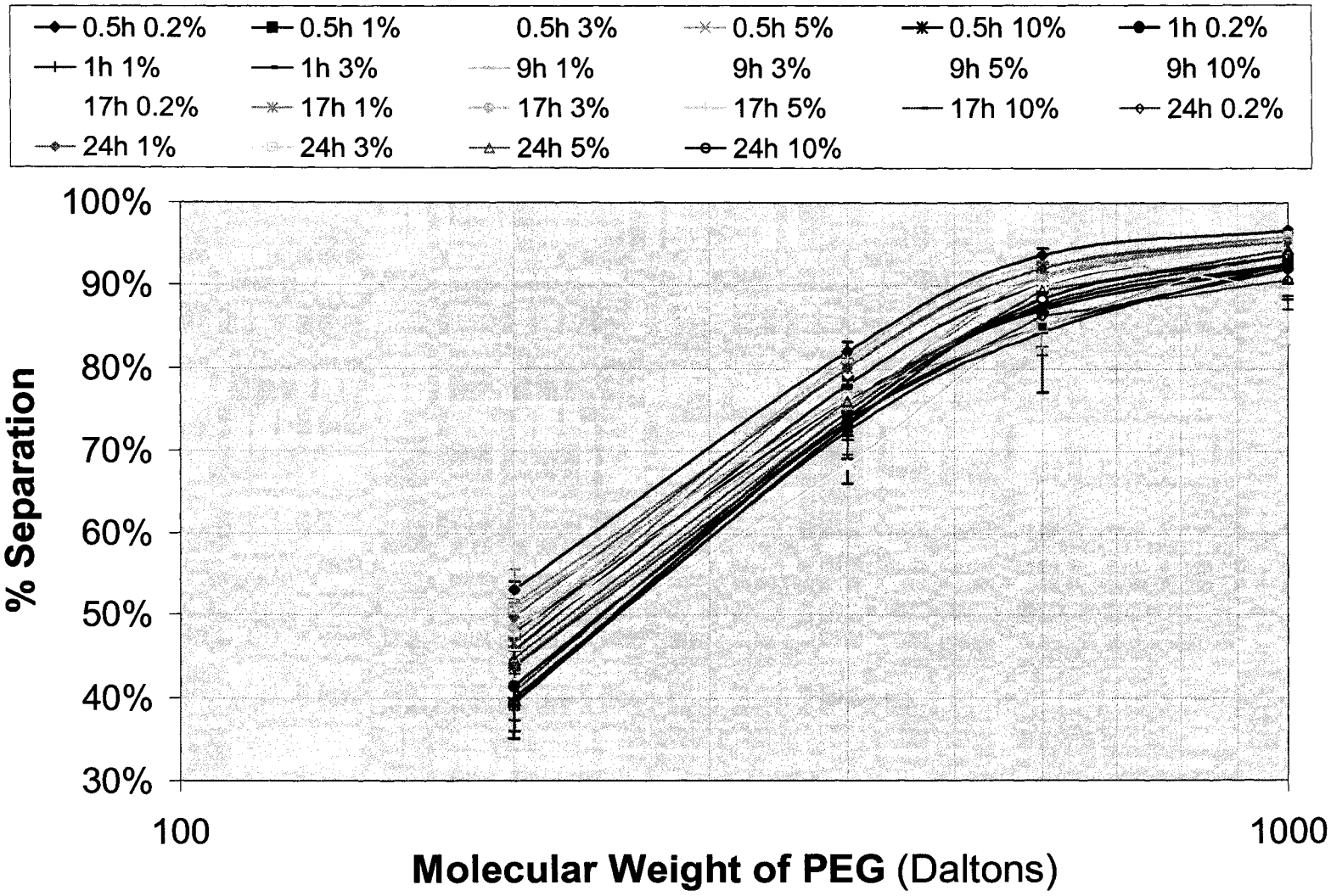

Figure 4.11 – % Separation of PEG solutes for IPACS(NX)L composite membranes based on cross linking time and concentration

Figures 4.10 and 4.11 show product rates and separation curves of all the tested IPACS(NX)L membranes. A matrix of experiments was performed, as shown in Table 4.3, and each experiment was repeated at least three times to characterize the membrane performance. The matrix consists of five (5) different concentrations of the cross linking solutions in which the membrane is soaked for at least five (5) different intervals of time resulting in a 5X5 matrix of experimental conditions. By implementing the same characterization procedure as described in Section 3.6, experimental results obtained have been reported in Table 4.3 and graphically displayed in Figure 4.9. MWCO's of the IPACS(NX)L membranes have also been summarized in Table 4.3 and Figure 4.9. Due to some mechanical limitations in the automated experimental system in which the membranes were tested, MWCO and PWP of some IPACS(NX)L composite membranes could not be obtained. Such membranes, commonly referred to as "damaged" in this thesis, were: IPACS(NX)L treated with 5% and 10% cross linking concentration and had been soaked in cross linking solution for a period of one hour. Similarly, IPACS(NX)L treated with 0.2%, 1%, 3%, 5%, and 10% cross linking concentration and soaked for four hours and IPACS(NX)L treated with 0.2% cross linking concentration and soaked for nine hours also were considered "damaged".

This limits the experimental characterization of the membrane cross linking behaviour and further characterization is based on the matrix of experimental results formed by eliminating the "damaged" test sub-matrix. This clearly limits the present work in obtaining the optimal cross linking concentration and period for Torlon®/Chitosan composite NF membrane, namely IPACS(NX)L. New membranes with those specific

soaking periods and concentrations need to be formulated in the future to advance the understanding of these parameters.

Separation curves for all membrane coupons show the expected plateau in separation and the separation increased with molecular weight of PEG solution. The complementary curve for product rate measurements is shown in Figure 4.10. The product rate decreased as the PEG solution concentration increased in most membrane coupons with the exception of IPACS(NX)L 0.5h 10%, 24h 5% and 24h 10%. At higher cross linking concentration, the membranes are more rigid indicating a possible loss of elastomeric properties. Visual observation, before loading membranes into test system, showed that membranes cross linked with 10% cross linking solution are more rigid than those made with lower concentrations. This increased rigidity translates to increased membrane brittleness and difficulty in handling. As a result of the rigidity, mechanical parts in the cell, such as top plates and O-rings, shown in Figure 3.8, may cause "membrane fracture". In particular, this problem was evident with IPACS(NX)L 0.5h 10% and 24h 10% membranes and the product rates obtained were higher than other membrane coupons with lower concentration with similar cross linking periods. As larger PEG solute concentrations are used (in close proximity to the membrane pore size), built up resistances due to pressure and solute concentrations cause the indicated fracture to extend the damage resulting in higher solute fluxes. IPACS(NX)L 24h 5% membrane coupons were also found to produce higher product rates and were expected to be plagued by the similar difficulties but the fracture in this case could not be confirmed by visual observation.

The MWCO of the composite membrane depends on the reaction time and the concentration of cross linking agent. Generally, the percentage separation increased with an

increase in cross linking concentration which leads to lower MWCO membrane. When the membrane cut-off reaches its minima, the composite membrane will cease to cross link and the separation performance of composite membrane is expected to reach a constant. MWCO is also expected to reach its minima and then start rising. This rise is explained as a flushing of excess cross linking agent into the permeate stream resulting in lower separation. The effect of cross linking concentration for given cross linking time on membrane cut-off is shown in Figure 4.9. Interestingly, in this research, the membrane separation curves show two minimum plateaus while cross linking concentration ranges from 0.2% to 10%. For instance, the MWCO for IPACS(NX)L 24h composite membrane decreased from 900 Daltons to 540 Daltons as the DEGDMA concentration increased from 0.2% to 1%. As the cross linking concentration increased to 5%, the MWCO oddly increased to 800 Daltons before it decreased again to 620 Daltons. At present, there is no explanation for the observed results. Detailed experiments at shorter intervals of cross linking time and concentrations need to be conducted in order to verify if the plateaus are an experimental anomaly. Since this work would be far beyond the scope of this study, IPACS(NX)L with 5% w/v cross linking concentration and 9 hours cross linking time was adopted for the remainder of this work and the resistance toward industrial solvents was investigated.

4.4 Comparison of membrane performances

The impact of Chitosan coating and cross linking on Torlon® base membranes are evident in all of the composite membranes prepared no matter what technique was performed. All composite membranes showed MWCO less than 1 000 Daltons which are in NF range.

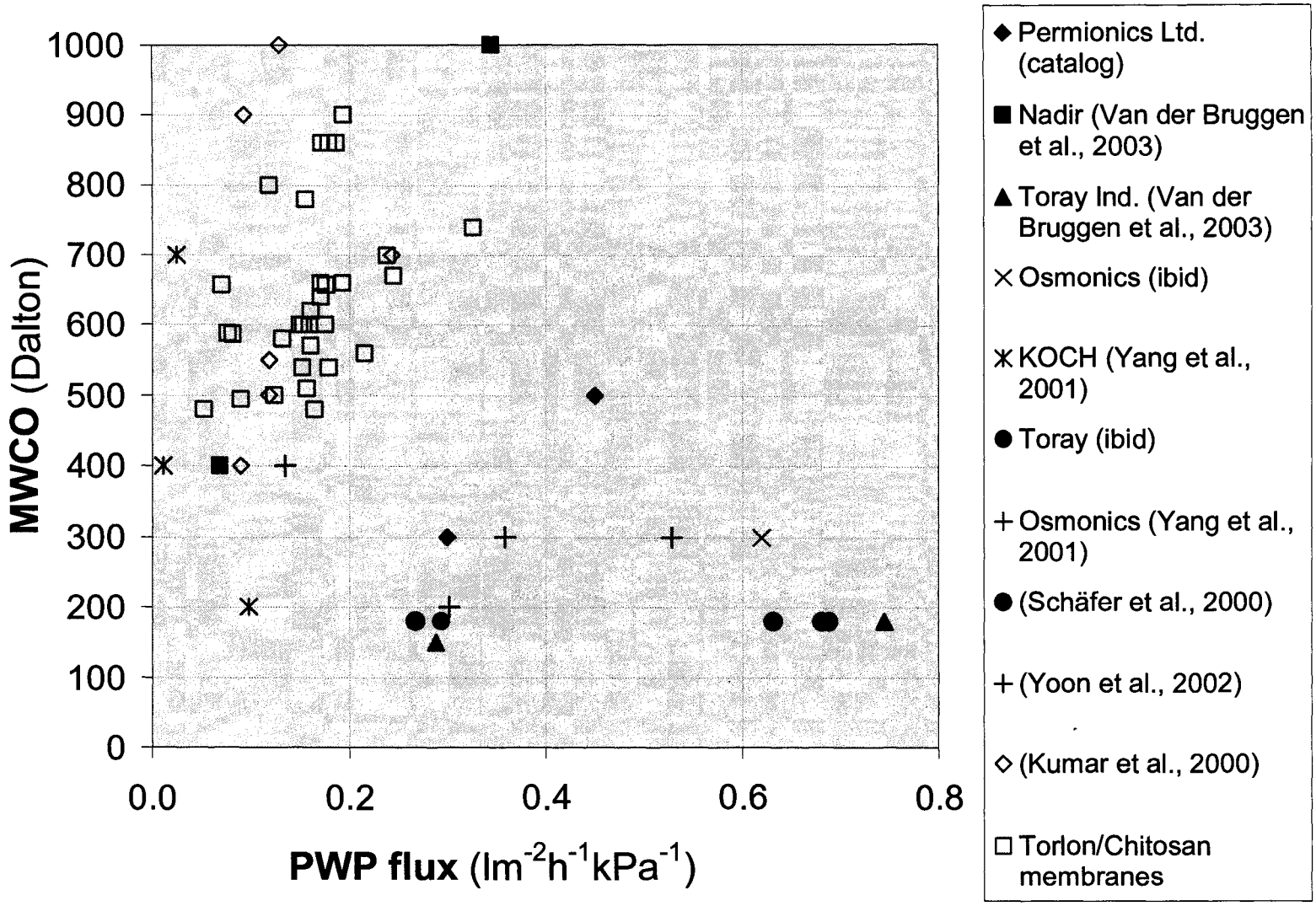

Figure 4.12 – MWCO and PWP flux of Torlon®/Chitosan composite NF membranes among others

To identify if the performance of Torlon®/Chitosan composite NF membranes in this study are adequate, comparison of these membranes performance (MWCO and product rate) with other commercially available membranes are observed (detailed information for each individual membrane is listed in Appendix B). Figure 4.12 presents the PWP flux and MWCO of available commercial membranes with all of the composite membranes prepared in this work. Each commercial membrane is tested with specific pressure, testing environment and different solutes from the PEG used in this study. These factors lead to an inadequate comparison but it will offer a general idea about the standing of Torlon® and Chitosan composite membranes. It was also assumed that the pressure increased linearly with flux increase; therefore, PWP flux will be calculated in term of pressure differences.

Membranes from Permionics Ltd. show good PWP flux and low MWCO but it is also mentioned in the catalog that the membranes have low alcohol compatibility. Thus these membranes are not suitable for solvent resistance performance. Whu *et al.* (2000) investigated NF in methanol solutions using MPF solvent resistant membranes and observed that rejections were generally significantly lower than the manufacturer-specified MWCO values. Yang *et al.* (2001) also found that the retention of organic solutes in different solvents was quite different and the manufacturer-specified nominal MWCO did not seem to reflect solute retention in organic solvents. Evidently, the MeOH and EtOAc fluxes measured by Yang *et al.* (2001) for MPF-60 were lower than those claimed by the manufacturer. The authors also pointed out that the relative difference of membrane discs used in the test and the time needed to allows steady state or to wash out the pre-conditioning agent might have given rise to some variation. Another illustration of such a variation is that UTC-20 membrane (procured from Toray Ind.) tested by Yang *et al.* (2001)

gave a PWP flux of 0.04 $lm^{-2}h^{-1}kPa^{-1}$ where as the same membrane when tested by Van der Bruggen *et al.* (2003) showed PWP flux as high as 0.11 $lm^{-2}h^{-1}kPa^{-1}$.

Aside from all of the above variation, the best comparison for the membranes performance is with Kumar *et al.* (2000) given that the authors used the same PEG solute for MWCO measurement. The figure showed that Torlon®/Chitosan composite NF membranes formed in this study generally gave a reasonable performance to begin with. However detailed investigation and an extended study are still needed to improve membrane performance and reproducibility.

4.5 Reproducibility of data (IPACS(NX)L composite membrane)

In order to ensure that the experiments performed provided consistent results reproducibility of data collected throughout the experiments is important. A brief study was conducted to determine the reproducibility of the selected technique for the production of IPACS(NX)L membranes for solvent resistance studies. The procedure was tested by preparing a new set of IPACS(NX)L 9h 5% membrane by following the previously explained procedures as close as possible and comparing it with the preceding IPACS(NX)L 9h 5% results tabulated in Table 4.3. Twelve membrane coupons were tested in conventional membrane system and average percent separation curves and product rates are shown in Figure 4.13 below.

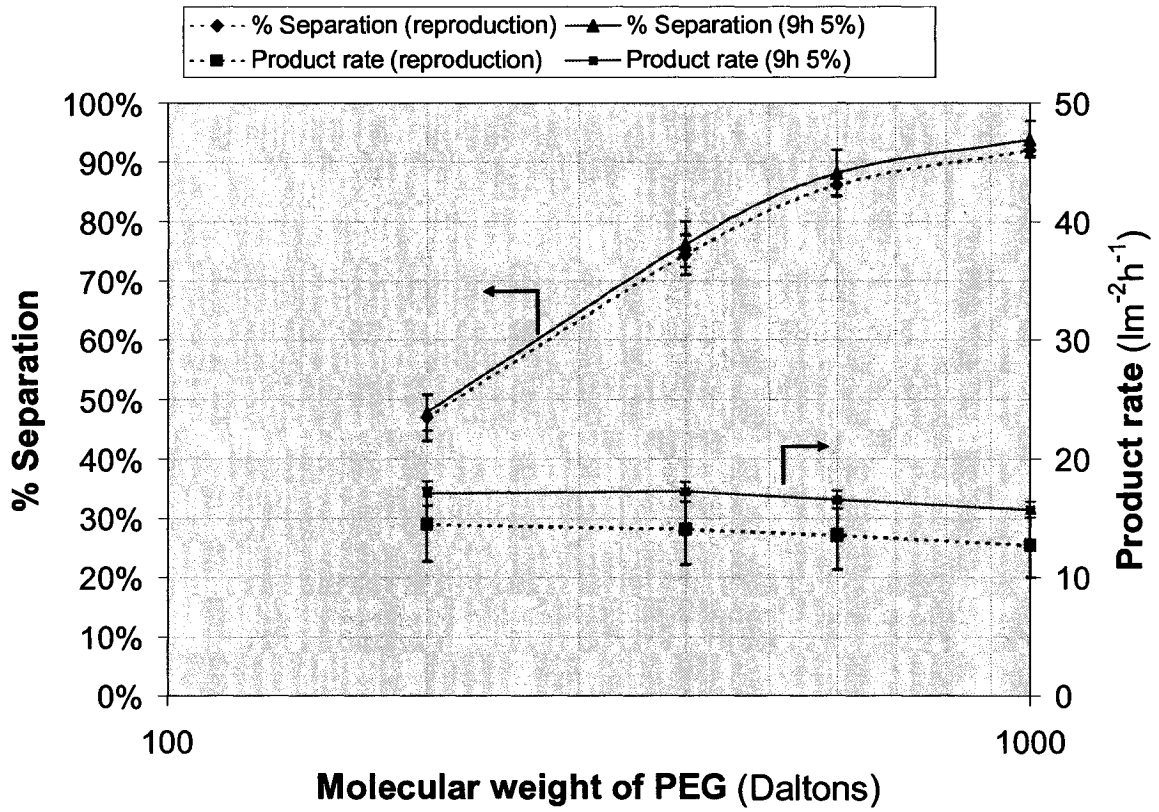

Figure 4.13 – MWCO and solute flux of reproduction and original IPACS(NX)L 9h 5% membranes for reproducibility study

The PEG solutes rejection or separation curves of replicate and original IPACS(NX)L 9h 5% membranes are comparable and showed standard errors of 1 to 2%. Although the replicate and original IPACS(NX)L 9h 5% product rates indicate a slight difference of 3 $lm^{-2}h^{-1}$ (20% error), the differences in product rate between the various PEG solutions are fairly consistent. Product rate variations between these membranes could be accounted for on the basis of differences in the pore size distributions. Small deviations in the pore size and pore size distribution can yield dramatic changes in permeation rates. Based upon this performance data (tabulated in Appendix C), it was concluded that the

membrane modification procedure implemented on IPACS(NX)L is fairly reproducible and the composite membranes formed by using this technique can be considered stable.

4.6 Membrane morphology by SEM

Before studying the IPACS(NX)L 9h 5% actual solvent resistance performance, the membrane was characterized more thoroughly in order to allow a better understanding of the coating and base membrane structure before and after cross linking process. Cross sectional photos of Torlon® 20-0 are shown in Figure 4.14 and composite membranes before and after cross linking are shown in Figures 4.15 and 4.16, respectively. As can be seen from Figure 4.14, base UF Torlon® membrane clearly shows the presence of sponge or finger-like structure. The supporting membrane after coating of Chitosan solution diluted with IPA (overlook the effect of before and after cross linking process) showed the finger-like structure characterized with an asymmetric dense layer on the membrane surface (Figures 4.15 and 4.16). Both figures also show that cross linking indeed partakes a major effect in the active layer formation. Composite membrane without cross linking formed undesirable active layer with observable lump on surface which could alter membrane performance and effect in large discrepancies in the end results. Composite membranes undergo a cross linking step shown in Figure 4.16 give a preferably uniform dense active layer with measured thickness of 0.429 μm (standard deviation of 0.087 μm).

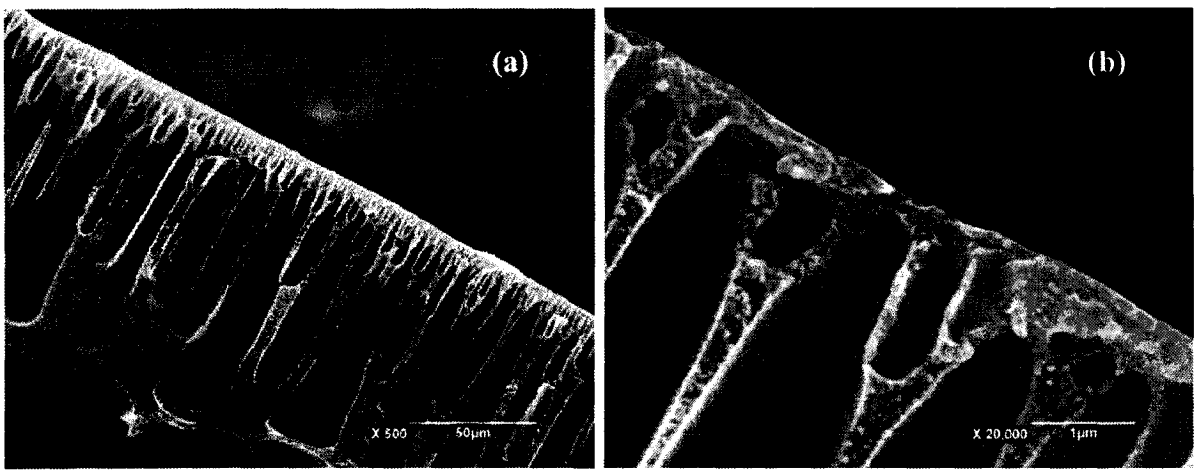

Figure 4.14 – Scanning electron micrograph of cross section of Torlon® base membrane with 500x (a) and 20,000x (b) magnification

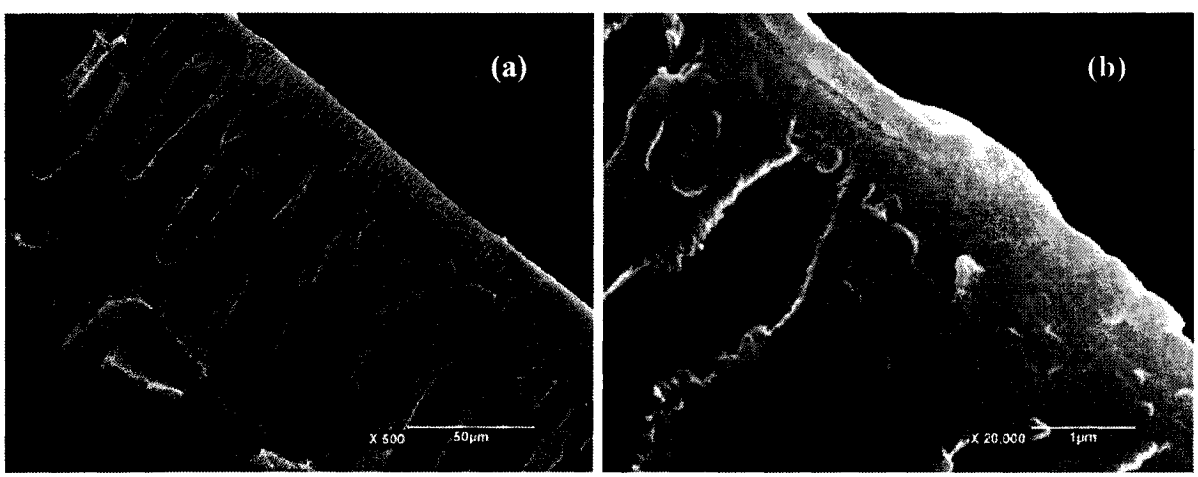

Figure 4.15 – Scanning electron micrograph of cross section of IPACS(NX)L 9h 5% composite membrane before cross linking process with 500x (a) and 20,000x (b) magnification

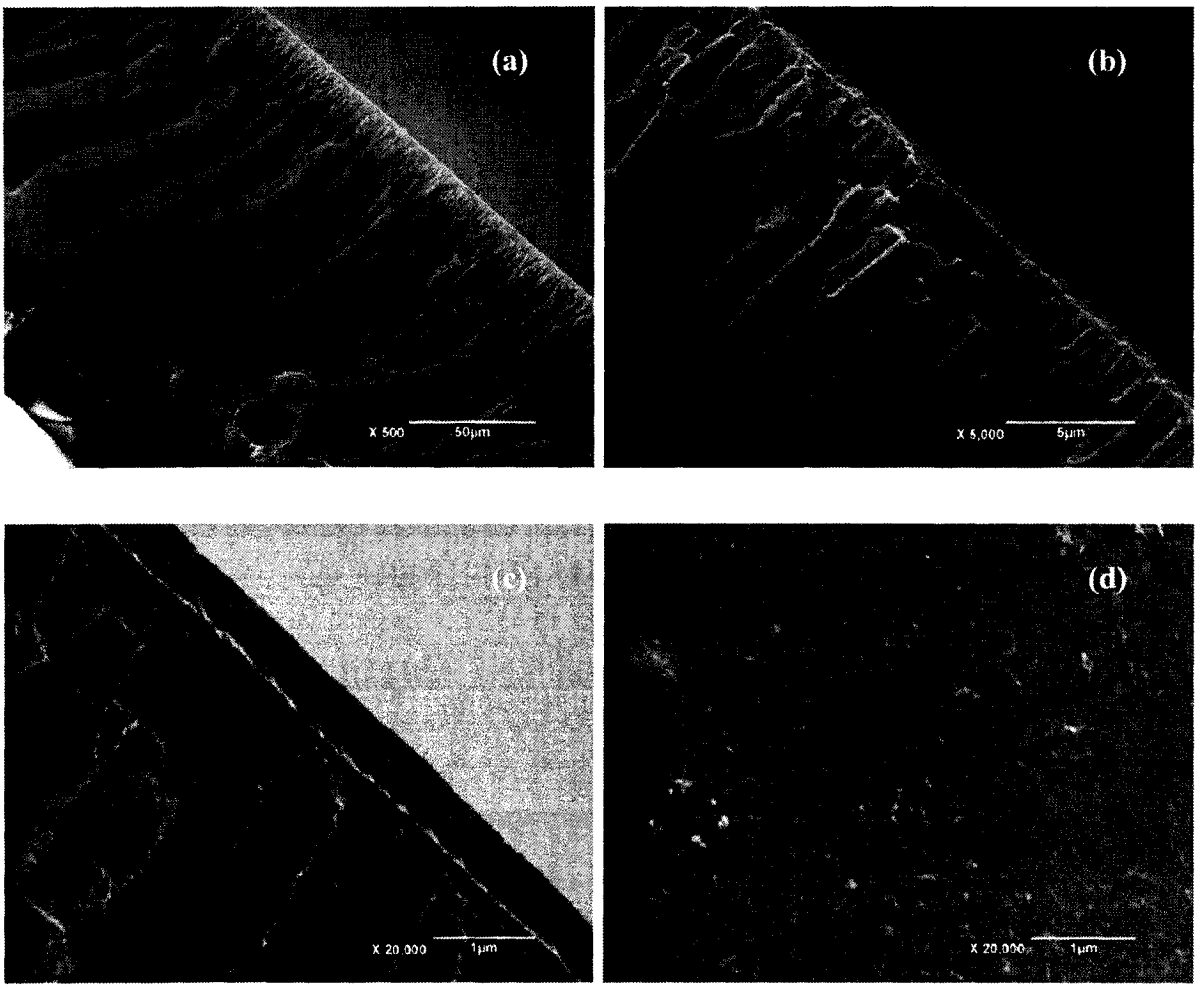

Figure 4.16 – Scanning electron micrograph of cross section and surface of IPACS(NX)L 9h 5% composite membrane after cross linking process with 500x (a); 5,000x (b); and 20,000x (c, d) magnification

4.7 Surface characterization by XPS

The atomic composition (%) measured by XPS of surfaces of Torlon®, IPACS(NX)L 9h 5% before and after cross linking, and Chitosan (Musale *et al.*, 1999) membranes are shown in Table 4.4.

Table 4.4 – XPS measurement of area and atomic composition (%) of surfaces of membrane

Membrane	Area		
	Carbon (C)	Oxygen (O)	Nitrogen (N)
Torlon® 20-0	14580	2831	1395
IPACS(NX)L 9h5% before cross linked	11658	6317	1527
IPACS(NX)L 9h5% after cross linked	11750	6380	1412

Membrane	Composition			Ratio	
	C	O	N	C/O	C/N
Torlon® 20-0	77.5	15.1	7.4	5.2	10.5
IPACS(NX)L 9h5% before cross linked	59.8	32.4	7.8	1.8	7.6
IPACS(NX)L 9h5% after cross linked	60.1	32.6	7.2	1.8	8.3
Chitosan	60.3	32.0	7.7	1.9	7.3

It is clear from the above table that the concentrations of carbon, oxygen, and nitrogen in both IPACS(NX)L membranes concur with those of Chitosan membrane described in literature. The C/O and C/N ratios of IPACS(NX)L are also comparable with those of Chitosan membrane which lead to confirmation of Chitosan layer formed on Torlon® base membrane. Small discrepancies between those numbers could be due to IPA solvent added into the Chitosan buffer for dilution purpose.

Further characterization of the coating surface has been outlined in Table 4.4. Table 4.4 shows the carbon and oxygen contents on IPACS(NX)L membrane surface after cross linking are higher than the one before cross linking. This phenomenon is expected since DEGDMA as cross linking agent contains carbon and oxygen (detailed can be found in Appendix D). The nitrogen content on the surface generally decreases as the cross linking agent used has no nitrogen atoms. The C/N ratio increase is expected from the reaction of Chitosan with DEGDMA. It is hypothesized that the DEGDMA cross linking agent were indeed cross linked with Chitosan chains.

Fourier transform Raman spectroscopy was used to confirm the evidence of cross linking between Chitosan layer and DEGDMA. Because of the coating layer is very thin, the first attempt showed that the sampling depth penetrates into the Torlon® region and as a result the Raman spectrum of the composite samples comprised of bands attributed to the Torlon® layer and unfortunately second attempt also did not provide any practical information. It is hypothesized that Fourier transform Infrared would provide more information about the composition of the composite membrane which could support the XPS results which confirm the formation of Chitosan layer on Torlon® base membrane.

4.8 pH Stability of membranes

Figure 4.17 shows the change in PWP and PEG rate after IPACS(NX)L 9h 5% composite membranes are treated with an aqueous acidic (pH 3.0) and basic (pH 11) solutions, respectively. All PWP and PEG product rate values in Figure 4.17 are the average of six membrane coupons for each aqueous solution. Bar charts are plotted with standard errors (around 3.2 to 5 $lm^{-2}h^{-1}$) calculated from the standard deviations of the experiment. It is shown that the changes in both PWP and PEG product rate after aqueous acidic solution treatment are less profound than the PWP and PEG transmission after aqueous basic solution. However, visual examination showed that the membrane coupons treated with aqueous acidic solution have degraded. There were spots on the membrane surface where the Chitosan layer became distorted. It is hypothesized that this phenomenon occurred because Chitosan is soluble in acidic solutions (pH less than 6.5) due to protonation of $-NH_2$ groups, though less number of $-NH_2$ groups of Chitosan remained after surface cross linking occurred. These protonation effects lead to swelling and distortion on Chitosan layer

subsequently reduced PWP and PEG flux. Large variance between membrane coupons shown could also be the result of this distortion. Sharma *et al.* (2003) also pointed that chemical effects including Van der Waals interactions, adsorption, and hydrogen bonding, may result in large discrepancies between the energy of diffusion within membrane pores and the solute permeability across the membrane.

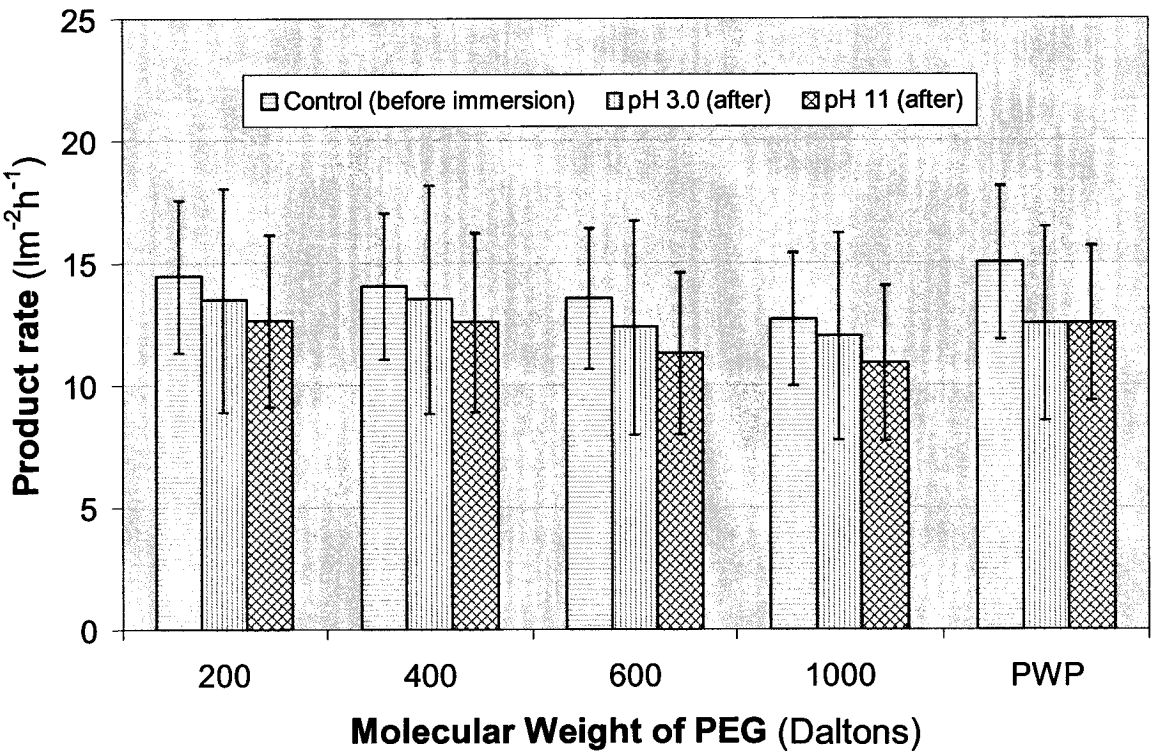

Figure 4.17 – PWP and PEG flux for IPACS(NX)L 9h 5% composite membranes before and after pH immersion

Aside from the protonation in aqueous acidic solution which resulted in distortion of Chitosan layer, membranes treated with aqueous basic solution show lower PWP and PEG flux than membranes treated with aqueous acidic solution. Also, similar trends in PWP and PEG flux variation could be observed. Swelling is likely to be the major cause of these

observations. Overall, even though PWP and PEG fluxes are lower for membrane coupons treated with aqueous basic solution, the visual observation indicate that the IPACS(NX)L 9h 5% composite membranes are more stable at pH 11 than at pH 3.0.

Aggressive chemicals can irreversibly degrade the membranes by oxidation, nitration, hydrolysis, and acid-catalysed hydrolysis processes. These processes eventually lead to chain scission, cross linking, and chemical modification (Platt *et al.*, 2004). The extent of attack is dependent on the concentration of chemical agent, duration of contact, temperature, and the chemical structure and morphology of the membranes. Scheirs (1983) and Platt *et al.* (2004) mentioned that the key indicators of chemical degradation are: embrittlement, surface cracking, blistering, pock-marks on the surface (due to etching), swelling or distortion, discolouration (due to oxidation), and voids or holes caused by selective dissolution. This chemical degradation effect is studied and observed in pH swelling experiment for Torlon®/Chitosan composite membranes prepared using IPACS(NX)L 9h 5% membranes. For this study, four Torlon®/Chitosan composite membrane coupons were used.

Experimental data presented in Figure 4.18 show that the swelling of the composite membranes is higher at pH 12. It is hypothesized that the higher swelling at pH 12 is due to formation of $-NH^-$ groups from the residual $-NH_2$ groups of Chitosan (Musale and Kumar, 2000) or slight effect of chemical degradation by hydrolysis and oxidation of Torlon®, which led to higher absorption of water. To study the degree of oxidation on these composite membranes, the same pH swelling procedures are repeated for Torlon® 20-0 base membranes. Torlon® coupons showed a complete discolouration on the whole membrane surface whilst only a small spot of discolouration occurred on Torlon®/Chitosan composite

membranes. Therefore, it is concluded that cross linking has decreased the effect of degradation on composite membranes.

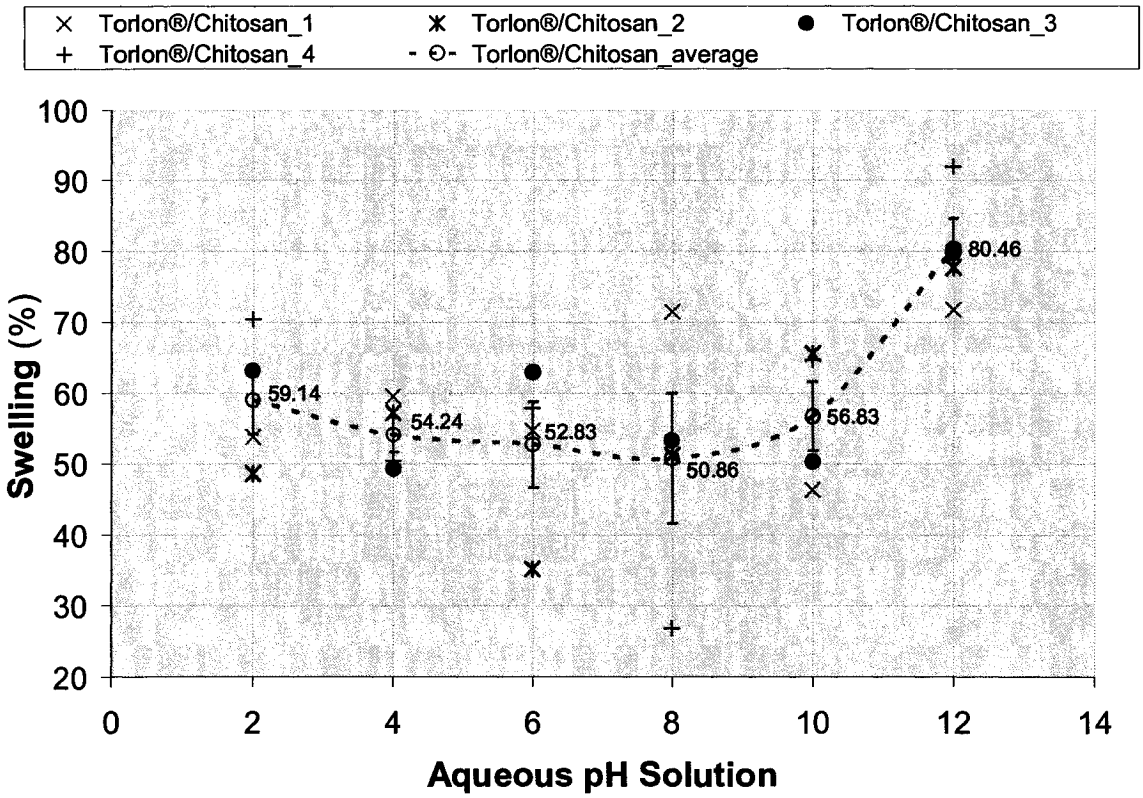

Figure 4.18 – Effect of pH on swelling of IPACS(NX)L 9h 5% composite membranes

The percentage of swelling at pH 2.0 shows that the swelling was less dramatic than those membranes exposed to pH 12. On the other hand, swelling in the pH ranges of 4.0 to 10 was relatively insignificant. Again, the difference or discrepancies in swelling percentage for these membranes could be affected by pore size distribution and thickness of membrane coupons. In general, cross linking in Torlon®/Chitosan composite NF membrane has improved the pH stability in the pH range of 4.0 to pH 10. However, there is scope for additional studies to enhance membrane performance and reproducibility.

4.9 Solvent stability of membranes

Since polyamides and polyimides are the type of materials susceptible to chemical degradation through hydrolysis (Platt *et al.*, 2004), swelling studies were done to verify the tolerance of Torlon®/Chitosan composite NF membranes for solvent degradation by soaking the membranes in solvents for a period of time. As in the pH swelling studies, four composite membrane coupons are tested for each test solvent. In addition, two Torlon® base membranes were also tested in this swelling study.

Interestingly, membrane instability can result in significantly large fluxes due to swelling and/or cracking of the membrane. It can also lead to negligible solvent permeation due to shrinking of the membrane matrix. The visual observations on the membranes after contact with organic test solvents are summarized in Table 4.5.

Table 4.5 – Observation of membrane compatibility with organic test solvent

Membrane	MeOH	EtOH	IPA	MEK	EtOAc	Hexane
Torlon® 20-0	Curled	Slightly curled	Slightly curled	Rolled	Rolled	Flat
IPACS(NX)L 9h5%	Curled	Flat	Curled	Rolled	Curled	Flat

It is evident that no immediate cracking occurred when the membranes were brought in contact with the test solvents, instead most of the membranes curled or rolled after few minutes of exposure to solvents. The membranes were soaked in test solvents for 24 h but the results for longer immersion time may be more significant. Yang *et al.* (2001) pointed that the swelling of one surface and shrinking of the other surface lead to membrane curling and rolling up which could result in unexpectedly high or low fluxes. Since Chitosan is

hydrophilic and Torlon® itself is known to have a good solvent resistance, no changes to the active surface of the membranes especially the IPACS(NX)L 9h 5% composite membranes were visually observed during the tests.

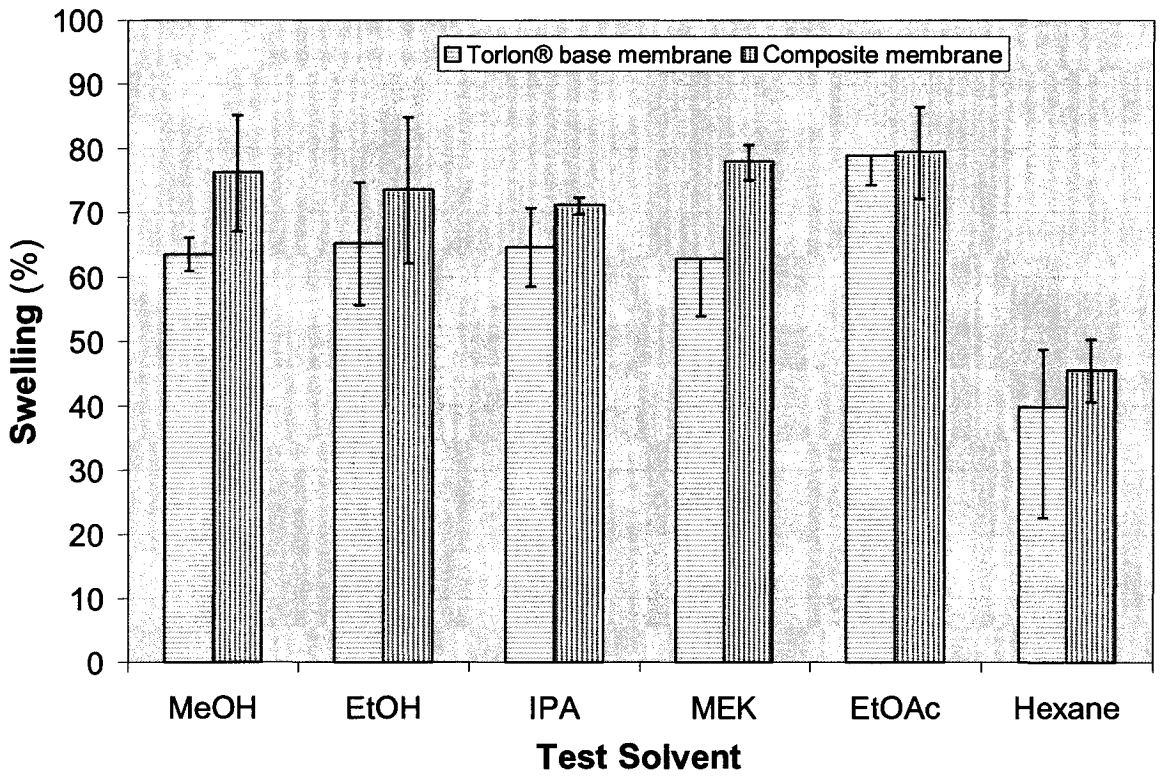

Figure 4.19 – Swelling effect of IPACS(NX)L 9h 5% and Torlon® 20-0 membranes after immersion in test solvent

On the other hand, Figure 4.19 show that both Torlon® 20-0 base and Torlon®/Chitosan composite membranes swelling percentage are relatively high. As the Chitosan coating is relatively thin in comparison to Torlon® base, the swelling percentage for each coating and base membrane layer is very hard to determine. Comparison of the swelling percentage on Torlon® 20-0 and the IPACS(NX)L 9h 5% composite membrane

shown in the figure, clearly shows that the swelling differences are quite insignificant. Perhaps it could be argued that predominant swelling occurs on Torlon® base membrane. It appears that swelling discrepancies between those two membranes are taking place due to an increase in hydrophobicity of membranes, caused by insertion of non polar $=CH-(CH_2)_3-CH=$ links between Chitosan chains which resulted in increased affinity with organic solvents (Musale and Kumar, 2000). It is also concluded that due to polar hydroxyl groups in Chitosan chains, membrane-solvent polar interactions and solvent's dielectric constant play a major role in membranes swelling. Figure 4.19 confirms that alcohols, which dielectric constants ranging from 18.3 to 32.6 and are the highest among the entire test solvents, tend to swell the membranes to a greater extend. The same phenomenon was observed for hexane which has the smallest dielectric constant of 1.9 and shows the least to swelling. Clearly with the same effect, membranes immersed in MEK and EtOAc, with dielectric constant of 15.4 and 6.02 respectively, are expected to swell less than alcohol but more than hexane. However, Figure 4.19 shows membranes immersed in MEK and EtOAC showed the highest swelling which could not be explained with the dielectric constant values alone. In order to eliminate the possibility of human or mechanical error, PWP measurements after solvent immersion were performed.

The importance of dielectric constant in membrane–solvent interaction has also been emphasized by Musale and Kumar (2000) in their study on the permeation of solvent through polyacrylonitrile and Chitosan composite membranes. The authors pointed that the trend in swelling of membranes with various solvents could also be correlated to the difference between solubility parameters of solvents and membrane. It was observed that Chitosan layer was more likely to swell in MEK and EtOAc, and less likely to swell in

alcohols. This literature observation supports the hypothesis drawn previously. The swelling trends, shown in Figure 4.19, indicate that contribution of Torlon® swelling could be higher in total swelling in the case of alcohols, where as in the case of MEK and EtOAc, Chitosan was likely to swell more than Torlon®.

4.10 Solvent immersion studies

The membrane characteristics could possibly change over time either due to the adsorption, fouling or other surface damages caused by trace contaminants. This outcome will be more acute for membrane coupon using various solutes at different temperatures, pressures and cross flow velocities in a longer term operation. Sharma *et al.* (2003) marked that changes in water permeability or neutral solute retention by a particular NF membrane coupon with time (for one set of operating conditions) indicated that its sieving characteristics such as thickness, surface porosity, and pore size distribution have changed during the course of experiments necessitating replacement of the coupon. Hence, to study the possible changes in membrane performance, PWP tests for IPACS(NX)L 9h 5% membranes were conducted before and after immersion in solvents.

Table 4.6 – PWP of IPACS(NX)L 9h 5% membranes before and after immersion in solvent

Solvent	PWP ($lm^{-2}h^{-1}$)	Difference (before – after) in $lm^{-2}h^{-1}$
Control (before immersion)	15.0 ± 3.1	0
Methanol	10.7 ± 2.7	-4.3
Ethanol	12.1 ± 5.0	-2.9
Iso-propanol	14.0 ± 4.5	-1.1
Methyl ethyl ketone	8.1 ± 1.7	-6.9
Ethyl acetate	8.9 ± 1.9	-6.1
Hexane	10.3 ± 3.2	-4.7

Table 4.6 summarizes the change in PWP of the membranes before and after immersion in various test solvents. The data show that PWP of the membranes has indeed decreased after solvent immersion. Membranes immersed in MEK and EtOAc show the most significant effect though the change was still considered to be tolerable in NF range. Geens *et al.* (2004) hypothesized that the changes in PWP after solvent treatment were caused by the reorganization of the membrane material, a shift of pore size distribution, and the change of surface hydrophilicity. It was reported that hydrophilic membranes showed lower rejections after solvent treatment indicating an increase of the pore size. On the other hand, the same membranes also showed a decrease of PWP after solvent exposure which was not expected when pore size would increase. Therefore, it was concluded that a decrease in the degree of surface hydrophilicity caused the lower water fluxes.

The swelling data on the membrane structures shown on Figure 4.19 may also influence the PWP fluxes. It is hypothesized that after solvent exposure, dense membranes become even denser, which correspond to a lower flux due to decreased free volume and decreased diffusivity (Geens *et al.*, 2004). Inversely, pores were larger in case of a porous

membrane showed a lower degree of swelling which correspond to a higher flux due to larger pores. The SEM image of Torlon®/Chitosan composite membrane after cross linking, previously shown in Figure 4.16, confirmed that the Chitosan layer can be categorized as a dense layer with no visible pores on the surface. The formation of Chitosan dense layers on Torlon® membranes surface are more profound to degree of swelling in contact with MEK and EtOAc, which explained the elevated swelling in membranes illustrated in Figure 4.19, thus leading to a lower PWP flux after immersion. Na *et al.* (2000) investigated the development of PVA composite membranes and showed that membrane modification using cross linking agents caused a lowering in the flux was attributed to the formation of a denser coating. Burczak *et al.* (1994) have also reported that the cross linking agent formed a denser cross linked PVA hydrogel network. They also observed that after cross linking the retention increased and the water fluxes decreased. However the different degree of swelling can not be excluded completely, it can be concluded from this observation that Torlon®/Chitosan composite membranes prepared via IPACS(NX)L 9h 5% technique sustain their physical and chemical structure after immersion in solvents.

4.11 Solvent permeation studies

The actual solvent permeation rates measured as a function of time are shown in Figure 4.20. As mentioned earlier, a fresh new membrane coupon was used for each test solvent in order to avoid the effect of "polymer memory". Difficulties in testing were noted while membrane coupons were tested with EtOH. Four coupons were tested but the first three EtOH fluxes could not be measured. After pressure in the test cell was adjusted (482.63 kPa), the flux through the membrane was very high and the beaker on the weight

balance filled in the matter of seconds hence flux was unreadable. Hence, it can be concluded that wetting or conditioning the membranes prior to use with EtOH decreased the swelling possibilities on membranes structure bearing in mind that average pore size distribution also plays a major role. On increasing the surface tension of the solvent from water to EtOH gradually, using EtOH-Water mixtures, the following procedure was used; soaking was done in 25% EtOH for a long period time[3], 50% EtOH for 30 minutes, and twice in EtOH for 30 minutes each has a strong effect on flux and membrane integrity thus improving the flux performance.

On the other hand, when hexane was used as test solute through the composite membrane, flux could not be observed. On repeating the experiment, it was found that the flux from a newly soaked membrane coupon could be recorded. From this result, it can be concluded that aside from pore size distribution, this phenomenon could be attributed to the fact that hexane had the lowest dielectric constant (non polar) and hydrophobicity.

[3] All prepared composite NF membrane coupons were immersed in 25% aqueous EtOH before they were further characterized. This method is to ensure that no possible fouling due to bacteria growth in membrane matrix can arise.

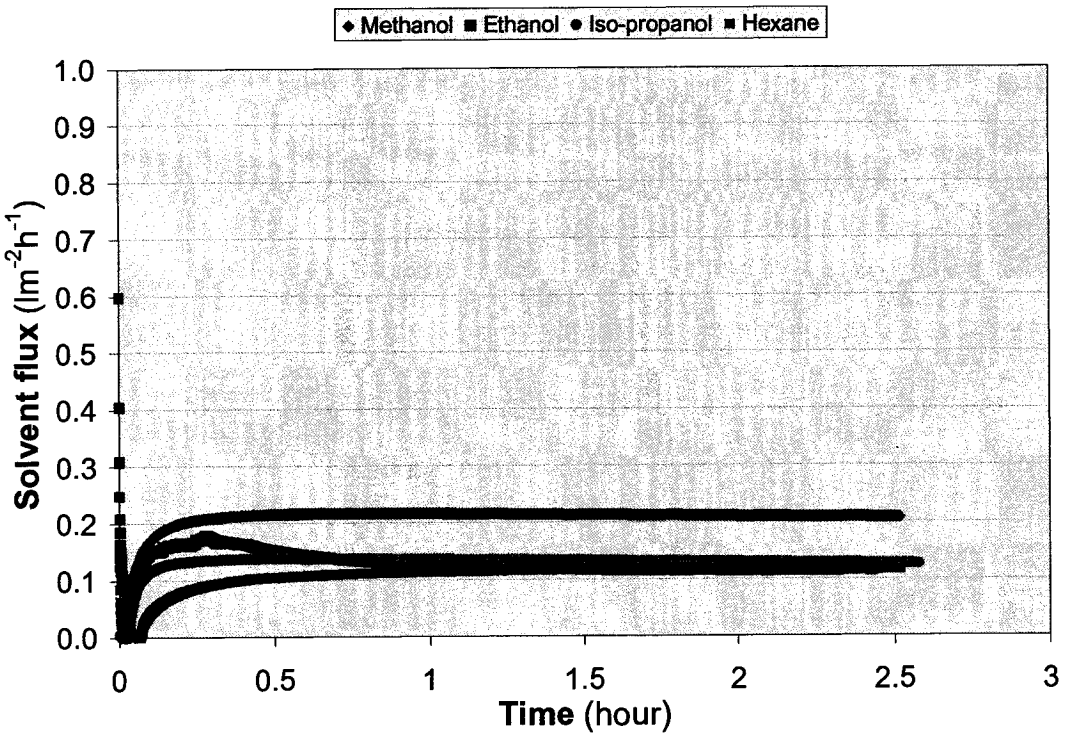

Figure 4.20 – Effect of operation time on solvent flux for IPACS(NX)L 9h 5% membranes

Figure 4.20 shows that the fluxes decline of EtOH and hexane, can be attributed to membrane compaction under pressure for all coupons tested. Membrane compatibility, especially in hexane, slight decreased in the effective membrane contact due to swelling and flattening of the O-ring in the stirred cell. As the time increased, the fluxes reached a steady state. Gibbins *et al.* (2002) indicated that the volume of solvent permeated before obtaining steady flux was a function of the membrane morphology, implying that a universal pre-fluxing volume could not be defined as it was dependent on the polymer from which the membrane was made. Yang *et al.* (2001) and Whu *et al.* (2000) also observed the transient period (initial flux decrease) when filtering solvents through membranes. Vankelecom *et al.* (2004) estimated the membrane was relatively swollen in the beginning of the NF experiment. Due to the applied pressure, the dense top layer was squeezed slowly till

equilibrium was reached subsequently resulting in a higher resistance for the migrating compounds.

For the alcohol series, flux changes can be represented as MeOH flux > EtOH flux > IPA flux. These verify the dependence of the flux on molecular size (smaller for MeOH), viscosity (lower for MeOH), and dielectric constant or polarity (higher for MeOH) among each homologous series of solvents. But there is no clear explanation to the reason why the EtOH flux started to decrease after 30 minutes experimentation time. Van der Bruggen *et al.* (2002) marked that immersion in ethanol caused a clustering effect on hydrophobic and hydrophilic groups in the membrane top layer. Hydrophilic membranes were postulated to become slightly more hydrophobic whereas hydrophobic membranes became more hydrophilic. Hestekin *et al.* in Nunes and Peinemann's membrane technology book (2001) also pointed out that increasing hydrophobicity of solvents in hydrophilic NF membranes were shown to decrease flux through membrane due mainly to membrane solubility and a decreased in pore size in the membrane polymer morphology. It is assumed that the particular membrane coupon became more and more hydrophobic after wetting or conditioning prior testing, compaction, and through out the test leading to a decrease in pore size. Figure 4.20 shows that alcohols (polar solvent) with higher flux than hexane (non polar solvent with low surface tension) confirms that Torlon®/Chitosan composite membrane are indeed a hydrophilic membrane.

The overall observations that can be summarized from Figure 4.20 are that solvent flux remains almost constant with operation for 2.5 h and solvent with higher polarity (dielectric constant) will permeate faster hence lower flux decrease compared to solvent with lower polarity. Hence it can be concluded that the performance of Torlon®/Chitosan

composite membrane depends on the effects of solubility parameter, dielectric constant, surface tension, and viscosity of solvents, it can be argued that this membrane has good solvent resistance. However, more permeation data with solvents is required for determining membrane durability and for reducing the discrepancies within membrane pores and the solute permeability across the membrane that are known to arise from non-homogeneity of the membrane coupon (i.e. variability of thickness, porosity, and pore size distribution in membrane active area).

CHAPTER 5

CONCLUSIONS

Polyamide imide (commonly known as Torlon®) ultrafiltration membranes with molecular weight cut-off (MWCO) around 13 000 Daltons and pure water permeation (PWP) value of 49.73 $lm^{-2}h^{-1}$ were prepared using phase inversion process. Asymmetric composite nanofiltration membranes using Torlon® and naturally available Chitosan biopolymer were prepared successfully. Torlon®/Chitosan membranes were prepared by coating the Chitosan solution on the Torlon® base membrane, subsequently curing followed by neutralization with $NaHCO_3$. From the results of these investigations, it was concluded that cross linking of top active layer of Torlon®/Chitosan with diethylene glycol dimethacrylate (DEGDMA) could lower molecular weight cut-offs to under 1 000 Daltons.

SEM studies revealed the presence of very thin coating layer of Chitosan on Torlon®, while XPS studies indicated the presence of atomic compositions that are characteristic of Chitosan on the surface of the composite membrane. An increase in C/N ratio resulted from XPS measurement also indicated a probable cross linking between DEGDMA and Chitosan on the membrane surface.

Torlon®/Chitosan composite membranes were found to be more stable at pH 11 than at pH 3.0. Cross linking used in the formation process has decreased the effect of degradation on membranes such as embrittlement, swelling or distortion, and discolouration. Based on the swelling studies, the cross linking also improved the pH stability of these composite membranes and recommended for practice at pH 4.0 up to pH 10.

The static swelling measured for these Torlon®/Chitosan membranes was least for non polar hexane and higher for alcohols. Aside from the unexpected advanced swelling from MEK and EtOAc, the swelling trend indicated a strong dependence on the effects of solubility parameter, dielectric constant, surface tension, and viscosity of solvents. High

degree of swelling in the membranes was attributed to the swelling of Torlon® base membranes. The results shown that Torlon® base swell more after contact with solvents thus lead to increase swelling degree in the composite membranes. On the other hand, characterization of these membranes through solvent immersion indicated that these composite membranes maintain their structure after contact with test solvents for appreciable time. After compaction stages, solvent fluxes were stabilized up to 2.5 hours which indicated excellent solvent resistance of these membranes.

Based on the MWCO, PWP measurements, and performance with test solvents data, it can be concluded that these hydrophilic NF membranes have a potential use for processing solvent containing feeds. New coating methods developed from commercially available biopolymer and straightforward cross linking process has been successfully achieved. However, further tests to increase the permeability of solvents are still necessary to develop a high-quality solvent resistance NF membrane.

CHAPTER 6

RECOMMENDATIONS

Further experiments should be conducted to verify the reproducibility and reliability of the membrane performance data. Torlon®/Chitosan NF membranes should be prepared in a more control environment to reduce any possible discrepancies due to non-homogeneity of the membrane coupons.

In the present study, the nanofiltration membranes were characterized with various test solvents. The membranes should also be characterized with multivalent salts and sugar solutions that were present in the forms of ions to investigate any change and understand further the permeation behaviour of these membranes with the charged and neutral solutes.

Pore size distribution studies should be done to verify if the Chitosan coating layer formed on the entire pore walls of the base membrane or simply located on the membrane surface or cover the base membrane pore walls only partially. FTIR should be carried out to determine the functional groups on the membrane surface which could corroborate the results obtained from XPS studies.

In most NF processes, the feed consists of more than one solute and the separation is carried out among different solutes, for example either the multivalent ions are separated from the monovalent ions or the organic solutes are separated from the monovalent salts. A detailed study is necessary to understand the effect of changes in permeability of the solutes in multi-component feed solutions in comparison to single solute solution.

It is usually hypothesized that a rise in temperature increases permeation flux through either reduction in solvent viscosity or an increase in solvent diffusion coefficient or by an increase in polymer chain mobility. It is also mentioned that an increase in average pore size and a corresponding increase in MWCO with increasing temperature indicated thermal expansion of the polymer constituting the active layer of thin film composite

membranes. Therefore, it would be interesting to determine if introducing heat treatment on Torlon®/Chitosan membranes formation would provide a higher permeability of solvents.

Development of less rigid membrane for support base membrane under Chitosan coating layer is also motivating. Polyvinylpyrrolidone (PVP) can be used as additive in Torlon® casting solution to create UF membranes with bigger pore size so that less resistance was offered to the permeation of solvents. It is theorized that Chitosan coating solution will penetrate more into the support porous walls providing a coat which will increase the compatibility of membrane to solvent resistance, reduce the swelling from the solvent contact, and thus increase solvents fluxes through the membrane.

BIBLIOGRAPHY

Books

Bloch, D. R., Polymer Handbook by Brandrup, J., Physical Constant of the Most Common Solvents for Polymers, 4th Edition, John Wiley & Sons Ltd., New York, 1999, pp. III/59-III/61.

Burggraaf, A. J., Cot, L., Fundamentals of Inorganic Membrane Science and Technology, Membrane Science and Technology Series (4), Elsevier Science B. V., Amsterdam, The Netherlands, 1996, pp. 1-34..

Daligaux, E., ICAM 99, Energetics Department, Implementation of an Automatic Bench Test used in the Characterization of Ultrafiltration Membranes, National Research Council of Canada, ICPET Institute for Chemical Process and Environmental Technology, Ottawa, Canada, 1999.

Johns, F. J., Membrane Technologies for Industrial and Municipal Wastewater Treatment and Reuse, Introduction to Membrane Technologies, Water Environment Federation, Alexandria, U.S.A., 2000.

Kurdi, J., Doctor of Philosophy Thesis, Molecular Engineering and Nanostructuring of Polymer Networks for High Performance Gas Separation Membranes, Department of Chemical Engineering, University of Ottawa, ON, Canada, 2003.

Li, N. N, Calo, J. M., Separation and Purification Technology, Marcel Dekker Inc., New York, U.S.A., 1992, pp. 1-17.

Long R. B., Separation Processes in Waste Minimization, Marcel Dekker Inc., New York, U.S.A., 1995, pp. 233-275.

Mark, H. F., Bikales, N., Overberger, C. G., Menges, G., Kroschwitz, J. I., Encyclopedia of Polymer Science and Engineering, Engineering Plactics, Vol. 6, 2nd Edition, John Wiley & Sons Ltd., New York, U.S.A., 1985, pp. 104-105.

Meares, P., Membrane Separation Processes, Elsevier Scientific Publishing Company, Amsterdam, The Netherlands, 1976.

Nunes, S. P., Peinemann, K. V., Membrane Technology in The Chemical Industry, Wiley-VCH Verlag Gmbh, Weinheim, Germany, 2001, pp.6-38, 173-187.

Rautenbach, R., Albrecht, R., Membrane Processes, Translated by V. Cottrell, John Wiley & Sons Ltd., New York, U.S.A., 1989, pp. 1-75.

Schäfer, A. I., Natural Organics Removal Using Membranes – Principles, Performances and Cost, Technomic Publishing Company Inc., Pennsylvania, U.S.A., 2001, pp. 92-130, 215-280.

Scheirs, J., Compositional and Failure Analysis of Polymers, John Wiley & Sons Inc., New York, U.S.A., 1983.

Scott, K., Handbook of Industrial Membranes, 1st Edition, Elsevier Science Publishers Ltd., Oxford, UK, 1995, pp. 3-257.

Sourirajan, S., Matsuura, T., Reverse Osmosis and Ultrafiltration, ACS Symposium Series 281, American Chemical Society, Washington, U.S.A., 1985.

Sperling, L. H., Introduction to Physical Polymer Science, 2nd Edition, John Wiley & Sons Inc., New York, U.S.A., 1992.

Stern, S. A., Noble, R. D., Membrane Separations Technology – Principles and Applications, Membrane Science and Technology Series (2), Elsevier Science B. V., Amsterdam, The Netherlands, 1995, pp. 1-40, 113-140.

Tan, L. S., Polymer Data Handbook, Poly(amide imide), Oxford University Press, JE Mark(ED) New York, U.S.A., 1999, pp. 260-265.

Tremblay, A. Y., Doctor of Philosopy Thesis, The Role of Structural Forces in Membrane Transport: Cellulose Membranes, Department of Chemical Engineering, University of Ottawa, ON, Canada, 1989.

Utracki, L. A., Polymer Blends, Rapra Review Reports – Expert overviews covering the science and technology of rubber and plastics, Vol. 11, No. 3, Rapra Technology Ltd., Shropshire, UK, 2000, pp. 3-28.

Watson, J. S., Separation Methods for Waste and Environmental Applications, Marcel Dekker Inc., New York, U.S.A., 1999, pp. 253-345.

Web Sites

Andersen, Niels Peder Raj, Chapter 6a – Membrane Technology,
http://www. .bio.auc.dk/~mlc/Chapter6aMembranes.pdf

Jijun, G., Yan, Y., Yongfang, C., Zhiying, Z., Hua, Z., Effect of Post-treatment on the Performance of the Particle-filled PAN Membrane, Chemical Journal on Internet, vol. 2, No. 2 (2000) p.10.
http://www.chemistrymag.org/cji/2000/022010ne.htm

Permionics Manufacturer of Reverse Osmosis Membranes, Ultrafiltration, Nanofiltration Membrane, Products – Proprietary Membranes,
http://www.permionics.com/prop_membranes.htm

Yongfang, C., Yan, Y., Jijun, G., Study of Alcohol Permselevtive Separation Membrane with a High Flux, Chemistry Online, http://hxtb.icas.ac.cn/col/2000/c00044.htm

http://www.comalc.com/

http://www.emdchemicals.com/corporate/emd_corporate.asp

http://www.fishersci.ca/

http://www.kochmembrane.com/sep_nf.html

http://www.millipore.com

http://www.sigmaaldrich.com/Local/SA_Splash.html

http://www.solvayadvancedpolymers.com

http://www.tech2004.umd.edu/2004posters/R-A_bioMEMS.pdf

Journals and articles

Ahmad, A. L., Ooi, B. S., Mohammad, A. W., Choudhury, J. P., Development of a Highly Hydrophilic Nanofiltration Membrane for Desalination and Water Treatment, Desalination 168 (2004) 215-221.

Ali, N., Mohammad, A. W., Ahmad, A. L., Use of Nanofiltration Predictive Model for Membrane Selection and System Cost Assessment, Separation and Purification Technology 41 (2005) 29-37.

Baker, R. W., Overview of Membrane Science and Technology, Membrane Technology and Applications (2004) 1-14.

Baker, R. W., Kaschemekat, J., Wijmans, J. G., Kamaruddin, H. D., Process for Removing an Organic Compound from Water, United States Patent: 5,273,572 (1993).

Bandini, S., Vezzani, D., Nanofiltration Modeling: the Role of Dielectric Exclusion in Membrane Characterization, Chemical Engineering Science 58 (2003) 3303-3326.

Barucci, M., Olivieri, E., Pasca, E., Risegari, L., Ventura, G., Thermal Conductivity of Torlon between 4.2 and 300 K, Cryogenics 45 (2005) 295-299.

Bellona, C., Drewes, J. E., The Role of Membrane Surface Charge and Solute Physico-chemical Properties in the Rejection of Organic Acids by NF Membranes, Journal of Membrane Science 249 (2005) 227-234.

Bershtein, V. A., Egorov, V. M., Egorova, L. M., Yakushev, P. N., David, L., Sysel, P., Sindelar, V., Pissis, P., Poly(amide-imide)-poly(ethylene adipate) Hybrid Networks. I. Nanostructure and Segmental Dynamics, Polymer 43 (2002) 6943-6953.

Bessarabov, D., Twardowski, Z., Industrial Application of Nanofiltration – New Perspectives, Membrane Technology 2002 (9) (2002) 6-9.

Bhanushali D., Bhattacharyya, D., Advances in Solvent Resistant Nanofiltration Membranes – Experimental Observations and Applications, Annual N. Y. Academic Science 984 (2003) 159-177.

Bhanushali, D., Kloos, S., Bhattacharyya, D., Solute Transport in Solvent-resistant Nanofiltration Membranes for Non-aqueous Systems: Experimental Results and the Role of Solute-solvent Coupling, Journal of Membrane Science 208 (2002) 343-359.

Bhanushali, D., Kloos, S., Kurth, C., Bhattacharyya, D., Performance of Solvent-resistant Membranes for Non-aqueous Systems: Solvent Permeation Results and Modeling, Journal of Membrane Science 189 (2001) 1-21.

Bhattacharjee, S., Kim, A. S., Elimelech, M., Concentration Polarization of Interacting Solute Particles in Cross-flow Membrane Filtration, Journal of Colloid and Interface Science 212 (1999) 81-99.

Blume, I., Peinemann, K. V., Pinnau, I., Wijmans, J. G., Composite membranes for Fluid Separations, United States Patent : 5,085,776 (1992).

Blume, I., Pinnau, I., Composite Membrane, Method of Preparation and Use, United States Patent 4,963,165 (1990).

Bonina, P., Petrova, Ts., Manolova, N., pH-Sensitive Hyrdogels Composed of Chitosan and Polyacrylamide – Preparation and Properties, Journal of Bioactive and Compatible Polymers 19 (2004) 101-116.

Bowen, W. R., Cassey, B., Jones, P., Oatley, D. L., Modeling the Performance of Membrane Nanofiltration – Application to an Industrial Relevant Separation, Journal of Membrane Science 242 (2004) 211-220.

Bowen, W. R., Mukhtar, H., Characterization and Prediction of Separation Performance of Nanofiltration Membranes, Journal of Membrane Science 112 (1996) 263-274.

Bryce, R. M., Nguyen, H. T., Nakeeran, P., Clement, T., Haugen, C. J., Tykwinski, R. R., DeCorby, R. G., McMullin, J. N., Polyamide-imide Polymer Thin Films for Integrated Optics, Thin Solid Films 458 (2004) 233-236.

Burczak, K., Fujisato, T., Hatada, M., Ikada, Y., Protein Permeation through Poly(vinyl alcohol) Hydrogel Membranes, Biomaterials 15 (1994) 231-238.

Castro, R. P., Baker, R. W., Wijmans, J. G., Multilayer Interfacial Composite Membrane, United States Patent: 5,049,167 (1991).

Chen, S., Chang, D., Liou, R., Hsu, C., Lin, S., Preparation and Separation Properties of Polyamide Nanofiltration Membrane, Journal of Applied Polymer Science 83 (2002) 1112-1118.

Chern, Y., Wu, B., Preparation of Composite Membranes with Polyimides and Poly(amide-imide)s Skin via Interfacial Condensation for Air Separation, Institute of Chemical Engineering, National Taiwan Institute of Technology, China (1997) 693-701.

Dal-Cin, M. M., Kumar, A., Kirpalani, D. M., Daligaux, E., Jubely, D., Lalangue, F., Gabbard, D., An Apparatus for Automated Cross Flow Solute Permeation Characterization of Membranes, Instrumentation Science and Technology (2005) In Press.

Dal-Cin, M. M., Striez, C. N., Tam, C. M., Tweddle, T. A., Ung, K., Reproducibility of Membrane Testing Procedures, National Research Council Canada Report, Ottawa, Canada (1995) 1-21.

Dal-Cin, M. M., Striez, C. N., Tweddle, T. A., Membrane Casting Reproducibility, National Research Council Canada Report, Ottawa, Canada (1991) 1-51.

Du, R., Zhao, J., Properties of Poly(N,N-dimethylaminoethyl methacrylate)/polysulfone Positively Charged Composite Nanofiltration Membrane, Journal of Membrane Science 239 (2004) 183-188.

Ebert, K., Cuperus, P., Solvent Resistant Nanofiltration Membranes in Edible Oil Processing, Membrane Technology 107 (1999) 5-8.

Ebert, K., Fritsch, D., Koll, J., Tjahjawiguna, C., Influence of Inorganic Fillers on the Compaction Behaviour of Porous Polymer Based Membranes, Journal of Membrane Science 233 (2004) 71-78.

Feng, X., Huang, R. Y. M., Pervaporation with Chitosan Membranes. I. Separation of Water from Ethylene Glycol by a Chitosan/polysulfone Composite Membrane, Journal of Membrane Science 116 (1996) 67-76.

Freeman, B. D., Pinnau, I., Gas and Liquid Sperations Using Membranes: An Overview, American Chemical Society Symposium Series 876 (2004) 1-22.

Freger, V., Bottino, A., Capannelli, G., Perry, M., Gitis, V., Belfer, S., Characterization of Novel Acid-stable NF Membranes Before and After Exposure to Acid Using ATR-FTIR, TEM and AFM, Journal of Membrane Science 256 (2005) 134-142.

Fritsch, D., Peinemann, K. V., Novel Highly Permselective 6F-poly(amide-imide)s as Membrane Host for Nano-sized Catalysts, Journal of Membrane Science 99 (1995) 29-38.

Geens, J., Van der Bruggen, B., Vandecasteele, C., Characterisation of the Solvent Stability of Polymeric Nanofiltration Membranes b Measurement of Contact Angles and Swelling, Chemical Engineering Science 59 (2004) 1161-1164.

Gésan-Guiziou, G., Boyaval, E., Daufin, G., Nanofiltration for the Recovery of Cauting Cleaning-in-place Solutions: Robustness towards Large Variations of Composition, Desalination 149 (2002) 127-129.

Gibbins, E., D'Antonio, M., Nair, D., White L. S., Frietas dos Santos, L. M., Vankelecom, I. F. J., Livingston, A. G., Observations on Solvent Flux and Solute Rejection across Solvent Resistant Nanofiltration Membranes, Desalination 147 (2002) 307-313.

Guizard, C., Ayral, A., Julbe, A., Potentiality of Organic Solvents Filtration with Ceramic Membranes. A comparison with Polymer Membranes, Desalination 147 (2002) 275-280.

Hicke, H., Lehmann, I., Malsch, G., Ulbricht, M., Becker, M., Preparation and Characterization of a Novel Solvent-resistant and Autoclavable Polymer Membrane, Journal of Membrane Science 198 (2002) 187-196.

Hsiao, S., Yang, C., Chen, C., Liou, G., Synthesis and Properties of Novel Poly(amide-imide)s Containing Pendent Diphenylamino Groups, European Polymer Journal 41 (2005) 511-517.

Hu, Q., Marand, E., In situ Formation of Nanosized TiO_2 Domains within Poly(amide-imide) by a Sol-gel Process, Polymer 40 (1999) 4833-4843.

Hu, Q., Marand, E., Dhingra, S., Fritsch, D., Wen, J., Wilkes, G., Poly(amide-imide)/TiO_2 Nano-composite Gas Separation Membranes: Fabrication and Characterization, Journal of Membrane Science 135 (1997) 65-79.

Huai-min, G., Xian-su, C., Study of Cobalt(II)-Chitosan Coordination Polymer and its Catalytic Activity and Selectivity for Vinyl Monomer Polymerization, Polymers for Advanced Technologies 15 (2001) 89-92.

Huang, J., Cranford, R. J., Matsuura, T., Roy, C., Sorption and Transport Behaviour of Water Vapor in dense and Asymmetric Polyimide Membranes, Journal of Membrane Science 241 (2004) 187-196.

Huang, J., Cranford, R. J., Matsuura, T., Roy, C., Water Vapor Permeation Properties of Aromatic Polyimides, Journal of Membrane Science 215 (2003) 129-140.

Huang, J., Guo, Q., Ohya, H., Fang, J., The Characteristics of Crosslinked PAA Composite Membrane for Separation of Aqueous Organics Solutions by Reverse Osmosis, Journal of Membrane Science 144 (1998) 1-11.

Huang, J., Zhu, Z., Yin, J., Qian, X., Sun, Y., Poly(etherimide)/montmorillonite Nanocomposites Prepared by Melt Intercalation : Morphology, Solvent Resistance Properties and Thermal Properties, Polymer 42 (2001) 873-877.

Huang, R. Y. M., Moon, G. Y., Pal, R., N-acetylated Chitosan Membranes for the Pervaporation Separation of Alcohol/toluene Mixtures, Journal of Membrane Science 176 (2000) 223-231.

Huang, R. Y. M., Pal, R., Moon, G. Y., Crosslinked Chitosan Composite Membrane for the Pervaporation Dehydration of Alcohol Mixtures and Enhancement of Structural Stability of Chitosan/polysulfone Composite Membranes, Journal of Membrane Science 160 (1999) 17-30.

Jones, K., Characterization of Ion-Implanted Nanofiltration Membranes, NNUN REU Program at MSRCE, Howard University (2003) 44-45.

Kanapitsas, A., Pissis, P., Delides, C. G., Sysel, P., Sindelar, V., Bershtein, V. A., Poly(imide-amide)-poly(ethylene adipate) Hybrid Networks. II. Dielectric Studies, Polymer 43 (2002) 6955-6963.

Kim, I., Jegal, J., Lee, K., Effect of Aqueous and Organic Solutions on the Performance of Polyamide Thin-Film-Composite Nanofiltration Membranes, Journal of Polymer Science: Part B: Polymer Physics 40 (2002) 2151-2163.

Kim, I., Lee, K., Preparation of Interfacially Synthesized and Silicone-Coated Composite Polyamide Nanofiltration Membranes with High Performance, Ind. Eng. Chem. Res. 41 (2002) 5523-5528.

Kim, B. K., Oh, Y. S., Lee, Y. M., Yoon, L. K., Lee, S., Modified Polyacrylonitrile Blends with Cellulose Acetate: Blend Properties, Polymer 41 (2000) 385-390.

Kölsch, P., Sziládi, M., Noack, M., Caro, J., Kotsis, L., Kotsis, I., Sieber, I., Ceremic Membranes for Water Separation from Organic Solvents, Review, Chemical Engineering Technology 25 (2002) 357-362.

Koops, G. H., Nolten, J. A. M., Mulder, M. H. V., Smolders, C. A., Poly(vinyl chloride)polyacrylonitrile Composite Membranes for the Dehydration of Acetic Acid, Journal of Membrane Science 81 (1993) 57-70.

Koyuncu, I., Topacik, D., Wiesner, M. R., Factors Influencing Flux Decline during Nanofiltration of Solutions Containing Dyes and Salts, Water Research 38 (2004) 432-440.

Kumar, A., Musale, D., Composite Solvent Resistance Nanofiltration Membranes, United States Patent: 6,113,794 (2000).

Kurdi, J., Tremblay, A. Y., Preparation of Defect-Free Asymmetric Membranes for Gas Separations, Journal of Applied Polymer Science 73 (1999) 1471-1482.

Laîné, J. M., Clark, M. M., Mallevialle, J., Hagstrom, J. P., Effects of Ultrafiltration Membrane Composition, Journal of American Water Works Association (1989) 61-67.

Lebrun, R. E., Xu, Y., Dynamic Characterization of Nanofiltration and Reverse Osmosis Membranes, Separation Science and Technology 34 (8) (1999) 1629-1641.

Lenki, R. W., Williams, S., Effect of Nonaqueous Solvents on the Flux Behaviour of Ultrafiltration Membranes, Journal of Membrane Science 101 (1995) 43-51.

Lee, K., Kim, I., Yun, H., Silicon-coated Organic Solvent Resistant Polyamide Composite Nanofiltration Membrane, and Method for Preparing the same, Korea Res Inst Chem Tech: EP1356856.

Lee, S., Shim, Y., Kim, I. S., Sohn, J., Yim, S. K., Cho, J., Determination of Mass Transport Characteristics for Natural Organic Matter (NOM) in Ultrafiltration (UF) and Nanofiltration (NF) Membranes, Water Science and Technology: Water Supply Vol. 2 No. 2 (2002) 151-160.

Li, F., Liu, W. G., Yao, K. D., Preparation of Oxidized Glucose-crosslinked N-alkylated Chitosan Membrane and In Vitro Studies of pH-sensitive Drug Delivery Behaviour, Biomaterial 23 (2002) 343-347.

Liu, Y., Su, Y., Lee, K., Lai, J., Crosslinked Organic-inorganic Hybrid Chitosan Membranes for Pervaporation Dehydration of Isopropanol-water Mixtures with a Long-term Stability, Journal of Membrane Science 251 (2005) 233-238.

Lu, X., Bian, X., Shi, L., Preparation and Characterization of NF Composite Membrane, Journal of Membrane Science 210 (2002) 3-11.

Machado, D. R., Hasson, D., Semiat, R., Effect of Solvent Properties on Permeate Flow through Nanofiltration membranes. Part I. Investigation of Parameters Affecting Solvent Flux, Journal of Membrane Science 163 (1999) 93-102.

Matienzo, L. J., Winnacker, S. K., Dry Processes for Surface Modification of a Biopolymer: Chitosan, Macromolecular Materials and Engineering 287 (12) (2002) 871-880.

Mika, A. M., Childs, R. F., Dickson, J. M., McCarry, B. E., Gagnon, D. R., Porous, Polyelectrolyte-filled Membranes: Effect of cross-linking on Flux and Separation, Journal of Membrane Science 135 (1997) 81-92.

Mohammad, A. W., Ali, N., Ahmad, A. L., Hilal, N., Optimized Nanofiltration Membranes: Relevance to Economic Assessment and Process Performance, Desalination 165 (2004) 243-250.

Mohammad, A. W., Hilal, N., Nizam Abu Seman, M., A Study on Producing Composite Nanofiltration Membranes with Optimized Properties, Desalination 158 (2003) 73-78.

Mohammad, A. W., Othaman, R., Hilal, N., Potential Use of Nanofiltration Membranes in Treatment of Industrial Wastewater from Ni-P Electroless Plating, Desalination 168 (2004) 241-252.

Mohammad, A. W., Takriff, M. S., Predicting Flux and Rejection of Multicomponent Salts Mixture in Nanofiltration Membranes, Desalination 157 (2003) 105-111.

Musale, D. A., Kumar, A., Effect of Surface Crosslinking on Sieving Characteristics of Chitosan/Poly(acrylonitrile) Composite Nanofiltration Membranes, Separation and Purification Technology 21 (2000) 27-38.

Musale, D. A., Kumar, A., Solvent and pH Resistance of Surface Crosslinked Chitosan/Poly(acrylonitrile) Composite Nanofiltration Membranes, Journal of Applied Polymer Science 77 (2000) 1782-1793.

Musale, D. A., Kumar, A., Pleizier, G., Formation and Characterization of Poly(acrylonitirle)/Chitosan Composite Ultrafiltration Membranes, Journal of Membrane Science 154 (1999) 163-173.

Na, L., Zhongzhou, L., Shuguang, T., Dynamically Formed Poly(vinyl alcohol) Ultrafiltation Membranes with Good Anti-fouling Characteristics, Journal of Membrane Science 169 (2000) 15.

Nair, D., Luthra, S. S., Scarpello, J. T., White, L. S., Freitas dos Santos, L. M., Livingston, A. G., Homogeneous Catalyst Separation and Re-use through Nanofiltration of Organic Solvents, Desalination 147 (2002) 301-306.

Nam, S. Y., Chun, H. J., Lee, Y. M., Pervaporation Separation of Water-Isopropanol Mixture Using Carbxymethylated Poly(vinyl alcohol) Composite Membranes, Journal of Applied Polymer Science 72 (1999) 241-249.

Nam, S. Y., Lee, Y. M., Pervaporation and Properties of Chitosan-poly(acrylic acid) Complex Membranes, Journal of Membrane Science 135 (1997) 161-171.

Nishikata, Y., Kakimoto, M., Morikawa, A., Imai, Y., Preparation and Characterization of Poly(amide-imide) Multilayer Films, Thin Solid Films 160 (1988) 15-20.

Nwuha, V., Novel Studies on Membrane Extraction of Bioactive Components of Green Tea in Organic Solvents: Part I, Journal of Food Engineering 44 (4) (2000) 233-238.

Oh, N., Jegal, J., Lee, K., Preparation and Characterization of Nanofiltration Composite Membranes Using Polyacrylonitrile (PAN). II. Preparation and Characterization of Polyamide Composite Membranes, Journal of Applied Polymer Science 80 (2001) 2729-2736.

Paul, D. R., Garcin, M., Garmon, W. E., Solute Diffusion through Swollen Polymer Membranes, Journal of Applied Polymer Science 20 (1976) 609-625.

Peeva, L. G., Gibbins, E., Luthra, S. S., White, L. S., Stateva, R. P., Livingston, A. G., Effect of Concentration Polarisation and Osmotic Pressure on Flux in Organic Solvent Nanofiltration, Journal of Membrane Science 236 (2004) 121-136.

Petersen, Robert J., Composite Reverse Osmosis and Nanofiltration Membranes, Journal of Membrane Science 83 (1993) 81-150.

Platt, S., Nyström, M., Bottino, A., Capannelli, G., Stability of NF Membranes under Extreme Acidic Conditions, Journal of Membrane Science 239 (2004) 91-103.

Qin, J. J., Oo, M. H., Lee, H., Coniglio, B., Effect of Feed pH on Permeate pH and Ion Rejection under Acidic Conditions in NF Process, Journal of Membrane Science 232 (2004) 153-159.

Rami Reddy, A. V., Synthesis and Characterization of Poly(amide-imide)s and Their Precursors as Materials for Membranes, Journal of Applied Polymer Science 75 (2000) 1721-1727.

Ranade, A., D'Souza, N. A., Gnade, B., Exfoliated and Intercalated Polyamide-imide Nanocomposites with Montmorillonite, Polymer 43 (2002) 3759-3766.

Rao, A. P., Joshi, S. V., Trivedi, J. J., Devmurari, C. V., Shah, V. J., Structure-performance Correlation of Polyamide Thin Film Composite Membranes: Effect of Coating Conditions on Film Formation, Journal of Membrane Science 211 (2003) 13-24.

Rautenbach, R., Gröschl, A., Separation Potential of Nanofiltration Membranes, Desalination 77 (1990) 73-84.

Razdan, U., Joshi, S. V., Shah, V. J., Novel Membrane Processes for Separation of Organics, Current Science 85 No. 6 (2003) 761-771.

Roberts, S. L., Koval, C. A., Noble, R. D., Strategy for Selection of Composite Membrane Materials, Ind. Eng. Chem. Res. 39 (2000) 1673-1682.

Robertson, G. P., Guiver, M. D., Yoshikawa, M., Brownstein, S., Structural Determination of Torlon® 4000T Polyamide-imide by NMR Spectroscopy, Polymer 45 (2004) 1111-1117.

Robinson, J. P., Tarleton, E. S., Millington, C. R., Nijmeijer, A., Solvent Flux through Dense Polymeric Nanofiltration Membranes, Journal of Membrane Science 230 (2004) 29-37.

Rohindra, D. R., Nand, A. V., Khurma, J. R., Swelling Properties of Chitosan Hydrogels, The South Pacific Journal of Natural Science 22 (2004) 32-35.

Schäfer, A. I., Fane, A. G., Waite, T. D., Fouling Effects on Rejection in the Membrane Filtration of Natural Waters, Conference on Membranes in Drinking and Industrial Water Production, Vol. 1, Desalination Publication (2000) 411-420.

Schäfer, A. I., Pihlajamäki, A., Fane, A. G., Waite, T. D., Nyström, M., Natral Organic Matter Removal by Nanofiltration: Effects of Solution Chemistry on Retention of Low Molar Mass Acids versus Bulk Organic Matter, Journal of Membrane Science 242 (2004) 73-85.

Schmidt, M., Mirza, S., Schubert, R., Rodicker, H., Kattanek, S., Malisz, J., Nanofiltration Membranes for Problems in Organic Solutions, Chemie Ingenieur Technik 71 (1999) 199-206.

Sharma, R. R., Agrawal, R., Chellam, S., Temperature Effects on Sieving Characteristics of Thin-film Composite Nanofiltration Membranes: Pore size Distributions and Transport Parameters, Journal of Membrane Science 223 (2003) 69-87.

Sheth. J. P., Qin, Y., Sirkar, K. K., Baltzis, B. C., Nanofiltration-based Diafiltration Process for Solvent Exchange in Pharmaceutical Manufacturing, Journal of Membrane Science 211 (2003) 251-261.

Shi, L., Yang L., Chen, J., Pei, Y., Chen, M., Hui, B., Li, J., Preparation and Characterization of pH-sensitive Hydrogel of Chitosan/poly(acrylic acid) co-polymer, Journal of Biomaterial Science Polymer Education 15 (4) (2004) 465-474.

Shukla, R., Cheryan, M., Performance of Ultrafiltration Membranes in Ethanol-water Solutions: Effect of Membrane Conditioning, Journal of Membrane Science 198 (2002) 75-85.

Šindelář, V., Sysel, P., Hynek, V., Friess, K., Šípek, M., Castaned, N., Transport of Gases and Organic Vapours through Membranes made of Poly(amide-imide)s Crosslinked with Poly(ethylene adipate), Collect. Czech. Chem. Commun. 66 (2001) 533-540.

Song, L., A New Model for the Calculation of the Limiting Flux in Ultrafiltration, Journal of Membrane Science 144 (1998) 173-185.

Song, W., Ravindran, V., Koel, B. E., Pirbazari, M., Nanofiltration of Natural Organic Matter with H_2O_2/UV Pretreatment: Fouling Mitigation and Membrane Surface Characterization, Journal of Membrane Science 241 (2004) 143-160.

Spivak, D. A., Sibrian-Vazquez, M., Development of Improved Crosslinking Monomers for Molecularly Imprinted Materials, Materials Research Society Symposia Proceedings 723 (2002) 5-10.

Srinivasa, P. C., Ramesh, M. N., Kumar, K. R., Tharanathan, R. N., Properties of Chitosan Films Prepared under Different Drying Conditions, Journal of Food Engineering 63 (2004) 79-85.

Sroog, C. E., Polyimides, Prog. Polym. Sci., 16 (1991) 561-694.

Stafie, N., Stamatialis, D. F., Wessling, M., Effect of PDMS cross-lingking Degree on the Permeation Performance of PAN/PDMS Composite Nanofiltration Membranes, Separation and Purification Technology, Article in Press (2005).

Stafie, N., Stamatialis, D. F., Wessling, M., Insight into the Transport of Hexane-solute Sstems through Tailor-made Composite Membranes, Journal of Membrane Science 228 (2004) 103-116.

Szoke, S., Patzay, G., Weiser, L., Characteristics of Thin-film Nanofiltration Membranes at Various pH-values, Desalination 151 (2002) 123-129.

Tin, P. S., Chung, T. S., Liu, Y., Wang, R., Liu, S. L., Pramoda, K. P., Effects of Cross-linking Modification on Gas Separation Performance of Matrimid Membranes, Journal of Membrane Science 225 (2003) 77-90.

Tsui, E. M., Cheryan, M., Characteristics of Nanofiltration Membranes in Aqueous Ethanol, Journal of Membrane Science 237 (2004) 61-69.

Tweddle, T. A., Striez, C. N., Membrane Fabrication and Testing Manual, National Research Council Canada Report, Ottawa, Canada (1994) 1-14.

Tweddle, T. A., Striez, C. N., Kutowy, O., Hazlett, J. D., Equipment and Procedures for testing Small Coupon Samples of RO an UF Membranes, National Research Council Canada Report, Division of Chemistry Chemical Engineering (1990) 1-33.

Unishi, T., Preparation of Aromatic Polyimide-amide, Polymer Letters 3 (1965) 679-683.

Van der Bruggen, B., Braeken, L., Vandecasteele, C., Flux Decline in Nanofiltration due to Adsorption of Organic Compounds, Separation and Purification Technology 29 (2002) 23-31.

Van der Bruggen, B., Geens, J., Vandecasteele, C., Influence of Organic Solvents on the Performance of Polymeric Nanofiltration Membranes, Separation Science and Technology 37 (4) (2002) 783-797.

Van der Bruggen, B., Geens, J., Vandecasteele, C., Fluxes and Rejections for Nanofiltration with Solvent Stable Polymeric Membranes in Water, Ethanol and n-Hexane, Chemical Engineering Science 57 (2002) 2511-2518.

Van der Bruggen, B., Hawrijk, I., Cornelissen, E., Vandecasteele, C., Direct Nanofiltration of Surface Water Using Capillary Membranes: Comparison with Flat Sheet Membranes, Separation and Purification Technology 31 (2003) 193-201.

Van der Bruggen, B., Kim, J. H., DiGiano, F. A., Geens, J., Vandecasteele, C., Influence of MF Pretreatment on NF Performance for Aqueous Solutions Containing Particles and an Organic Foulant, Separation and Purification Technology 36 (2004) 203-213.

Van der Bruggen, B., Schaep, J., Wilms, D., Vandecasteele, C., Influence of Molecular size, Polarity and Charge on the Retention Organic Molecules by Nanofiltration, Journal of Membrane Science 156 (1999) 29-41.

Vandezande, P., Gevers, L. E. M., Paul, J. S., Vankelecom, I. F. J., Jacobs, P. A., High throughput Screening for Rapid Developmenr of Membranes and Membranes Processes, Journal of Membrane Science 250 (2005) 305-310.

Vankelecom, I. F. J., Smet, K. D., Gevers, L. E. M., Livingston, A., Nair, D., Aerts, S., Kuypers, S., Jacobs, P. A., Physico-chemical Interpretation of the SRNF Transport Mechanism for Solvents through Dense Silicone Membranes, Journal of Membrane Science 231 (2004) 99-108.

Wang, H., Fang, Y., Yan, Y., Surface Modification of Chitosan Membranes by alkane Vapor Plasma, Journal of Materials Chemistry 11 (2001) 1374-1377.

Wang, K. Y., Chung, T., The Characterization of Flat Composite Nanofiltration Membranes and Their Applications in the Separation of Cephalexin, Journal of Membrane Science 247 (2005) 37-50.

White, L. S., Transport Properties of a Polyimide Solvent Resistant Nanofiltration Membrane, Journal of Membrane Science 205 (2002) 191-202.

White, L. S., Nitsch, A. R., Solvent Recovery from Lube Oil Filtrates with a Polyimide Membrane, Journal of Membrane Science 179 (2000) 267-274.

Whu, J. A., Batlzis, B. C., Sirkar, K. K., Modelling of Nanofiltration Asisted Organic Synthesis, Journal of Membrane Science 1163 (1999) 319-331.

Whu, J. A., Batlzis, B. C., Sirkar, K. K., Nanofiltration Studies of Larger Organic Microsolutes in Methanol Solutions, Journal of Membrane Science 170 (2000) 159-172.

Won, W., Feng, X., Lawless, D., Separation of Dimethyl Carbonate/methanol/water Mixtures by Pervaporation Using Crosslinked Chitosan Membranes, Separation and Purification Technology 31 (2003) 129-140.

Wu, C., Xu, T., Gong, M., Yang, W., Synthesis and Characterizations of New Negatively Charged Organic–inorganic Hybrid Materials: Part II. Membrane Preparation and Characterizations, Journal of Membrane Science 247 (2005) 111-118.

Yanagashita, H., Kitamoto, D., Haraya, K., Nakane, T., Okada, T., Matsuda, H., Idemoto, Y., Koura, N., Separation Performance of Polyimide Composite Membrane Prepared by Dip Coating Process, Journal of Membrane Science 188 (2001) 165-172.

Yang, J. M., Su, W. Y., Leu, T. L., Yang, M. C., Evaluation of Chitosan/PVA Blended Hydrogel Membranes, Journal of Membrane Science 236 (2004) 39-51.

Yang, X. J., Livingston, A. G., Freitas dos Santos, L., Experimental Observations of Nanofiltration with Organic Solvents, Journal of Membrane Science 190 (2001) 45-55.

Yaroshchuk, A. E., The Role of Imperfections in the Solute Transfer in Nanofiltration, Journal of Membrane Science 239 (2004) 9-15.

Yoon, Y., Amy, G., Cho, J., Her, N., Effects of Retained Natural Organic Matter (NOM) on NOM Rejection and Membrane Flux Decline with Nanofiltration and Ultrafiltration, Desalination 173 (2005) 209-221.

Yoon, Y., Amy, G., Cho, J., Her, N., Pellegrino, J., Transport of Perchlorate (ClO_4^-) through NF and UF Membranes, Desalination 147 (2002) 11-17.

Yoshikawa, M., Guiver, M. D., Robertson, G. P., Molecularly Imprinted Films Derived from Torlon® Polyamide-imide, Journal of Molecular Structure 739 (2005) 41-46.

Yoshikawa, M., Higuchi, A., Ishikawa, M., Guiver, M. D., Robertson, G. P., Vapor Permeation of Aqueous 2-propanol Solutions through Gelatin/Torlon® Poly(amide imide) Blended Membranes, Journal of Membrane Science 243 (2004) 89-95.

Zhao, Z., Wang, Z., Wang S., Formation, Charged Characteristics and BSA Adsorption Behaviour of Carboxymethyl Chitosan/PES composite MF Membrane, Journal of Membrane Science 217 (2003) 151-158.

Zhang, S., Jian, X., Dai, Y., Preparation of Sulfonated Poly(phthalazinone ether sulfone ketone) Composite Nanofiltration Membrane, Journal of Membrane Science 246 (2005) 121-126.

Zhou, J. Childs, R. F., Mika, A. M., Pore-filled Nanofiltration Membranes Based on Poly(2-arylamido-2-methylpropanesulfonic acid) Gels, Journal of Membrane Science 254 (2005) 89-99.

APPENDIX A

PERMEATION DATA

Table A.1 – Experimental data for composite membrane coated with Chitosan buffer, following cross linking then neutralization step based on long curing period

Method	Membrane		Molecular weight of PEG (Dalton)					PWP
			200	600	1500	3000	6000	($lm^{-2}h^{-1}$)
Cross linked then neutralized	coupon #1	Product rate ($lm^{-2}h^{-1}$)	6.77	6.54	7.23	7.37	8.12	6.52
		% Separation	43%	81%	100%	100%	100%	
	coupon #2	Product rate ($lm^{-2}h^{-1}$)	8.57	8.12	8.94	9.28	10.83	8.19
		% Separation	53%	95%	100%	100%	100%	
	coupon #3	Product rate ($lm^{-2}h^{-1}$)	6.79	7.15	8.02	8.57	11.79	6.37
		% Separation	44%	87%	100%	100%	100%	
	average	***Product rate ($lm^{-2}h^{-1}$)***	7.38	7.27	8.06	8.41	10.25	7.03
		standard deviation	1.03	0.80	0.86	0.97	1.90	1.01
		standard error	0.60	0.46	0.49	0.56	1.10	0.58
		% Separation	47%	88%	100%	100%	100%	
		standard deviation	6%	7%	0%	0%	0%	
		standard error	3%	4%	0%	0%	0%	

Table A.2 – Experimental data for composite membrane coated with Chitosan buffer, following neutralization then cross linking process based on long curing period

Method	Membrane		Molecular weight of PEG (Dalton)					PWP
			200	600	1500	3000	6000	($lm^{-2}h^{-1}$)
Neutralized then cross linked	coupon #1	Product rate ($lm^{-2}h^{-1}$)	8.39	8.31	8.75	8.83	9.68	8.1
		% Separation	57%	81%	100%	100%	100%	
	coupon #2	Product rate ($lm^{-2}h^{-1}$)	7.08	6.72	7.94	8.11	10.31	5.92
		% Separation	57%	95%	100%	100%	100%	
	coupon #3	Product rate ($lm^{-2}h^{-1}$)	12.38	11.20	12.63	12.76	15.27	10.5
		% Separation	58%	96%	100%	100%	100%	
	average	***Product rate ($lm^{-2}h^{-1}$)***	9.28	8.74	9.77	9.90	11.75	8.17
		standard deviation	2.76	2.27	2.51	2.50	3.06	2.29
		standard error	1.59	1.31	1.45	1.45	1.77	1.32
		% Separation	57%	91%	100%	100%	100%	
		standard deviation	1%	8%	0%	0%	0%	
		standard error	0%	5%	0%	0%	0%	

Table A.3 – Experimental data for composite membrane coated with Chitosan buffer diluted with EtOH, following cross linking then neutralization step based on long curing period

Method	Membrane		Molecular weight of PEG (Dalton)					PWP
			200	600	1500	3000	6000	($lm^{-2}h^{-1}$)
Cross linked then neutralized	coupon #1	Product rate ($lm^{-2}h^{-1}$)	25.31	24.04	25.48	25.95	28.09	24.81
		% Separation	39%	84%	100%	100%	100%	
	coupon #2	Product rate ($lm^{-2}h^{-1}$)	21.03	20.01	21.26	21.64	23.76	20.43
		% Separation	47%	89%	100%	100%	100%	
	coupon #3	Product rate ($lm^{-2}h^{-1}$)	31.25	29.68	29.76	30.80	37.94	28.36
		% Separation	44%	88%	100%	100%	100%	
	average	***Product rate ($lm^{-2}h^{-1}$)***	25.86	24.58	25.50	26.13	29.93	24.53
		standard deviation	5.13	4.86	4.25	4.58	7.27	3.97
		standard error	2.96	2.80	2.45	2.65	4.20	2.29
		% Separation	43%	87%	100%	100%	100%	
		standard deviation	4%	3%	0%	0%	0%	
		standard error	2%	2%	0%	0%	0%	

Table A.4 – Experimental data for composite membrane coated with Chitosan buffer diluted with EtOH, following neutralization then cross linking process based on long curing period

Method	Membrane		Molecular weight of PEG (Dalton)					PWP
			200	600	1500	3000	6000	($lm^{-2}h^{-1}$)
Neutralized then cross linked	coupon #1	Product rate ($lm^{-2}h^{-1}$)	18.54	17.73	18.79	19.31	21.45	17.62
		% Separation	55%	92%	100%	100%	100%	
	coupon #2	Product rate ($lm^{-2}h^{-1}$)	26.44	25.78	27.90	29.01	37.20	22.74
		% Separation	55%	98%	100%	100%	100%	
	coupon #3	Product rate ($lm^{-2}h^{-1}$)	14.5	13.72	14.95	15.84	17.68	12.6
		% Separation	60%	95%	100%	100%	100%	
	average	***Product rate ($lm^{-2}h^{-1}$)***	19.83	19.08	20.55	21.39	25.44	17.65
		standard deviation	6.07	6.14	6.65	6.83	10.35	5.07
		standard error	3.51	3.55	3.84	3.94	5.98	2.93
		% Separation	57%	95%	100%	100%	100%	
		standard deviation	3%	3%	0%	0%	0%	
		standard error	2%	2%	0%	0%	0%	

Table A.5 – Experimental data for composite membrane coated with Chitosan buffer, following cross linking then neutralization step based on short curing period

Method	Membrane		Molecular weight of PEG (Dalton)					PWP
			200	600	1500	3000	6000	($lm^{-2}h^{-1}$)
Cross linked then neutralized	coupon #1	Product rate ($lm^{-2}h^{-1}$)	7.51	7.53	8.3	8.85	10.06	7.51
		% Separation	50%	89%	100%	100%	100%	
	coupon #2	Product rate ($lm^{-2}h^{-1}$)	7.08	7.08	7.84	8.41	9.94	7.15
		% Separation	51%	93%	100%	100%	100%	
	coupon #3	Product rate ($lm^{-2}h^{-1}$)	8.66	8.39	9.13	9.70	11.05	8.49
		% Separation	62%	90%	100%	100%	100%	
	average	***Product rate ($lm^{-2}h^{-1}$)***	7.75	7.67	8.42	8.99	10.35	7.72
		standard deviation	0.82	0.67	0.65	0.66	0.61	0.69
		standard error	0.47	0.38	0.38	0.38	0.35	0.40
		% Separation	54%	91%	100%	100%	100%	
		standard deviation	7%	2%	0%	0%	0%	
		standard error	4%	1%	0%	0%	0%	

Table A.6 – Experimental data for composite membrane coated with Chitosan buffer, following neutralization then cross linking process based on short curing period

Method	Membrane		Molecular weight of PEG (Dalton)					PWP
			200	600	1500	3000	6000	($lm^{-2}h^{-1}$)
Neutralized then cross linked	coupon #1	Product rate ($lm^{-2}h^{-1}$)	12.28	11.16	12.90	13.66	15.03	11.79
		% Separation	55%	96%	100%	100%	100%	
	coupon #2	Product rate ($lm^{-2}h^{-1}$)	20.26	17.11	19.53	21.17	21.33	20.26
		% Separation	57%	98%	100%	100%	100%	
	coupon #3	Product rate ($lm^{-2}h^{-1}$)	17.32	15.62	16.58	17.80	19.86	17.51
		% Separation	68%	94%	100%	100%	100%	
	average	***Product rate ($lm^{-2}h^{-1}$)***	16.62	14.63	16.34	17.54	18.74	16.52
		standard deviation	4.04	3.10	3.32	3.76	3.30	4.32
		standard error	2.33	1.79	1.92	2.17	1.90	2.49
		% Separation	60%	96%	100%	100%	100%	
		standard deviation	7%	2%	0%	0%	0%	
		standard error	4%	1%	0%	0%	0%	

Table A.7 – Experimental data for composite membrane coated with Chitosan buffer diluted with EtOH, following cross linking then neutralization step based on short curing period

Method	Membrane		Molecular weight of PEG (Dalton)					PWP
			200	600	1500	3000	6000	($lm^{-2}h^{-1}$)
Cross linked then neutralized	coupon #1	Product rate ($lm^{-2}h^{-1}$)	5.52	3.67	5.30	5.94	5.66	5.50
		% Separation	69%	89%	100%	100%	100%	
	coupon #2	Product rate ($lm^{-2}h^{-1}$)	5.19	4.51	5.25	5.98	6.37	5.25
		% Separation	85%	98%	100%	100%	100%	
	coupon #3	Product rate ($lm^{-2}h^{-1}$)	5.41	5.04	5.18	4.55	5.57	5.02
		% Separation	87%	91%	100%	100%	100%	
	average	***Product rate ($lm^{-2}h^{-1}$)***	5.37	4.41	5.24	5.49	5.87	5.26
		standard deviation	0.17	0.69	0.06	0.81	0.44	0.24
		standard error	0.10	0.40	0.03	0.47	0.25	0.14
		% Separation	80%	93%	100%	100%	100%	
		standard deviation	10%	5%	0%	0%	0%	
		standard error	6%	3%	0%	0%	0%	

Table A.8 – Experimental data for composite membrane coated with Chitosan buffer diluted with EtOH, following neutralization then cross linking process based on short curing period

Method	Membrane		Molecular weight of PEG (Dalton)					PWP ($lm^{-2}h^{-1}$)
			200	600	1500	3000	6000	
Neutralized then cross linked	coupon #1	Product rate ($lm^{-2}h^{-1}$)	7.44	6.73	7.26	9.02	7.69	7.46
		% Separation	75%	97%	100%	100%	100%	
	coupon #2	Product rate ($lm^{-2}h^{-1}$)	7.03	6.3	6.85	7.28	7.24	7.08
		% Separation	85%	92%	100%	100%	100%	
	coupon #3	Product rate ($lm^{-2}h^{-1}$)	12.54	11.75	11.67	12.14	12.12	12.49
		% Separation	69%	89%	100%	100%	100%	
	average	***Product rate ($lm^{-2}h^{-1}$)***	9.00	8.26	8.59	9.48	9.02	9.01
		standard deviation	3.07	3.03	2.67	2.46	2.70	3.02
		standard error	1.77	1.75	1.54	1.42	1.56	1.74
		% Separation	76%	93%	100%	100%	100%	
		standard deviation	8%	4%	0%	0%	0%	
		standard error	5%	3%	0%	0%	0%	

Table A.9 – Experimental data for composite membrane coated with Chitosan buffer diluted with IPA, following neutralization then cross linking process (24 hours and 10% w/v cross linking concentration in EtOH) based on long curing period

Method	Membrane		Molecular weight of PEG (Dalton)				PWP
			200	400	600	1000	($lm^{-2}h^{-1}$)
Neutralized then cross linked	coupon #1	Product rate ($lm^{-2}h^{-1}$)	15.12	14.06	13.65	13.43	16.96
		% Separation	43%	75%	91%	94%	
	coupon #2	Product rate ($lm^{-2}h^{-1}$)	8.92	8.35	7.82	7.80	10.07
		% Separation	51%	83%	93%	97%	
	coupon #3	Product rate ($lm^{-2}h^{-1}$)	14.92	14.44	13.24	13.10	16.97
		% Separation	45%	80%	86%	98%	
	coupon #4	Product rate ($lm^{-2}h^{-1}$)	6.79	6.29	10.50	5.83	7.62
		% Separation	61%	89%	86%	97%	
	coupon #5	Product rate ($lm^{-2}h^{-1}$)	8.51	7.96	7.54	7.67	9.61
		% Separation	41%	72%	94%	91%	
	coupon #6	Product rate ($lm^{-2}h^{-1}$)	12.22	11.3	5.75	10.61	13.90
		% Separation	44%	76%	83%	94%	
	coupon #7	Product rate ($lm^{-2}h^{-1}$)	3.78	3.46	4.09	3.14	8.33
		% Separation	54%	86%	89%	97%	
	coupon #8	Product rate ($lm^{-2}h^{-1}$)	3.08	2.96	2.81	2.87	4.60
		% Separation	31%	66%	80%	88%	
	coupon #9	Product rate ($lm^{-2}h^{-1}$)	4.96	4.44	3.15	3.95	6.73
		% Separation	40%	77%	94%	96%	
	coupon #10	Product rate ($lm^{-2}h^{-1}$)	3.28	2.99	3.73	2.75	5.18
		% Separation	50%	81%	91%	95%	
	coupon #11	Product rate ($lm^{-2}h^{-1}$)	2.79	2.57	2.33	2.39	6.92
		% Separation	57%	84%	93%	95%	
	coupon #12	Product rate ($lm^{-2}h^{-1}$)	4.3	3.92	2.70	3.66	5.68
		% Separation	44%	77%	91%	95%	
	average	***Product rate ($lm^{-2}h^{-1}$)***	7.39	6.90	6.44	6.43	9.38
		standard deviation	4.56	4.34	4.11	4.07	4.34
		standard error	1.32	1.25	1.19	1.17	1.25
		% Separation	47%	79%	89%	95%	
		standard deviation	8%	6%	5%	3%	
		standard error	2%	2%	1%	1%	

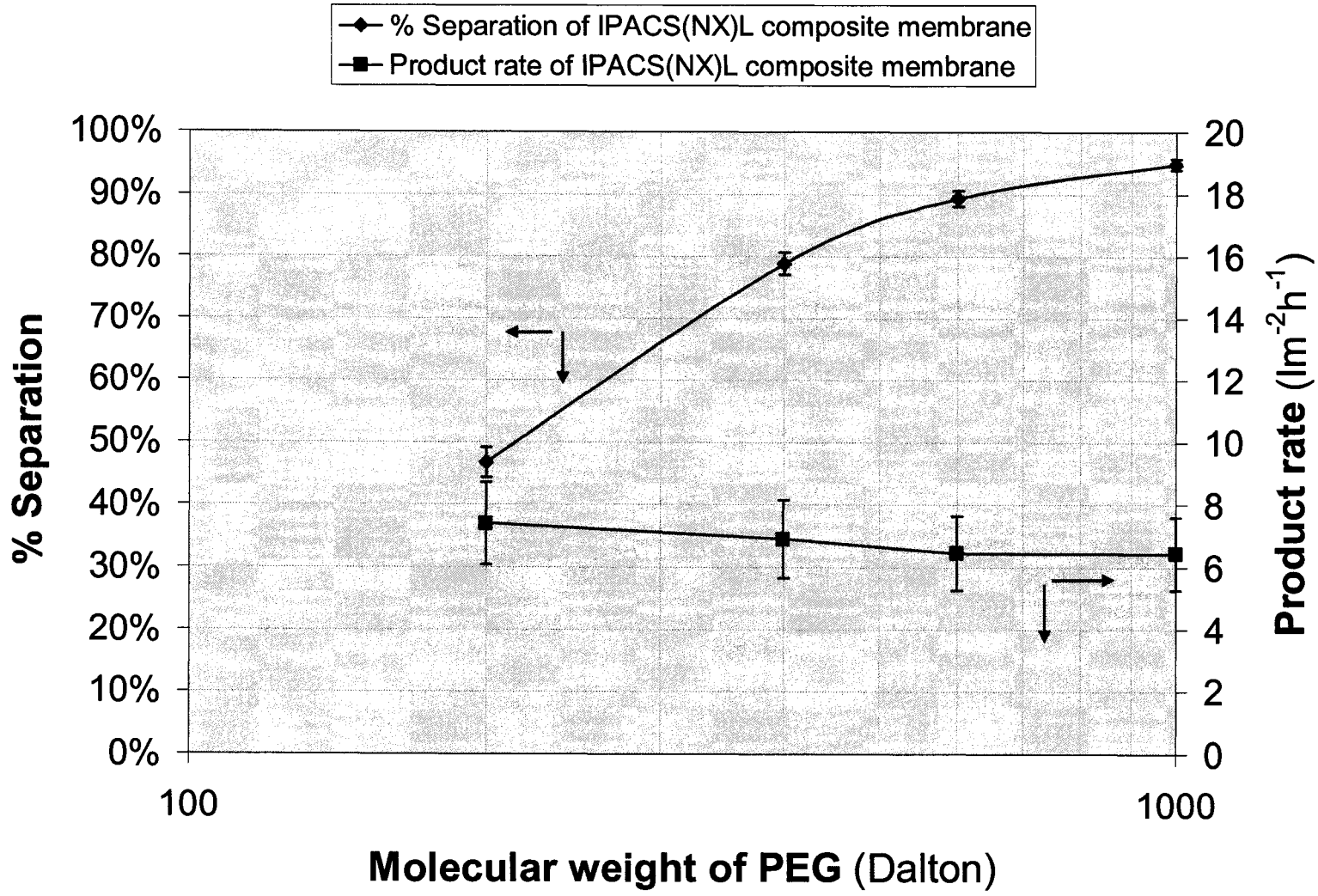

Figure A.1 – The average values of PEG separation and flux for IPACS(NX)L composite NF membranes (1st set of experiment)

Table A.10 – Experimental data for IPACS(NX)L composite membrane through 30 minutes cross linking time and 0.2% cross linking concentration

Method	Membrane		Molecular weight of PEG (Dalton)				PWP ($lm^{-2}h^{-1}$)
			200	400	600	1000	
30 min with 0.2% cross linking concentration	coupon #1	Product rate ($lm^{-2}h^{-1}$)	16.54	15.30	14.43	13.73	16.88
		% Separation	51%	80%	92%	96%	
	coupon #2	Product rate ($lm^{-2}h^{-1}$)	10.42	9.57	8.92	8.53	10.64
		% Separation	53%	82%	94%	97%	
	coupon #3	Product rate ($lm^{-2}h^{-1}$)	9.3	8.46	7.9	7.5	9.76
		% Separation	55%	84%	95%	97%	
	average	***Product rate ($lm^{-2}h^{-1}$)***	12.09	11.11	10.42	9.92	12.43
		standard deviation	3.90	3.67	3.51	3.34	3.88
		standard error	2.25	2.12	2.03	1.93	2.24
		% Separation	53%	82%	94%	97%	
		standard deviation	2%	2%	2%	1%	
		standard error	1%	1%	1%	0%	

Table A.11 – Experimental data for IPACS(NX)L composite membrane through 30 minutes cross linking time and 1% cross linking concentration

Method	Membrane		Molecular weight of PEG (Dalton)				PWP ($lm^{-2}h^{-1}$)
			200	400	600	1000	
30 min with 1% cross linking concentration	coupon #1	Product rate ($lm^{-2}h^{-1}$)	22.02	19.92	18.9	18.07	22.12
		% Separation	47%	79%	91%	95%	
	coupon #2	Product rate ($lm^{-2}h^{-1}$)	10.89	10.01	8.48	8.61	11.47
		% Separation	48%	76%	87%	94%	
	coupon #3	Product rate ($lm^{-2}h^{-1}$)	12.92	11.94	11.15	10.6	13.12
		% Separation	48%	73%	83%	88%	
	average	***Product rate ($lm^{-2}h^{-1}$)***	15.28	13.96	12.84	12.43	15.57
		standard deviation	5.93	5.25	5.41	4.99	5.73
		standard error	3.42	3.03	3.12	2.88	3.31
		% Separation	48%	76%	87%	92%	
		standard deviation	1%	3%	4%	4%	
		standard error	0%	2%	2%	2%	

Table A.12 – Experimental data for IPACS(NX)L composite membrane through 30 minutes cross linking time and 3% cross linking concentration

Method	Membrane		Molecular weight of PEG (Dalton)				PWP
			200	400	600	1000	($lm^{-2}h^{-1}$)
30 min with 3% cross linking concentration	coupon #1	Product rate ($lm^{-2}h^{-1}$)	18.95	19.22	14.47	14.47	19.37
		% Separation	44%	72%	90%	96%	
	coupon #2	Product rate ($lm^{-2}h^{-1}$)	15.93	16.15	12.45	12.36	16.58
		% Separation	38%	64%	82%	91%	
	coupon #3	Product rate ($lm^{-2}h^{-1}$)	11.55	10.98	8.13	8.03	17.79
		% Separation	43%	69%	83%	89%	
	average	***Product rate ($lm^{-2}h^{-1}$)***	15.48	15.45	11.68	11.62	17.91
		standard deviation	3.72	4.16	3.24	3.28	1.40
		standard error	2.15	2.40	1.87	1.90	0.81
		% Separation	42%	68%	85%	92%	
		standard deviation	3%	4%	4%	4%	
		standard error	2%	2%	3%	2%	

Table A.13 – Experimental data for IPACS(NX)L composite membrane through 30 minutes cross linking time and 5% cross linking concentration

Method	Membrane		Molecular weight of PEG (Dalton)				PWP ($lm^{-2}h^{-1}$)
			200	400	600	1000	
30 min with 5% cross linking concentration	coupon #1	Product rate ($lm^{-2}h^{-1}$)	9.39	8.85	8.27	7.92	10.37
		% Separation	49%	80%	94%	97%	
	coupon #2	Product rate ($lm^{-2}h^{-1}$)	17.8	16.73	15.82	15.11	18.12
		% Separation	44%	74%	90%	96%	
	coupon #3	Product rate ($lm^{-2}h^{-1}$)	19.05	18.06	17.17	16.48	19.53
		% Separation	39%	70%	87%	95%	
	average	***Product rate ($lm^{-2}h^{-1}$)***	15.41	14.55	13.75	13.17	16.01
		standard deviation	5.25	4.98	4.80	4.60	4.93
		standard error	3.03	2.87	2.77	2.65	2.85
		% Separation	44%	75%	90%	96%	
		standard deviation	5%	5%	4%	1%	
		standard error	3%	3%	2%	1%	

Table A.14 – Experimental data for IPACS(NX)L composite membrane through 30 minutes cross linking time and 10% cross linking concentration

Method	Membrane		Molecular weight of PEG (Dalton)				PWP
			200	400	600	1000	($lm^{-2}h^{-1}$)
30 min with 10% cross linking concentration	coupon #1	Product rate ($lm^{-2}h^{-1}$)	24.81	23.77	22.29	21.41	24.90
		% Separation	45%	78%	90%	96%	
	coupon #2	Product rate ($lm^{-2}h^{-1}$)	28.06	28.47	27.75	28.45	27.24
		% Separation	42%	80%	94%	98%	
	coupon #3	Product rate ($lm^{-2}h^{-1}$)	31.81	42.64	41.61	43.20	45.73
		% Separation	31%	64%	78%	84%	
	average	***Product rate ($lm^{-2}h^{-1}$)***	28.23	31.63	30.55	31.02	32.62
		standard deviation	3.50	9.82	9.96	11.12	11.41
		standard error	2.02	5.67	5.75	6.42	6.59
		% Separation	39%	74%	87%	93%	
		standard deviation	7%	9%	8%	8%	
		standard error	4%	5%	5%	4%	

Table A.15 – Experimental data for IPACS(NX)L composite membrane through 1 hour cross linking time and 0.2% cross linking concentration

Method	Membrane		Molecular weight of PEG (Dalton)				PWP
			200	400	600	1000	($lm^{-2}h^{-1}$)
1 hour with 0.2% cross linking concentration	coupon #1	Product rate ($lm^{-2}h^{-1}$)	16.92	16.22	15.17	14.23	16.74
		% Separation	43%	76%	90%	95%	
	coupon #2	Product rate ($lm^{-2}h^{-1}$)	20.60	19.17	18.08	17.41	20.81
		% Separation	37%	71%	83%	89%	
	coupon #3	Product rate ($lm^{-2}h^{-1}$)	13.07	12.15	11.1	10.24	13.95
		% Separation	44%	73%	82%	92%	
	average	***Product rate ($lm^{-2}h^{-1}$)***	16.86	15.85	14.78	13.96	17.17
		standard deviation	3.77	3.52	3.51	3.59	3.45
		standard error	2.17	2.04	2.02	2.07	1.99
		% Separation	41%	73%	85%	92%	
		standard deviation	4%	3%	4%	3%	
		standard error	2%	1%	3%	2%	

Table A.16 – Experimental data for IPACS(NX)L composite membrane through 1 hour cross linking time and 1% cross linking concentration

Method	Membrane		Molecular weight of PEG (Dalton)				PWP ($lm^{-2}h^{-1}$)
			200	400	600	1000	
1 hour with 1% cross linking concentration	coupon #1	Product rate ($lm^{-2}h^{-1}$)	14.02	13.07	12.19	11.12	14.11
		% Separation	46%	79%	91%	96%	
	coupon #2	Product rate ($lm^{-2}h^{-1}$)	15.15	13.93	12.98	12.29	15.06
		% Separation	46%	82%	95%	98%	
	coupon #3	Product rate ($lm^{-2}h^{-1}$)	16.08	15.01	13.94	13.11	16.92
		% Separation	45%	73%	84%	90%	
	average	***Product rate ($lm^{-2}h^{-1}$)***	15.08	14.00	13.04	12.17	15.36
		standard deviation	1.03	0.97	0.88	1.00	1.43
		standard error	0.60	0.56	0.51	0.58	0.83
		% Separation	46%	78%	90%	95%	
		standard deviation	1%	5%	6%	4%	
		standard error	0%	3%	3%	2%	

Table A.17 – Experimental data for IPACS(NX)L composite membrane through 1 hour cross linking time and 3% cross linking concentration[4]

Method	Membrane		Molecular weight of PEG (Dalton)				PWP ($lm^{-2}h^{-1}$)
			200	400	600	1000	
1 hour with 3% cross linking concentration	coupon #1	Product rate ($lm^{-2}h^{-1}$)	15.96	14.60	13.63	12.85	16.77
		% Separation	44%	81%	93%	97%	
	coupon #2	Product rate ($lm^{-2}h^{-1}$)	21.54	19.24	17.42	14.46	23.50
		% Separation	32%	60%	70%	85%	
	coupon #3	Product rate ($lm^{-2}h^{-1}$)	14.67	13.13	12.33	11.55	15.68
		% Separation	44%	76%	90%	96%	
	average	***Product rate ($lm^{-2}h^{-1}$)***	17.39	15.66	14.46	12.95	18.65
		standard deviation	3.65	3.19	2.64	1.46	4.24
		standard error	2.11	1.84	1.53	0.84	2.45
		% Separation	40%	72%	84%	93%	
		standard deviation	7%	11%	13%	7%	
		standard error	4%	6%	7%	4%	

[4] Note that the experimental data defined by IPACS(NX)L composite membrane through 1 hour (with 5% and 10% cross linking concentration), 4 hours (with 0.2%, 1%, 3%, 5%, and 10% cross linking concentration), and 9 hours (with 0.2%) cross linking time could not be measured due to the mechanical failure.

Table A.18 – Experimental data for IPACS(NX)L composite membrane through 9 hours cross linking time and 1% cross linking concentration

Method	Membrane		Molecular weight of PEG (Dalton)				PWP
			200	400	600	1000	($lm^{-2}h^{-1}$)
9 hours with 1% cross linking concentration	coupon #1	Product rate ($lm^{-2}h^{-1}$)	38.1	40.72	40.42	39.61	37.05
		% Separation	43%	73%	88%	95%	
	coupon #2	Product rate ($lm^{-2}h^{-1}$)	11.95	12.09	11.41	10.89	15.02
		% Separation	57%	82%	92%	96%	
	coupon #3	Product rate ($lm^{-2}h^{-1}$)	12.72	12.72	12.18	11.66	12.71
		% Separation	54%	83%	93%	97%	
	average	***Product rate ($lm^{-2}h^{-1}$)***	20.92	21.84	21.34	20.72	21.59
		standard deviation	14.88	16.35	16.53	16.36	13.44
		standard error	8.59	9.44	9.54	9.45	7.76
		% Separation	51%	79%	91%	96%	
		standard deviation	7%	6%	3%	1%	
		standard error	4%	3%	2%	1%	

Table A.19 – Experimental data for IPACS(NX)L composite membrane through 9 hours cross linking time and 3% cross linking concentration

Method	Membrane		Molecular weight of PEG (Dalton)				PWP ($lm^{-2}h^{-1}$)
			200	400	600	1000	
9 hours with 3% cross linking concentration	coupon #1	Product rate ($lm^{-2}h^{-1}$)	12.23	11.20	10.39	10.56	12.36
		% Separation	55%	82%	93%	97%	
	coupon #2	Product rate ($lm^{-2}h^{-1}$)	15.86	15.14	14.63	13.17	16.23
		% Separation	47%	82%	94%	97%	
	coupon #3	Product rate ($lm^{-2}h^{-1}$)	16.16	15.25	14.54	13.82	16.36
		% Separation	46%	74%	84%	89%	
	average	***Product rate ($lm^{-2}h^{-1}$)***	14.75	13.86	13.19	12.52	14.98
		standard deviation	2.19	2.31	2.42	1.73	2.27
		standard error	1.26	1.33	1.40	1.00	1.31
		% Separation	49%	79%	90%	94%	
		standard deviation	5%	5%	6%	5%	
		standard error	3%	3%	3%	3%	

Table A.20 – Experimental data for IPACS(NX)L composite membrane through 9 hours cross linking time and 5% cross linking concentration

Method	Membrane		Molecular weight of PEG (Dalton)				PWP ($lm^{-2}h^{-1}$)
			200	400	600	1000	
9 hours with 5% cross linking concentration	coupon #1	Product rate ($lm^{-2}h^{-1}$)	18.73	18.51	17.63	16.62	18.82
		% Separation	50%	78%	90%	96%	
	coupon #2	Product rate ($lm^{-2}h^{-1}$)	15.22	15.63	15.09	14.39	15.20
		% Separation	52%	82%	94%	98%	
	coupon #3	Product rate ($lm^{-2}h^{-1}$)	17.49	17.71	17.08	16.26	17.35
		% Separation	42%	69%	81%	88%	
	average	***Product rate ($lm^{-2}h^{-1}$)***	17.15	17.28	16.60	15.76	17.12
		standard deviation	1.78	1.49	1.34	1.20	1.82
		standard error	1.03	0.86	0.77	0.69	1.05
		% Separation	48%	76%	88%	94%	
		standard deviation	5%	7%	7%	5%	
		standard error	3%	4%	4%	3%	

Table A.21 – Experimental data for IPACS(NX)L composite membrane through 9 hours cross linking time and 10% cross linking concentration

Method	Membrane		Molecular weight of PEG (Dalton)				PWP ($lm^{-2}h^{-1}$)
			200	400	600	1000	
9 hours with 10% cross linking concentration	coupon #1	Product rate ($lm^{-2}h^{-1}$)	19.05	17.88	16.68	16.35	18.89
		% Separation	39%	68%	84%	91%	
	coupon #2	Product rate ($lm^{-2}h^{-1}$)	12.92	13.14	12.24	11.97	14.88
		% Separation	54%	83%	95%	98%	
	coupon #3	Product rate ($lm^{-2}h^{-1}$)	17.22	16.64	15.07	14.56	18.94
		% Separation	46%	77%	91%	95%	
	average	***Product rate ($lm^{-2}h^{-1}$)***	16.40	15.89	14.66	14.29	17.57
		standard deviation	3.15	2.46	2.25	2.20	2.33
		standard error	1.82	1.42	1.30	1.27	1.35
		% Separation	46%	76%	90%	95%	
		standard deviation	8%	8%	6%	4%	
		standard error	4%	4%	3%	2%	

Table A.22 – Experimental data for IPACS(NX)L composite membrane through 17 hours cross linking time and 0.2% cross linking concentration

Method	Membrane		Molecular weight of PEG (Dalton)				PWP
			200	400	600	1000	($lm^{-2}h^{-1}$)
17 hours with 0.2% cross linking concentration	coupon #1	Product rate ($lm^{-2}h^{-1}$)	12.82	11.81	11.17	10.43	12.95
		% Separation	52%	83%	93%	97%	
	coupon #2	Product rate ($lm^{-2}h^{-1}$)	23.99	22.52	21.48	20.24	24.58
		% Separation	42%	76%	88%	93%	
	coupon #3	Product rate ($lm^{-2}h^{-1}$)	10.30	9.38	8.75	8.25	10.80
		% Separation	52%	82%	91%	92%	
	average	***Product rate ($lm^{-2}h^{-1}$)***	15.70	14.57	13.80	12.97	16.11
		standard deviation	7.29	6.99	6.76	6.39	7.41
		standard error	4.21	4.04	3.90	3.69	4.28
		% Separation	49%	80%	91%	94%	
		standard deviation	6%	4%	3%	3%	
		standard error	3%	2%	1%	2%	

Table A.23 – Experimental data for IPACS(NX)L composite membrane through 17 hours cross linking time and 1% cross linking concentration[5]

Method	Membrane		Molecular weight of PEG (Dalton)				PWP ($lm^{-2}h^{-1}$)
			200	400	600	1000	
17 hours with 1% cross linking concentration	coupon #1	Product rate ($lm^{-2}h^{-1}$)	20.49	19.45	18.35	17.29	20.26
		% Separation	47%	79%	91%	95%	
	coupon #2	Product rate ($lm^{-2}h^{-1}$)	53.83	45.36	25.00	15.73	111.36
		% Separation	11%	24%	42%	65%	
	coupon #3	Product rate ($lm^{-2}h^{-1}$)	14.52	13.23	12.56	11.92	15.63
		% Separation	46%	81%	93%	97%	
	average	***Product rate ($lm^{-2}h^{-1}$)***	17.51	16.34	15.46	14.61	17.95
		standard deviation	4.22	4.40	4.09	3.80	3.27
		standard error	2.99	3.11	2.89	2.69	2.32
		% Separation	47%	80%	92%	96%	
		standard deviation	1%	1%	1%	1%	
		standard error	1%	1%	1%	1%	

[5] Data gathered from coupon #2 was not taken into average calculation considering the coupon was damaged (scratch or pin holes).

Table A.24 – Experimental data for IPACS(NX)L composite membrane through 17 hours cross linking time and 3% cross linking concentration

Method	Membrane		Molecular weight of PEG (Dalton)				PWP ($lm^{-2}h^{-1}$)
			200	400	600	1000	
17 hours with 3% cross linking concentration	coupon #1	Product rate ($lm^{-2}h^{-1}$)	16.71	16.81	12.67	12.74	17.94
		% Separation	43%	71%	87%	94%	
	coupon #2	Product rate ($lm^{-2}h^{-1}$)	10.39	10.47	8.08	8.11	11.05
		% Separation	50%	77%	93%	97%	
	coupon #3	Product rate ($lm^{-2}h^{-1}$)	10.05	10.09	7.80	7.79	10.62
		% Separation	52%	78%	93%	97%	
	average	***Product rate ($lm^{-2}h^{-1}$)***	12.38	12.46	9.52	9.55	13.20
		standard deviation	3.75	3.77	2.73	2.77	4.11
		standard error	2.17	2.18	1.58	1.60	2.37
		% Separation	48%	75%	91%	96%	
		standard deviation	5%	4%	3%	2%	
		standard error	3%	2%	2%	1%	

Table A.25 – Experimental data for IPACS(NX)L composite membrane through 17 hours cross linking time and 5% cross linking concentration

Method	Membrane		Molecular weight of PEG (Dalton)				PWP
			200	400	600	1000	($lm^{-2}h^{-1}$)
17 hours with 5% cross linking concentration	coupon #1	Product rate ($lm^{-2}h^{-1}$)	13.37	12.23	11.72	10.69	13.36
		% Separation	49%	81%	93%	96%	
	coupon #2	Product rate ($lm^{-2}h^{-1}$)	15.37	14.04	13.15	15.42	16.08
		% Separation	50%	82%	92%	76%	
	coupon #3	Product rate ($lm^{-2}h^{-1}$)	17.83	16.34	15.34	14.26	17.80
		% Separation	43%	80%	92%	97%	
	average	***Product rate ($lm^{-2}h^{-1}$)***	15.52	14.20	13.40	13.46	15.75
		standard deviation	2.23	2.06	1.82	2.47	2.24
		standard error	1.29	1.19	1.05	1.42	1.29
		% Separation	47%	81%	92%	90%	
		standard deviation	4%	1%	1%	12%	
		standard error	2%	1%	0%	7%	

Table A.26 – Experimental data for IPACS(NX)L composite membrane through 17 hours cross linking time and 10% cross linking concentration

Method	Membrane		Molecular weight of PEG (Dalton)				PWP ($lm^{-2}h^{-1}$)
			200	400	600	1000	
17 hours with 10% cross linking concentration	coupon #1	Product rate ($lm^{-2}h^{-1}$)	25.48	25.75	22.9	22.38	25.65
		% Separation	45%	78%	93%	96%	
	coupon #2	Product rate ($lm^{-2}h^{-1}$)	25.4	25.34	23.51	22.93	25.32
		% Separation	38%	70%	86%	92%	
	coupon #3	Product rate ($lm^{-2}h^{-1}$)	18.7	15.29	14.49	12.94	20.72
		% Separation	39%	76%	84%	93%	
	average	***Product rate ($lm^{-2}h^{-1}$)***	23.19	22.13	20.30	19.42	23.90
		standard deviation	3.89	5.92	5.04	5.62	2.76
		standard error	2.25	3.42	2.91	3.24	1.59
		% Separation	41%	75%	88%	94%	
		standard deviation	4%	4%	5%	2%	
		standard error	2%	2%	3%	1%	

Table A.27 – Experimental data for IPACS(NX)L composite membrane through 24 hours cross linking time and 0.2% cross linking concentration

Method	Membrane		Molecular weight of PEG (Dalton)				PWP ($lm^{-2}h^{-1}$)
			200	400	600	1000	
24 hours with 0.2% cross linking concentration	coupon #1	Product rate ($lm^{-2}h^{-1}$)	17.77	16.95	15.51	15.07	18.08
		% Separation	46%	79%	92%	96%	
	coupon #2	Product rate ($lm^{-2}h^{-1}$)	17.1	17.55	15.68	15.62	17.19
		% Separation	49%	78%	90%	92%	
	coupon #3	Product rate ($lm^{-2}h^{-1}$)	20.60	19.00	17.52	16.56	23.10
		% Separation	36%	65%	77%	84%	
	average	***Product rate ($lm^{-2}h^{-1}$)***	18.49	17.83	16.24	15.75	19.46
		standard deviation	1.86	1.05	1.11	0.75	3.19
		standard error	1.07	0.61	0.64	0.44	1.84
		% Separation	44%	74%	86%	91%	
		standard deviation	7%	8%	8%	6%	
		standard error	4%	5%	5%	4%	

Table A.28 – Experimental data for IPACS(NX)L composite membrane through 24 hours cross linking time and 1% cross linking concentration

Method	Membrane		Molecular weight of PEG (Dalton)				PWP ($lm^{-2}h^{-1}$)
			200	400	600	1000	
24 hours with 1% cross linking concentration	coupon #1	Product rate ($lm^{-2}h^{-1}$)	15.17	14.73	13.38	13.05	15.02
		% Separation	49%	78%	91%	94%	
	coupon #2	Product rate ($lm^{-2}h^{-1}$)	13.45	13.18	11.98	11.71	13.12
		% Separation	52%	82%	93%	96%	
	coupon #3	Product rate ($lm^{-2}h^{-1}$)	17.10	16.78	15.24	14.97	17.68
		% Separation	48%	80%	92%	96%	
	average	***Product rate ($lm^{-2}h^{-1}$)***	15.24	14.90	13.53	13.24	15.27
		standard deviation	1.83	1.81	1.64	1.64	2.29
		standard error	1.05	1.04	0.94	0.95	1.32
		% Separation	50%	80%	92%	95%	
		standard deviation	2%	2%	1%	1%	
		standard error	1%	1%	1%	1%	

Table A.29 – Experimental data for IPACS(NX)L composite membrane through 24 hours cross linking time and 3% cross linking concentration

Method	Membrane		Molecular weight of PEG (Dalton)				PWP
			200	400	600	1000	($lm^{-2}h^{-1}$)
24 hours with 3% cross linking concentration	coupon #1	Product rate ($lm^{-2}h^{-1}$)	13.24	13.40	11.47	11.5	13.90
		% Separation	47%	75%	90%	92%	
	coupon #2	Product rate ($lm^{-2}h^{-1}$)	10.44	10.45	8.35	8.33	11.24
		% Separation	49%	75%	82%	95%	
	coupon #3	Product rate ($lm^{-2}h^{-1}$)	9.49	9.31	7.19	7.10	10.52
		% Separation	56%	80%	83%	98%	
	average	***Product rate ($lm^{-2}h^{-1}$)***	11.06	11.05	9.00	8.98	11.89
		standard deviation	1.95	2.11	2.21	2.27	1.78
		standard error	1.13	1.22	1.28	1.31	1.03
		% Separation	51%	77%	85%	95%	
		standard deviation	5%	3%	4%	3%	
		standard error	3%	2%	3%	2%	

Table A.30 – Experimental data for IPACS(NX)L composite membrane through 24 hours cross linking time and 5% cross linking concentration

Method	Membrane		Molecular weight of PEG (Dalton)				PWP
			200	400	600	1000	($lm^{-2}h^{-1}$)
24 hours with 5% cross linking concentration	coupon #1	Product rate ($lm^{-2}h^{-1}$)	22.24	21.38	23.26	22.32	21.33
		% Separation	42%	73%	87%	92%	
	coupon #2	Product rate ($lm^{-2}h^{-1}$)	13.24	12.9	14.23	13.68	12.90
		% Separation	47%	78%	91%	96%	
	coupon #3	Product rate ($lm^{-2}h^{-1}$)	14.78	13.94	15.24	14.59	14.20
		% Separation	45%	77%	90%	95%	
	average	***Product rate ($lm^{-2}h^{-1}$)***	16.75	16.07	17.58	16.86	16.14
		standard deviation	4.81	4.63	4.95	4.75	4.54
		standard error	2.78	2.67	2.86	2.74	2.62
		% Separation	45%	76%	89%	94%	
		standard deviation	3%	3%	2%	2%	
		standard error	1%	2%	1%	1%	

Table A.31 – Experimental data for IPACS(NX)L composite membrane through 24 hours cross linking time and 10% cross linking concentration

Method	Membrane		Molecular weight of PEG (Dalton)				PWP
			200	400	600	1000	($lm^{-2}h^{-1}$)
24 hours with 10% cross linking concentration	coupon #1	Product rate ($lm^{-2}h^{-1}$)	21.48	21.23	23.69	22.56	20.28
		% Separation	43%	76%	90%	95%	
	coupon #2	Product rate ($lm^{-2}h^{-1}$)	14.64	13.39	14.32	13.92	14.96
		% Separation	39%	73%	87%	90%	
	coupon #3	Product rate ($lm^{-2}h^{-1}$)	23.49	22.85	24.95	24.38	22.77
		% Separation	36%	70%	88%	96%	
	average	***Product rate ($lm^{-2}h^{-1}$)***	19.87	19.16	20.99	20.29	19.34
		standard deviation	4.64	5.06	5.81	5.59	3.99
		standard error	2.68	2.92	3.35	3.23	2.30
		% Separation	39%	73%	88%	94%	
		standard deviation	4%	3%	2%	3%	
		standard error	2%	2%	1%	2%	

APPENDIX B

COMMERCIAL NF MEMBRANES

Table B.1 – Commercial NF membrane and its properties gathered from literature[6]

Manufacturer (Source)	Membrane	Applied pressure		PWP	Adjustment to	MWCO	Solute
		pressure	unit	($lm^{-2}h^{-1}$)	($\mathbf{lm^{-2}h^{-1}kPa^{-1}}$)	(dalton)	tested
Permionics Ltd. (catalog)	HFNF300	200	psi	60	0.04	300	n.i.
	HFNF500	200	psi	90	0.07	500	n.i.
Nadir (Van der Bruggen *et al.*, 2003)	NF PES 10	40	bar	200	0.05	1000	n.i.
	N30F	40	bar	40	0.01	400	n.i.
Toray Ind. (Van der Bruggen *et al.*, 2003)	UTC-20	7.5	bar	81	0.11	180	n.i.
	UTC-60	6.7	bar	28	0.04	150	n.i.
Osmonics (ibid)	Desal 51 HL	6.9	bar	62.1	0.09	300	n.i.
KOCH (Yang *et al.*, 2001)	MPF-44	30	bar	43	0.01	200	n.i.
	MPF-50	30	bar	11	0.004	700	Sudan IV
	MPF-60	30	bar	4.9	0.002	400	Sudan IV
Toray (ibid)	UTC-20	30	bar	128	0.04	180	n.i.
Osmonics (Yang *et al.*, 2001)	Desal-5	30	bar	230	0.08	300	n.i.
	Desal-DK	30	bar	156	0.05	300	n.i.
(Schäfer *et al.*, 2000)	CA-UF	5	bar	49.9	0.10	180	Dektran
	TFC-SR	5	bar	45.8	0.09	180	Dektran
	TFC-S	5	bar	49.4	0.10	180	Dektran
	TFC-ULP	5	bar	19.4	0.04	180	Dektran
(Yoon *et al.*, 2002)	ESNA	-	-	1.05	0.04	200	n.i.
	MX07	-	-	0.47	0.02	400	n.i.

[6] Yoon *et al.* (2002) presented the PWP units in terms of $ld^{-1}m^{-2}kPa^{-1}$.

Table B.1 – Commercial NF membrane and its properties gathered from literature (continued)

Manufacturer (Source)	Membrane	Applied pressure		PWP	Adjustment to	MWCO	Solute
		pressure	unit	($lm^{-2}h^{-1}$)	($lm^{-2}h^{-1}kPa^{-1}$)	(dalton)	tested
(Kumar *et al.*, 2000)	PANCHINF (0.02% 0.5h)	69.6	psi	17	0.04	700	PEG
	PANCHINF (0.08% 0.5h)	69.6	psi	8.3	0.02	550	PEG
	PANCHINF (0.2% 0.5h)	69.6	psi	8.3	0.02	500	PEG
	PANCHINF (0.08% 1h)	69.6	psi	9.0	0.02	1000	PEG
	PANCHINF (0.2% 1h)	69.6	psi	6.3	0.01	400	PEG
	PANCHINF (0.5% 1h)	69.6	psi	6.5	0.01	900	PEG

APPENDIX C

REPRODUCIBILITY DATA

Table C.1 – Reproducibility data of IPACS(NX)L 9h 5% composite NF membranes chosen for solvent resistant studies

Membrane		PEG (Dalton)				PWP ($lm^{-2}h^{-1}$)
		200	400	600	1000	
Coupon #1	Product rate ($lm^{-2}h^{-1}$)	30.33	29.00	27.41	25.75	28.02
	% Separation	33%	64%	84%	91%	
Coupon #2	Product rate ($lm^{-2}h^{-1}$)	22.86	21.97	21.51	20.17	22.22
	% Separation	37%	69%	86%	94%	
Coupon #3	Product rate ($lm^{-2}h^{-1}$)	20.10	19.76	19.78	18.87	20.46
	% Separation	40%	70%	86%	94%	
Coupon #4	Product rate ($lm^{-2}h^{-1}$)	26.52	25.96	25.11	24.17	24.74
	% Separation	28%	59%	80%	91%	
Coupon #5	Product rate ($lm^{-2}h^{-1}$)	22.70	22.89	21.92	20.39	28.55
	% Separation	33%	60%	78%	88%	
Coupon #6	Product rate ($lm^{-2}h^{-1}$)	24.20	22.70	21.61	19.85	27.03
	% Separation	35%	66%	82%	90%	
Coupon #7	Product rate ($lm^{-2}h^{-1}$)	6.05	5.66	5.34	5.12	6.56
	% Separation	58%	86%	93%	96%	
Coupon #8	Product rate ($lm^{-2}h^{-1}$)	2.65	2.58	2.56	2.50	2.82
	% Separation	63%	85%	87%	87%	
Coupon #9	Product rate ($lm^{-2}h^{-1}$)	3.04	2.92	2.73	2.66	2.97
	% Separation	64%	90%	96%	96%	
Coupon #10	Product rate ($lm^{-2}h^{-1}$)	5.23	5.06	4.76	4.51	5.6
	% Separation	57%	84%	91%	92%	
Coupon #11	Product rate ($lm^{-2}h^{-1}$)	4.73	5.20	5.13	3.97	6.29
	% Separation	57%	73%	76%	89%	
Coupon #12	Product rate ($lm^{-2}h^{-1}$)	5.10	4.86	4.61	4.40	4.98
	% Separation	60%	89%	95%	97%	
Average	***Product rate ($lm^{-2}h^{-1}$)***	14.46	14.05	13.54	12.70	15.02
	standard deviation	10.75	10.37	9.98	9.44	10.89
	standard error	3.10	2.99	2.88	2.73	3.14
	% Separation	47%	74%	86%	92%	
	standard deviation	14%	12%	7%	3%	
	standard error	4%	3%	2%	1%	

APPENDIX D

XPS MEASUREMENT

Table D.1 – Stoichiometric of theoretical atomic concentration of different elemental chemical states for different components and their range of binding energies[7]

Component	Formula	Total atoms	Carbon							
			(C=C)	(C=O)-O	NH-(C=O)	O-CH_2-O	CH_2-O-CH_2	CH_2-OH	CH_2-NH	CH_x
Chitosan	$C_{628}O_{414}N_{100}$	1142	0	0	1.2	8.8	17.5	17.5	8.8	1.2
AcOH	C_2O_2	4	0	25	0	0	0	0	0	25
N_aOAc	C_2O_2	4	0	25	0	0	0	0	0	25
Water	O_1	1	0	0	0	0	0	0	0	0
DEGDMA	$C_{12}O_5$	17	11.8	11.8	0	0	0	0	0	47.1
IPA	C_3O_1	4	0	0	0	0	0	25	0	50
Torlon®	$C_{192}O_{37}N_{20}$	249	24.5	0	12	0	2.8	0	8	29.7
NMP	$C_5O_1N_1$	7	0	0	14.3	0	0	0	0	57.1
Binding energy (eV)			285	289.4	288.4	288	286.8	286.6	285.6	285

[7] Binding energies for each group is calculated from www.tech2004.umd.edu/2004posters/R-A_bioMEMS.pdf

Table D.1 – Stoichiometric of theoretical atomic concentration of different elemental chemical states for different components and their range of binding energies (continued)

Component	Formula	Total atoms	Oxygen					Nitrogen	
			(C=O)-O*	CH_2-OH	CH_2O-CH_2	(C=O)	H_2O	NH-(C=O)	NH_2-CH
Chitosan	$C_{628}O_{414}N_{100}$	1142	0	17.5	17.5	1.2	0	1.2	7.5
AcOH	C_2O_2	4	25	0	0	25	0	0	0
N_aOAc	C_2O_2	4	25	0	0	25	0	0	0
Water	O_1	1	0	0	0	0	100	0	0
DEGDMA	$C_{12}O_5$	17	0	0	17.6	11.8	0	0	0
IPA	C_3O_1	4	0	25	0	0	0	0	0
Torlon®	$C_{192}O_{37}N_{20}$	249	0	0	2.8	12	0	4	4
NMP	$C_5O_1N_1$	7	0	0	0	14.3	0	14.3	0
Binding energy (eV)			533.5	532.7	531.7	531.4	535	400.2	399.5

Table D.2 – Theoretical atomic concentration (%) in terms of carbon, oxygen, and nitrogen ratio

Component	Formula	Total atoms	Carbon (C)	Oxygen (O)	Nitrogen (N)	C/O	C/N
Chitosan	$C_{628}O_{414}N_{100}$	1142	54.99	36.25	8.76	1.52	6.28
AcOH	C_2O_2	4	50	50	-	1	-
N_aOAc	C_2O_2	4	50	50	-	1	-
Water	O_1	1	-	100	-	0	-
DEGDMA	$C_{12}O_5$	17	70.59	29.41	-	2.40	-
IPA	C_3O_1	4	75	25	-	3	-
N_aHCO_3	C_1O_3	7	14	43	-	0.33	-
Torlon®	$C_{192}O_{37}N_{20}$	249	77.11	14.86	8.03	5.19	9.60
NMP	$C_5O_1N_1$	7	71.43	14.29	14.29	5	5

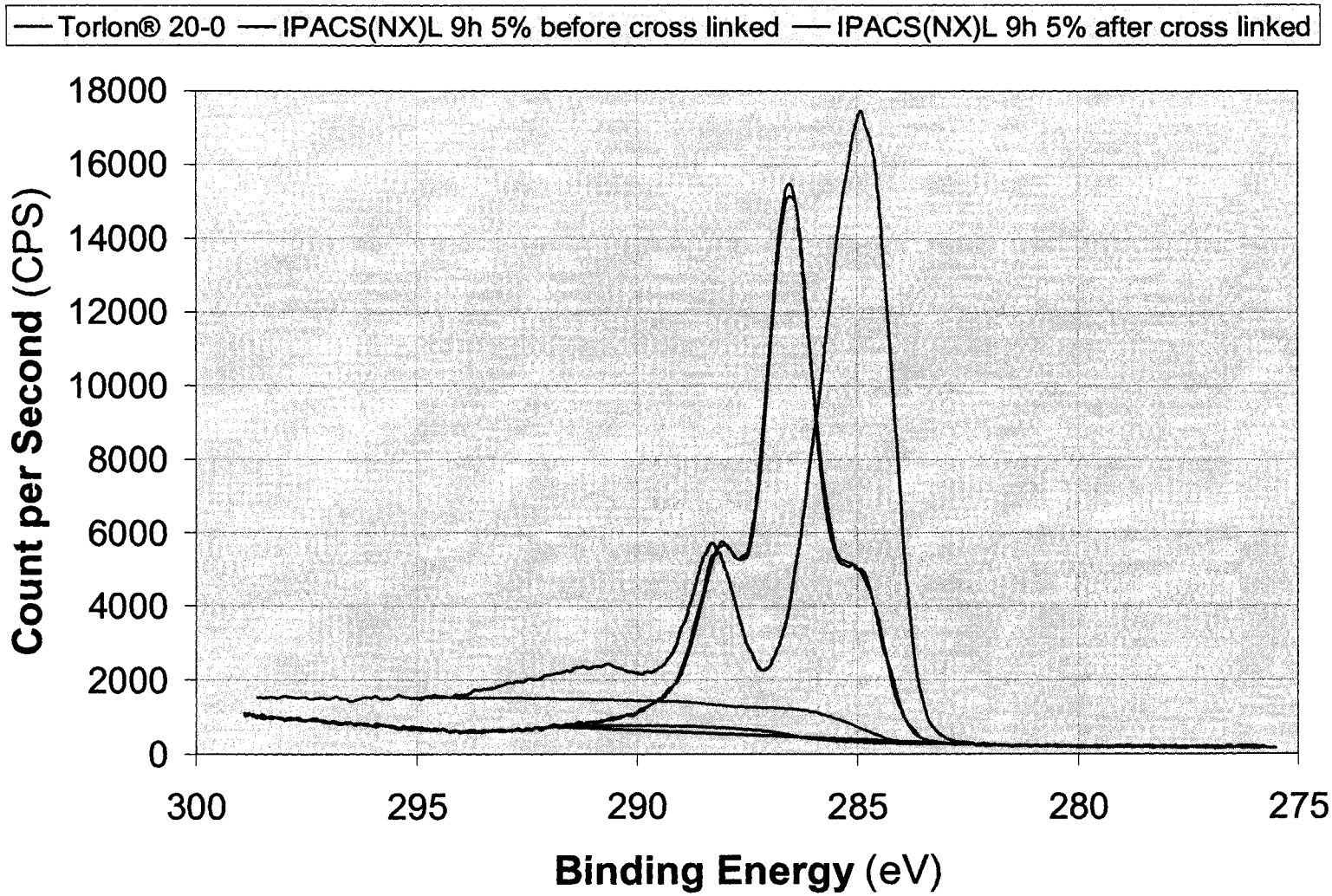

Figure D.1 – Carbon 1s spectrum for Torlon®, IPACS(NX)L 9h 5% before and after cross linking process

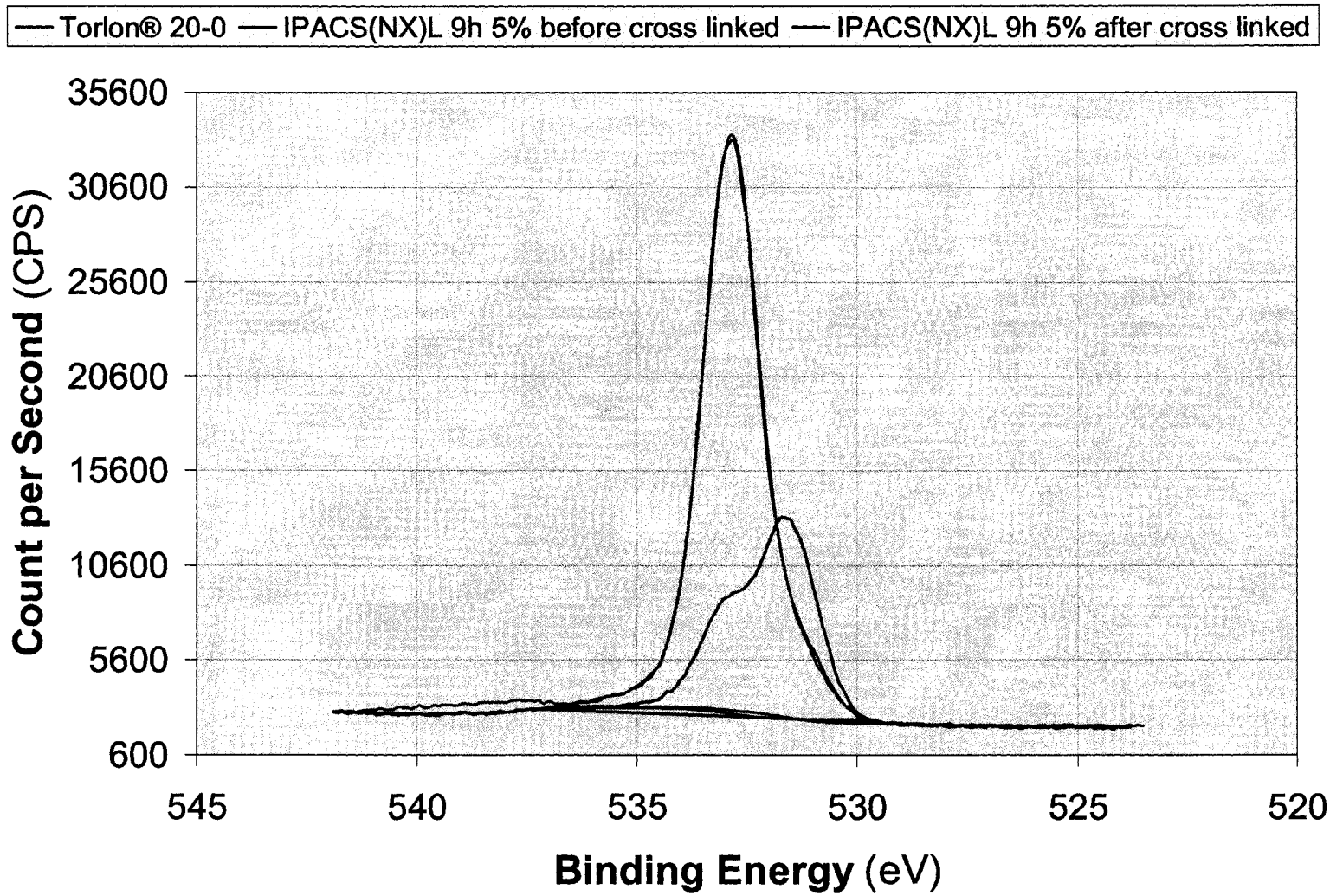

Figure D.2 – Oxygen 1s spectrum for Torlon®, IPACS(NX)L 9h 5% before and after cross linking process

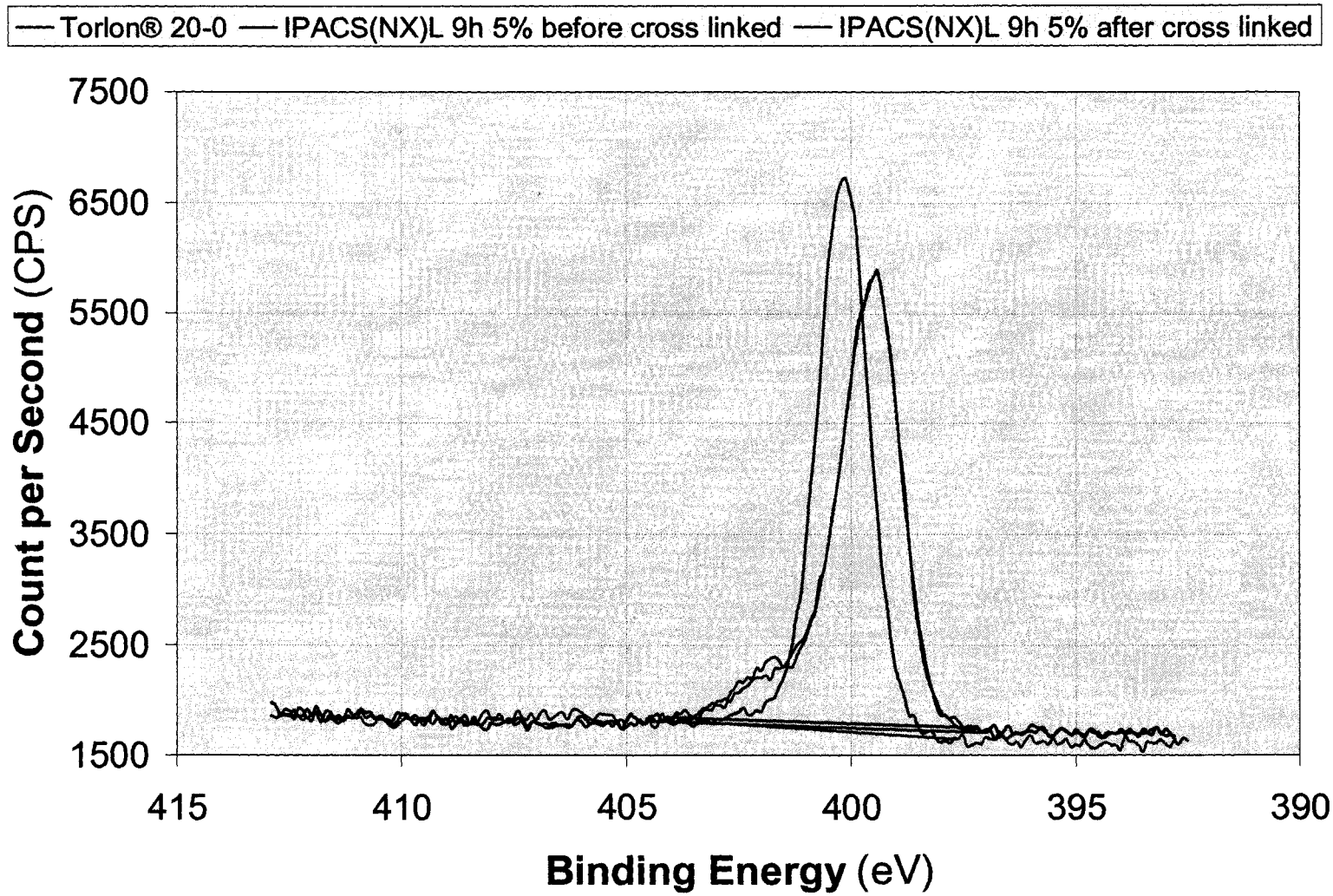

Figure D.3 – Nitrogen 1s spectrum for Torlon®, IPACS(NX)L 9h 5% before and after cross linking process

APPENDIX E

SWELLING AND PERMEATION DATA FOR IPACS(NX)L 9h5%

Table E.1 – Permeation data for IPACS(NX)L 9h 5% membranes at pH 3.0

pH	Membrane		PEG (Dalton)				PWP ($lm^{-2}h^{-1}$)
			200	400	600	1000	
pH 3.0	Coupon #1	Product rate ($lm^{-2}h^{-1}$)	25.13	25.06	24.74	22.81	23.06
		% Separation	43%	74%	86%	91%	
	Coupon #2	Product rate ($lm^{-2}h^{-1}$)	29.03	29.50	26.51	26.41	25.66
		% Separation	43%	74%	89%	95%	
	Coupon #3	Product rate ($lm^{-2}h^{-1}$)	13.49	13.76	11.53	11.77	12.52
		% Separation	50%	75%	91%	92%	
	Coupon #4	Product rate ($lm^{-2}h^{-1}$)	6.51	6.43	5.80	5.61	6.44
		% Separation	63%	89%	100%	99%	
	Coupon #5	Product rate ($lm^{-2}h^{-1}$)	4.14	3.93	3.41	3.30	4.79
		% Separation	59%	81%	93%	92%	
	Coupon #6	Product rate ($lm^{-2}h^{-1}$)	2.64	2.51	2.26	2.20	2.74
		% Separation	72%	90%	98%	98%	
	Average	***Product rate ($lm^{-2}h^{-1}$)***	13.49	13.53	12.38	12.02	12.54
		standard deviation	11.23	11.42	10.76	10.36	9.76
		standard error	4.59	4.66	4.39	4.23	3.98
		% Separation	55%	80%	93%	94%	
		standard deviation	12%	8%	5%	4%	
		standard error	5%	3%	2%	1%	

Table E.2 – Permeation data for IPACS(NX)L 9h 5% membranes at pH 11

pH	Membrane		PEG (Dalton)				PWP ($lm^{-2}h^{-1}$)
			200	400	600	1000	
pH 11.0	Coupon #1	Product rate ($lm^{-2}h^{-1}$)	19.38	19.30	17.25	16.99	19.07
		% Separation	41%	70%	86%	92%	
	Coupon #2	Product rate ($lm^{-2}h^{-1}$)	13.89	13.38	11.86	11.57	13.97
		% Separation	42%	68%	82%	89%	
	Coupon #3	Product rate ($lm^{-2}h^{-1}$)	25.81	26.61	24.11	22.92	23.97
		% Separation	33%	62%	81%	89%	
	Coupon #4	Product rate ($lm^{-2}h^{-1}$)	4.70	4.38	3.90	3.80	5.35
		% Separation	59%	83%	95%	97%	
	Coupon #5	Product rate ($lm^{-2}h^{-1}$)	6.00	5.82	5.16	4.99	6.33
		% Separation	60%	86%	97%	98%	
	Coupon #6	Product rate ($lm^{-2}h^{-1}$)	6.07	5.94	5.42	5.14	6.55
		% Separation	62%	89%	99%	100%	
	Average	***Product rate ($lm^{-2}h^{-1}$)***	12.64	12.57	11.28	10.90	12.54
		standard deviation	8.61	8.94	8.09	7.75	7.76
		standard error	3.52	3.65	3.30	3.17	3.17
		% Separation	49%	76%	90%	94%	
		standard deviation	12%	11%	8%	5%	
		standard error	5%	5%	3%	2%	

Table E.3 – Swelling data for IPACS(NX)L 9h 5% membranes at pH 2.0

pH	Membrane		Dry weight (gram)	Wet weight (gram)	% Swelling (%)	Standard deviation (%)	Standard error (%)
2.0	Torlon® base membrane	coupon #1	0.46	0.76	65.22		
		coupon #2	0.49	0.70	42.86		
		average			54.04	15.81	11.18
	Composite membrane	coupon #1	0.51	0.79	53.97		
		coupon #2	0.51	0.76	48.73		
		coupon #3	0.51	0.83	63.29		
		coupon #4	0.49	0.83	70.57		
		average			59.14	9.71	4.86

Table E.4 – Swelling data for IPACS(NX)L 9h 5% membranes at pH 4.0

pH	Membrane		Dry weight (gram)	Wet weight (gram)	% Swelling (%)	Standard deviation (%)	Standard error (%)
4.0	Torlon® base membrane	coupon #1	0.44	0.68	53.92		
		coupon #2	0.49	0.63	29.71		
		average			41.81	17.12	12.10
	Composite membrane	coupon #1	0.49	0.78	59.71		
		coupon #2	0.50	0.78	57.26		
		coupon #3	0.54	0.80	49.45		
		coupon #4	0.52	0.79	50.53		
		average			54.24	5.02	2.51

Table E.5 – Swelling data for IPACS(NX)L 9h 5% membranes at pH 6.0

pH	Membrane		Dry weight (gram)	Wet weight (gram)	% Swelling (%)	Standard deviation (%)	Standard error (%)
6.0	Torlon® base membrane	coupon #1	0.48	0.65	36.41		
		coupon #2	0.47	0.71	51.03		
		average			43.72	10.34	7.31
	Composite membrane	coupon #1	0.48	0.75	54.89		
		coupon #2	0.53	0.72	35.26		
		coupon #3	0.50	0.81	63.11		
		coupon #4	0.50	0.79	58.06		
		average			52.83	12.19	6.10

Table E.6 – Swelling data for IPACS(NX)L 9h 5% membranes at pH 8.0

pH	Membrane		Dry weight (gram)	Wet weight (gram)	% Swelling (%)	Standard deviation (%)	Standard error (%)
8.0	Torlon® base membrane	coupon #1	0.46	0.71	53.71		
		coupon #2	0.53	0.63	20.00		
		average			36.86	23.84	16.86
	Composite membrane	coupon #1	0.42	0.72	71.67		
		coupon #2	0.48	0.72	51.32		
		coupon #3	0.49	0.75	53.44		
		coupon #4	0.48	0.61	27.00		
		average			50.86	18.34	9.17

Table E.7 – Swelling data for IPACS(NX)L 9h 5% membranes at pH 10

pH	Membrane		Dry weight (gram)	Wet weight (gram)	% Swelling (%)	Standard deviation (%)	Standard error (%)
10.0	Torlon® base membrane	coupon #1	0.49	0.70	41.53		
		coupon #2	0.47	0.76	63.27		
		average			52.40	15.37	10.87
	Composite membrane	coupon #1	0.53	0.78	46.48		
		coupon #2	0.50	0.82	65.59		
		coupon #3	0.53	0.80	50.40		
		coupon #4	0.51	0.84	64.84		
		average			56.83	9.82	4.91

Table E.8 – Swelling data for IPACS(NX)L 9h 5% membranes at pH 12

pH	Membrane		Dry weight (gram)	Wet weight (gram)	% Swelling (%)	Standard deviation (%)	Standard error (%)
12.0	Torlon® base membrane*	coupon #1	0.50	1.24	148.20		
		coupon #2	0.48	1.24	158.17		
		average			153.19	7.05	4.99
	Composite membrane~	coupon #1	0.51	0.88	71.94		
		coupon #2	0.49	0.88	77.81		
		coupon #3	0.52	0.93	79.99		
		coupon #4	0.50	0.96	92.12		
		average			80.46	8.48	4.24

* Membranes changed colour after pH immersion (white)

~ Membranes changed colour but trace of yellow from Torlon® still noticeable

Table E.9 – Swelling data for IPACS(NX)L 9h 5% membranes contact with methanol

Solvent	Membrane		Dry weight (gram)	Wet weight (gram)	% Swelling (%)	Standard deviation (%)	Standard error (%)
Methanol	Torlon® base membrane	coupon #1	0.48	0.80	66.04		
		coupon #2	0.53	0.86	60.84		
		average			63.44	3.68	2.60
	Composite membrane	coupon #1	0.50	0.82	64.23		
		coupon #2	0.52	0.84	62.19		
		coupon #3	0.48	0.84	76.73		
		coupon #4	0.48	0.96	101.55		
		average			76.18	18.10	9.05

Table E.10 – Swelling data for IPACS(NX)L 9h 5% membranes contact with ethanol

Solvent	Membrane		Dry weight (gram)	Wet weight (gram)	% Swelling (%)	Standard deviation (%)	Standard error (%)
Ethanol	Torlon® base membrane	coupon #1	0.47	0.82	74.65		
		coupon #2	0.49	0.76	55.61		
		average			65.13	13.47	9.52
	Composite membrane	coupon #1	0.49	0.87	76.01		
		coupon #2	0.45	0.92	104.40		
		coupon #3	0.52	0.84	61.66		
		coupon #4	0.53	0.80	52.00		
		average			73.52	22.83	11.41

Table E.11 – Swelling data for IPACS(NX)L 9h 5% membranes contact with iso-propanol

Solvent	Membrane		Dry weight (gram)	Wet weight (gram)	% Swelling (%)	Standard deviation (%)	Standard error (%)
Iso-propanol	Torlon® base membrane	coupon #1	0.49	0.84	70.66		
		coupon #2	0.50	0.79	58.48		
		average			64.57	8.62	6.09
	Composite membrane	coupon #1	0.50	0.88	74.46		
		coupon #2	0.50	0.85	68.65		
		coupon #3	0.50	0.84	69.63		
		coupon #4	0.53	0.91	71.93		
		average			71.17	2.59	1.30

Table E.12 – Swelling data for IPACS(NX)L 9h 5% membranes contact with MEK

Solvent	Membrane		Dry weight (gram)	Wet weight (gram)	% Swelling (%)	Standard deviation (%)	Standard error (%)
Methyl ethyl ketone	Torlon® base membrane	coupon #1	0.49	0.84	71.53		
		coupon #2	0.55	0.84	53.85		
		average			62.69	12.51	8.84
	Composite membrane	coupon #1	0.49	0.90	85.49		
		coupon #2	0.50	0.89	78.43		
		coupon #3	0.52	0.90	73.11		
		coupon #4	0.52	0.90	74.52		
		average			77.89	5.55	2.77

Table E.13 – Swelling data for IPACS(NX)L 9h 5% membranes contact with ethyl acetate

Solvent	Membrane		Dry weight (gram)	Wet weight (gram)	% Swelling (%)	Standard deviation (%)	Standard error (%)
Ethyl acetate	Torlon® base membrane	coupon #1	0.48	0.88	83.33		
		coupon #2	0.47	0.82	74.25		
		average			78.79	6.43	4.54
	Composite membrane	coupon #1	0.49	0.91	86.70		
		coupon #2	0.50	0.97	95.33		
		coupon #3	0.54	0.88	63.60		
		coupon #4	0.52	0.89	72.11		
		average			79.44	14.26	7.13

Table E.14 – Swelling data for IPACS(NX)L 9h 5% membranes contact with hexane

Solvent	Membrane		Dry weight (gram)	Wet weight (gram)	% Swelling (%)	Standard deviation (%)	Standard error (%)
Hexane	Torlon® base membrane	coupon #1	0.54	0.66	22.59		
		coupon #2	0.48	0.76	56.99		
		average			39.79	24.33	17.20
	Composite membrane	coupon #1	0.53	0.72	37.09		
		coupon #2	0.50	0.75	50.63		
		coupon #3	0.51	0.70	37.31		
		coupon #4	0.47	0.74	56.71		
		average			45.44	9.83	4.91

Table E.15 – PWP data for IPACS(NX)L 9h 5% membranes after immersion in solvents

Solvent	Composite membrane	PWP ($lm^{-2}h^{-1}$)	Standard deviation ($lm^{-2}h^{-1}$)	Standard error ($lm^{-2}h^{-1}$)
Methanol	coupon #1	15.21		
	coupon #2	15.55		
	coupon #3	5.46		
	coupon #4	6.57		
	average	10.70	5.43	2.71
Ethanol	coupon #1	11.24		
	coupon #2	26.50		
	coupon #3	5.03		
	coupon #4	5.72		
	average	12.12	9.98	4.99
Iso-propanol	coupon #1	14.12		
	coupon #2	26.72		
	coupon #3	8.45		
	coupon #4	6.56		
	average	13.96	9.09	4.54
Methyl ethyl ketone	coupon #1	12.04		
	coupon #2	10.10		
	coupon #3	5.07		
	coupon #4	5.41		
	average	8.15	3.46	1.73
Ethyl acetate	coupon #1	13.26		
	coupon #2	11.08		
	coupon #3	5.37		
	coupon #4	5.94		
	average	8.91	3.88	1.94
Hexane	coupon #1	13.79		
	coupon #2	17.53		
	coupon #3	3.86		
	coupon #4	5.94		
	average	10.28	6.45	3.23

Table E.16 – Methanol flux for IPACS(NX)L 9h 5% membranes as a function of time

Time (second)	Pressure (kPa)	Mass (gram)	Rate (gram/second)	Solvent flux ($lm^{-2}h^{-1}$)
2	1.851	0.001	0.000	0.008
238	479.786	1.217	0.005	0.135
474	478.944	3.296	0.007	0.184
710	478.524	5.372	0.008	0.200
946	478.103	7.421	0.008	0.207
1182	481.890	9.441	0.008	0.211
1418	481.048	11.465	0.008	0.214
1654	481.048	13.472	0.008	0.215
1890	480.628	15.475	0.008	0.216
2126	480.628	17.473	0.008	0.217
2362	480.628	19.436	0.008	0.217
2598	480.207	21.390	0.008	0.218
2834	480.628	23.324	0.008	0.218
3070	480.207	25.282	0.008	0.218
3306	480.207	27.206	0.008	0.217
3542	480.207	29.123	0.008	0.217
3778	480.207	30.988	0.008	0.217
4014	480.207	32.868	0.008	0.216
4250	479.786	34.746	0.008	0.216
4486	479.786	36.607	0.008	0.216
4722	479.786	38.485	0.008	0.215
4958	479.786	40.338	0.008	0.215
5194	479.786	42.169	0.008	0.215
5430	479.786	44.048	0.008	0.214
5666	479.786	45.881	0.008	0.214
5902	479.366	47.727	0.008	0.214
6138	479.366	49.511	0.008	0.213
6374	479.786	51.269	0.008	0.213
6610	479.366	53.070	0.008	0.212
6846	479.366	54.849	0.008	0.212
7082	479.366	56.647	0.008	0.211
7318	479.366	58.424	0.008	0.211
7554	479.366	60.183	0.008	0.211
7790	479.366	61.961	0.008	0.210
8026	478.944	63.741	0.008	0.210
8262	478.944	65.495	0.008	0.210
8498	478.944	67.247	0.008	0.209
8734	478.944	68.987	0.008	0.209
8970	478.944	70.715	0.008	0.208
9058	479.366	71.368	0.008	0.208

Table E.17 – Ethanol flux for IPACS(NX)L 9h 5% membranes as a function of time

Time (second)	Pressure (kPa)	Mass (gram)	Rate (gram/second)	Solvent flux ($lm^{-2}h^{-1}$)
2	478.103	0.101	0.050	1.337
238	476.000	1.024	0.004	0.114
474	475.579	2.722	0.006	0.152
710	475.158	4.426	0.006	0.165
946	475.158	6.156	0.007	0.172
1182	475.158	7.555	0.006	0.169
1418	478.524	8.782	0.006	0.164
1654	478.944	9.755	0.006	0.156
1890	478.524	10.690	0.006	0.150
2126	481.048	11.601	0.005	0.145
2362	479.786	12.500	0.005	0.140
2598	479.786	13.390	0.005	0.137
2834	479.366	14.276	0.005	0.133
3070	479.786	15.094	0.005	0.130
3306	479.366	16.012	0.005	0.128
3542	479.366	17.016	0.005	0.127
3778	479.366	17.958	0.005	0.126
4014	479.366	18.877	0.005	0.125
4250	479.366	19.797	0.005	0.123
4486	479.366	20.672	0.005	0.122
4722	479.366	21.582	0.005	0.121
4958	479.366	22.298	0.004	0.119
5194	478.944	23.219	0.004	0.118
5430	482.310	24.147	0.004	0.118
5666	482.310	25.055	0.004	0.117
5902	482.310	26.041	0.004	0.117
6138	482.310	27.126	0.004	0.117
6374	481.890	28.021	0.004	0.116
6610	481.890	29.190	0.004	0.117
6846	481.890	30.054	0.004	0.116
7082	481.890	31.111	0.004	0.116
7318	481.469	32.002	0.004	0.116
7554	475.579	33.020	0.004	0.116
7790	475.579	34.105	0.004	0.116
8026	482.471	35.007	0.004	0.116
8262	475.579	36.072	0.004	0.116
8498	475.579	37.325	0.004	0.116
8734	475.579	38.225	0.004	0.116
8970	475.579	39.129	0.004	0.116
9058	475.579	39.810	0.004	0.116

Table E.18 – Iso-propanol flux for IPACS(NX)L 9h 5% membranes as a function of time

Time (second)	Pressure (kPa)	Mass (gram)	Rate (gram/second)	Solvent flux ($lm^{-2}h^{-1}$)
2	485.255	-0.0141	-0.007	-0.188
238	482.310	0.827	0.003	0.093
474	481.890	2.202	0.005	0.124
710	481.890	3.512	0.005	0.132
946	481.890	4.797	0.005	0.135
1182	481.890	5.537	0.005	0.125
1418	481.890	7.339	0.005	0.138
1654	481.469	8.609	0.005	0.139
1890	481.890	9.854	0.005	0.139
2126	481.890	11.060	0.005	0.139
2362	481.890	12.269	0.005	0.138
2598	481.890	13.484	0.005	0.138
2834	481.469	14.689	0.005	0.138
3070	481.469	15.897	0.005	0.138
3306	481.469	17.079	0.005	0.138
3542	481.890	18.255	0.005	0.137
3778	481.890	19.428	0.005	0.137
4014	481.469	20.584	0.005	0.137
4250	481.890	21.741	0.005	0.136
4486	481.469	22.884	0.005	0.136
4722	481.890	24.020	0.005	0.135
4958	481.469	25.150	0.005	0.135
5194	481.469	26.278	0.005	0.135
5430	481.469	27.357	0.005	0.134
5666	481.890	28.461	0.005	0.134
5902	481.469	29.559	0.005	0.133
6138	481.469	30.599	0.005	0.133
6374	481.469	31.689	0.005	0.132
6610	481.469	32.777	0.005	0.132
6846	481.469	33.854	0.005	0.132
7082	481.469	34.928	0.005	0.131
7318	481.469	35.979	0.005	0.131
7554	481.469	37.004	0.005	0.130
7790	481.469	38.038	0.005	0.130
8026	481.469	39.075	0.005	0.130
8262	481.469	40.109	0.005	0.129
8498	481.469	41.091	0.005	0.129
8734	481.469	42.123	0.005	0.128
8970	481.469	43.142	0.005	0.128
9206	481.048	44.135	0.005	0.128

Table E.19 – Hexane flux for IPACS(NX)L 9h 5% membranes as a function of time

Time (second)	Pressure (kPa)	Mass (gram)	Rate (gram/second)	Solvent flux ($lm^{-2}h^{-1}$)
2	478.944	0.016	0.008	0.250
238	479.786	-0.010	0.000	-0.001
474	479.366	0.882	0.002	0.059
710	479.366	1.759	0.002	0.078
946	478.944	2.671	0.003	0.089
1182	478.944	3.595	0.003	0.096
1418	478.944	4.527	0.003	0.101
1654	478.944	5.484	0.003	0.104
1890	478.944	6.370	0.003	0.106
2126	478.944	7.295	0.003	0.108
2362	478.944	8.205	0.003	0.109
2598	478.944	9.157	0.004	0.111
2834	478.944	10.106	0.004	0.112
3070	478.944	11.057	0.004	0.113
3306	478.944	11.945	0.004	0.114
3542	478.944	12.842	0.004	0.114
3778	478.944	13.800	0.004	0.115
4014	478.524	14.758	0.004	0.116
4250	478.944	15.670	0.004	0.116
4486	478.944	16.568	0.004	0.116
4722	478.524	17.557	0.004	0.117
4958	478.944	18.480	0.004	0.117
5194	478.524	19.374	0.004	0.117
5430	478.944	20.251	0.004	0.117
5666	478.944	21.147	0.004	0.118
5902	478.944	22.050	0.004	0.118
6138	478.944	22.980	0.004	0.118
6374	478.524	23.870	0.004	0.118
6610	478.944	24.755	0.004	0.118
6846	478.944	25.655	0.004	0.118
7082	478.944	26.581	0.004	0.118
7318	478.524	27.441	0.004	0.118
7554	478.524	28.320	0.004	0.118
7790	478.524	29.228	0.004	0.118
8026	478.524	30.048	0.004	0.118
8262	478.524	30.966	0.004	0.118
8498	478.524	31.808	0.004	0.118
8734	478.944	32.667	0.004	0.118
8970	478.524	33.543	0.004	0.118
9058	478.524	33.877	0.004	0.118

APPENDIX F

SOLVENT PHYSICAL PROPERTIES

Table F.1 – Physical properties of test solvents used in this work

Solvent	Molecular weight (g/mol)	Dielectric constant (ϵ)	Viscosity (cP)	Surface tension (mN/m)
Water	18	80.4	0.89	72.7
Methanol	32	32.6	0.6	22.6
Ethanol	46	24.3	1.08	22.8
Iso-propanol	60	18.3	2.0	20.7
Methyl ethyl ketone	72	15.4	0.41	23.9
Ethyl Acetate	88	6.02	0.45	24
Hexane	86	1.9	0.31	18.2